PREPARATION AND CHARACTERIZATION OF HERBAL EXTRACT LOADED BILAYER SPONGES FOR WOUND DRESSING APPLICATIONS

A Thesis Submitted to
The Graduate School of Engineering and Sciences of
İzmir Institute of Technology
in Partial Fulfillment of the Requirements for the Degree of

MASTER OF SCIENCE

in Chemical Engineering

by
Sibel DEĞER

July 2019
İZMİR

.We approve the thesis of **Sibel DEĞER**

Examining Committee Members:

_____
Prof. Dr. Funda TIHMINLIOĞLU
Department of Chemical Engineering, İzmir Institute of Technology

_____
Prof. Dr. Oğuz BAYRAKTAR
Department of Chemical Engineering, Ege University

_____
Asst. Prof. Dr. Ayben TOP
Department of Chemical Engineering, İzmir Institute of Technology

12 July 2019

_____
Prof. Dr. Funda TIHMINLIOĞLU
Supervisor,
Department of Chemical Engineering,
İzmir Institute of Technology

_____
Prof. Dr. Erol ŞEKER
Head of the Department of Chemical
Engineering

_____
Prof. Dr. Aysun SOFUOĞLU
Dean of the Graduate School of
Engineering and Sciences

ACKNOWLEDGMENTS

ABSTRACT

PREPARATION AND CHARACTERIZATION OF HERBAL EXTRACT LOADED BILAYER SPONGES FOR WOUND DRESSING APPLICATIONS

Recently, the use of biomaterials with natural extracts have been rapidly increasing as an alternative to antibiotic-loaded biomaterials in wound healing applications. *Cissus quadrangularis* (CQ) is a natural extract which has anti-inflammatory, anti-bacterial and anti-fungal activities. CQ has been used as a natural therapy in India to treat many problems such as bone repair, skin infection and wound. In this thesis study, it was aimed to prepare and characterize a bilayer wound dressing consisting of CQ extract that can mimic skin structure and to investigate extract release from the wound dressing. CQ loaded chitosan nanofibers were coated on the chitosan/POSS composite sponges with the electrospinning method as a bilayer wound dressing to treat exudate wounds. The morphology and encapsulation efficiency of the extract-loaded chitosan nanofibers are optimized to achieve controlled release of the extract. Morphologies of nanofibers were observed by scanning electron microscopy (SEM) analysis. Bilayer sponges were characterized by FT-IR, swelling, porosity, mechanical properties, antimicrobial activity, and cytotoxicity analyzes. The diameters of the nanofibers were found between 77.9±4 nm and 97.4±4 nm. The water vapor permeability of the wound dressings is between 4021 and 4609 g/m^{2}day which is found in the appropriate range for wound healing. Bilayer dressings reached 78% to 80% cumulative release at the end of fourth day and release medium showed antimicrobial activity against *E. coli* and *S. epidermidis*. Wound dressings have not shown any toxic effects on the 3T3 cell line. Consequently, the extract loaded bilayer sponges are found as potential candidates for wound dressing.

ÖZET

YARA ÖRTÜSÜ UYGULAMALARINDA KULLANILMAK ÜZERE DOĞAL EKSTRAKT YÜKLÜ ÇİFT TABAKA SÜNGERLERİN HAZIRLANMASI VE KARAKTERİZASYONU

Son zamanlarda, yara iyileşme uygulamalarında, doğal özlü biyomalzemelerin kullanımı antibiyotik yüklü biyomalzemelere alternatif olarak hızla artmaktadır. *Cissus quadrangularis* (CQ), anti-enflamatuar, anti-bakteriyel ve anti-fungal aktiviteleri olan doğal bir ekstraktır. CQ, Hindistan'da kemik onarımı, cilt enfeksiyonu ve yara gibi birçok sorunu tedavi etmek için doğal bir terapi olarak kullanılmaktadır. Bu çalışmada, cilt yapısını taklit edebilen CQ ekstraktından oluşan iki tabakalı bir yara örtüsünün hazırlanması ve karakterize edilmesi ve yara örtüsünden ekstrakt salınımının araştırılması amaçlandı. CQ yüklü kitosan nano lifleri, eksuda yaralarını tedavi etmek için iki tabakalı yara sargısı olarak elektroeğirme yöntemi ile kitosan/POSS kompozit süngerlerin üzerine kaplandı. Ekstrakt yüklü kitosan nano liflerinin morfolojisi ve enkapsülasyon verimliliği, ekstraktın kontrollü salımını sağlamak için optimize edilmiştir. Taramalı elektron mikroskobu (SEM) analizi ile nano liflerin morfolojileri gözlendi. İki katmanlı süngerler, FT-IR, şişme, gözeneklilik, mekanik özellikler, antimikrobiyal aktivite ve sitotoksisite analizleri ile karakterize edildi. Nano liflerin çapları 77.9 ± 4 nm ile 97.4 ± 4 nm arasında bulundu. Yara örtücülerin su buharı geçirgenliği 4021 ve 4609 g/m^2gün aralığındadır ve bu değerler yara iyileşmesi için uygun bulunmuştur. İki tabakalı örtücüler dördüncü günün sonunda kümülatif ekstrakt salımı % 78 ile % 80'e ulaştı ve salım ortamı *E. coli* ve *S. epidermidis*'e karşı antimikrobiyal aktivite gösterdi. Yara pansumanları, 3T3 hücre çizgisi üzerinde herhangi bir toksik etki göstermemiştir. Sonuç olarak, ekstrakt yüklü iki katmanlı süngerler potansiyel yara örtüsü olmaya adaydır.

TABLE OF CONTENTS

LIST OF FIGURES

LIST OF TABLES

CHAPTER 1

INTRODUCTION

The skin forms a large part of human body and acts as a barrier to body (Kolarsick et al. 2011). The wound can occur from some traumatic events, burning or chronic disease in the skin. After the injury, clinical methods are used to regenerate the skin tissue. In clinical methods, tissue transplantation is performed from the person, the same genus or another genus, and applied to the damaged area but this method has many disadvantages. Skin transplantation applications take a very long time and late healing occurs in the wound area. Also, there is a risk of transport of some diseases such as AIDS and Hepatitis B and C in consequence of skin transplantation (Ramos-e-Silva and Ribeiro de Castro 2002; Zhong et al. 2010). Therefore, recently, biomaterials have been used for wound healing.

Wound dressings are made of synthetic and natural polymers. In recent years, natural polymers are more preferred than synthetic polymers. Hence, natural polymers play a positive role in cell binding and binding has the ability to support wound healing. Chitosan, which is a natural polymer, is a biocompatible, biodegradable and having an antimicrobial effect. Moreover, it promotes granulation tissue formation in wound healing and helps blood clotting (Dai et al. 2011). Chitosan is an easily processable polymer in different forms such as hydrogel, sponge, film, and fiber. Chitosan membranes have been tested in animal model and humans. It was found that the membranes supported healing in the wound area (Azad et al. 2004). In addition to its advantages in wound healing, chitosan has low stability problems. In order to overcome this problem, generally polyelectrolyte complex is formed with polymers such as alginate, gelatin or a crosslinker is used (e.g., glutaraldehyde, genipin). In other respects, composite materials can be formed using nanofiller (e.g., silica, clay, polyhedral oligomeric silsesquioxane) to increase the stability of wound dressings and accelerate the wound healing (Lai et al. 2012; Mane et al. 2015; Park et al. 2018)

In addition, herbal extract loaded wound dressings have gained more attention due to wound healing effect. *Cissus quadrangularis* (CQ) is a herbal extract which has antibacterial and anti-inflammatory effects (Jabamalai 2014). Also, CQ provides support in wound healing due to its content such as quercetin, ascorbic acid, Vitamin C and

phenols (Mohanty et al. 2010). Recently, it is reported as one of the bioactive agents that supports wound healing (Matadeen et al. 2014). An ideal wound dressing should have biocompatibility as well as suitable mechanical properties and elasticity. It should also protect the wound from bacteria (Mutlu 2014; Dhivya et al. 2015). There are many types of wound dressings in different structure such as semi-permeable film, foam, hydrocolloid, hydrogel, and nanofiber forms. In recent years, the bilayer wound dressings are highly preferred in literature because of their ability to mimic the extracellular matrix structure (Deepthi et al. 2015).

The aim of this study, is therefore to design a bioactive containing bilayer wound dressing that can mimic skin structure and to investigate bioactive extract (CQ) release and to characterize the bilayer wound dressing. In accordance with this purpose, firstly extract loaded nanofibers were optimized for the uniform morphology and distribution. After the appropriate parameters were found, CQ loaded nanofibers were coated on the composite sponges by electrospinning method and bilayer wound dressings were obtained. The encapsulation efficiency of the nanofibers, and *in vitro* release behavior of the extract were determined. The antimicrobial activity of the extract loaded nanofiber coated sponges was investigated. FT-IR analysis was used to determine the interaction between extract-chitosan and chitosan/POSS composite. The porosity, swelling percentages and water vapor permeability of wound dressings were investigated. The cytotoxicity of bilayer sponges was determined using the 3T3 fibroblast cell line.

The progress of the thesis, Chapter 1 includes the literature review about skin structure, wound healing and the aim of the study. Literature review about wound dressing materials is given in Chapter 2. Production and characterization of nanofiber and composite sponges are explained in Chapter 3. The results of the study are given and discussed in Chapter 4. Chapter 5 consists of the conclusion and future plans.

CHAPTER 2

LITERATURE REVIEW

2.1. Skin and Skin Structure

Skin is the largest organ that covers the whole body. It forms an average of 15-16% of body weight. The skin is an active organ which senses sensations such as pain and touch, balances body temperature and prevents excessive water loss. It is composed of three layers known as epidermis, dermis, and hypodermis as shown in Figure 2.1. (Kolarsick et al. 2011; Kanitakis 2002).
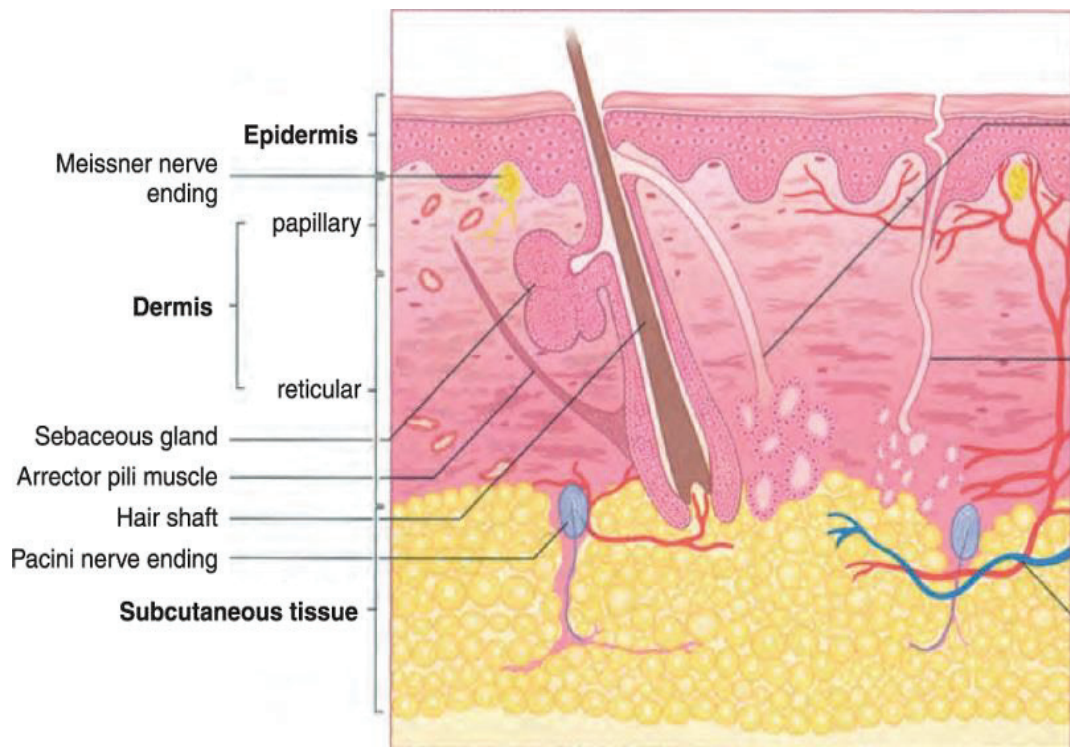
Figure 2. 1. Structure of the Skin (Source: Kolarsick et al. 2011)

2.1.1. Epidermis

Epidermis is the outer layer of the skin and mostly consists of keratinocytes cells. Apart from keratinocytes, melanocytes, langerhans and merkel cells are other components of epidermis. The epidermis does not contain vascular structures, and consists of 4 layers which are stratum basale, stratum spinosum, stratum granulose and stratum corneum.

These layers vary according to the body region due to the difference of keratin maturation. The thickness of the epidermis is 0.05 mm in the eyelids as the thinnest layer and 0.8 ± 1.5 mm in the soles and the palms.

The bottom layer is defined as stratum basale. It locates directly above the dermis. This layer consists of single-row basal cells, merkel cells (cells that transmit the sensation to the nerves) and melanocytes. Stratum spinosum layer comprise of keratinocytes. On the other hand, langerhans cells (immune system cells) locates in stratum spinosum layer. Stratum granulosum layer is composed of keratinocytes that generates large amounts of the proteins (keratin & keratohyalin) and accumulates as lamellar layer. It is also known as transition layer in skin tissue. Stratum corneum layer protects the skin from external factors. The cells in the stratum corneum layer are not alive. However, they are biochemically active. (Kolarsick et al. 2011)

2.1.2. Dermis

Dermis is the second layer of the skin tissue, and composed of fibroblast cells. Blood vessels which are responsible for blood stream, transport nutrient and oxygen and lymphatic structures for acquired immune system, are also located in dermis. Collagen and elastin are fibrous support proteins of dermis which give tension and elasticity to the skin, respectively. Furthermore, the dermis consists of two different regions as papillary and reticular layers. The papillary is thin layer whereas, the reticular is thick layer in dermis. Collagen fibers in the papillary layer are thin and loose. It is also perpendicular to the skin surface. Papillary layer forms the upper layer of the dermis. In the reticular layer, the collagen fibers are thicker and parallel to the skin. Reticular layer is transit area to the hypodermis (Kolarsick et al. 2011)

2.1.3. Hypodermis (Subcutaneous tissue)

Hypodermis is the lowest layer of the skin. It consists of fatty, connective tissue, nervous cells and blood vessels. Thickness of hypodermis varies according to the regions in body and nutrition. Hypodermis protects the body from temperature changes and provides the skin to be moving.

2.2. Wound and Wound Types

Wound is a deterioration of the integrity and function of tissues or organs by the reason of various factors. Wounds are generally divided into two groups according to their structures as acute and chronic wounds.

2.2.1. Acute Wound

Acute wound is sudden damage on the skin. There are different types of acute wounds as traumatic, surgical and burn disease. This type of wounds heal in the expected time (Ramasastry 2005). In order to treat the acute wound, the immune cells first migrate to the wound site and cleans the pathogens, and the wound healing process begins. Cell migration from the epidermal edges in the wound area. Furthermore, fibroblasts proliferate to form granulation tissue at the wound site. New blood vessels are formed by angiogenesis in the wound area. The wound area is coated with nerves that positively affects wound healing. (Martin and Nunan 2015).

2.2.2. Chronic Wound

Chronic wound is a class of wounds that does not heal over 3 months. Venous wounds, diabetic wounds and pressure sore are the major types of chronic wounds. These types of wounds slowly heal or do not heal in some cases. Besides, these kind of wounds often repeat (Izadi&Ganchi 2005;Wolcott et al. 2010).

2.3. Wound Healing

Wound healing begins with traumatic events and tissue integrity is ensured with new cell formation. The wound healing process is composed of a chain of biochemical events. This process consists of 3 intertwined stages as hemostatis and inflammation, proliferation, remodeling and maturation.

2.3.1. Hemostasis and inflammation

In a skin injury, bleeding immediately occurs due to the destruction of blood vessel integrity. Hemostasis is the first stage of wound healing. The first aim of this stage is to stop blood loss. (Singer and Clark 1999). Right after the injury, blood platelets come together to secrete growth factors and after that, healing process begins. Various precursor factors (fibrinogen, thrombospodia, etc.) that stimulate coagulation are released from injured cells for the onset of coagulation. The maintenance of the healing process directly depends on the hemostasis. Inflammation, neutrophils and lymphocytes are predominant cells. The inflammation phase is observed in last 3-5 days in normal conditions. Furthermore, hemostatis is the fundamental stage to make the wound ready for repairing process by preventing inflammation and providing blood platelet coagulation (Velnar et al. 2009).

2.3.2. Proliferation

Proliferation begins in the third day after injury and lasts for 2-3 weeks. Proliferation phase is characterized by new vessel formation (angiogenesis) and proliferation of epithelial cells (epithelialization). In this stage, first microcirculation is arranged to meet the oxygen demand of newly formed tissues. At the same time, rapidly and large of amount collagen is synthesized from fibroblasts in the wound area. Thus, growth factor excreting fibroblasts contribute to the process of wound healing. Afterwards, the basal layer around the wound disintegrates, causing endothelial cells forming the tissue to move into the wound to form budding. The buds come together to form a capillary network after branching. At the end of the proliferation stage, tissue formation of granules occurs (Velnar et al. 2009; Öztopalan et al. 2017).

2.3.3. Remodeling and Maturation

The final stage of wound healing is maturation and epithelial tissue formation is observed in this stage. The range of this phase changes from 21th day to 2 years after injury [Witte et al. 1997]. The maturation period varies depending on age, genetic structure and the type of wound. Produced collagen in proliferation stage increasingly

gets strength in maturation stage. Collagen fibrils are crosslinked to form a more regular form. By this way, tension strength of the scar tissue increases with time. The density of capillaries and the number of fibroblasts decrease during wound healing occurs. In the wound area, blood flow and metabolic activity reduce since the capillary vascular growth stops. Over the time, capillary vascular growth stops, blood flow and metabolic activity slows down (Baum and Arpey 2005). When the all stages are completed, strong and resistant scar tissue is formed.

2.4. Wound Dressings For Skin Regeneration

Wound dressing is a medicinal product that is used to protect the wound area from the germs and infections as well as supporting wound healing. The main purpose of a wound dressing is to provide the optimum conditions for wound healing at the defect site. There are some key factors to design an ideal wound dressing (Mutlu 2014; Dhivya et al. 2015):

Biocompatibility and biodegradability: The wound dressing should not show toxic or allergic reactions in the defect area. When applied to the wound dressing on the wound structure should not be disturbed and should not cause unwanted reactions. In the wound region should ensure the proliferation of cells proliferation. It should provide required mechanical properties for tissue.

Microbial control and physical barrier: The wound cover should act as a barrier against any microbial and bacterial infections from the external environment. It should prevent liquid build-up and allow water-vapor permeability to allow the injured area to breathe. Water vapor permeability for healthy skin is 204 g/m^2day, depending on the type of wound in a wounded skin it varies between 279 to 5138 g/m^2day (Patel et al. 2018).

Fluid control: The wound cover should provide required humidity at the defect site. Body fluid should not leak through the bandages to prevent bacterial growth.

Low stickiness: The dressing material should not adhere to the wound surface and not cause trauma during removal. Therefore material should not lose its integrity during wound healing process.

Elasticity: Wound dressing should be able to maintain elasticity even in dry state to provide integrity.

The application of appropriate treatment to the wound is the most significant point of the wound healing process. In this point of view, the contribution of the wound dressing to wound healing process is crucial. Many traditional methods have been applied for wound covering studies for centuries. In the past, honey, resin, vegetable and animal origin materials and oils were used and today these treatments continue with the use of wound dressings. In B.C. 460-370, wounds were cleaned with water and wine before the invention of wound dressings. Later, wool was used to cover the wound by boiling it in water and wine. In the treatment of wounds and burns, castor oil was also used to treat the defect area (Daunton et al. 2012). In addition, gauze was used as a wound dressing in 1800s. The transition to modern dressings has been observed in the 20th century. Ancient Egyptian expert Edwen Smith believed that the wounds would heal faster if kept dry and exposed. In 1948, the humid room was used to heal the ulcer. Modern dressings have been started to be used in materials that provide moist environment in early 1980s (Dhivya et al. 2015).

2.4.1. Skin Transplantation

Tissue transplantation is performed using autograft, allograft, xeonograft or alloplastic (biomaterials) materials. Autografts are the tissue that is taken from the person himself and transferred to the damaged area. Even though, this method has many advantages such as easier integration and adaptation, it has disadvantages like obtaining a limited amount and performing the more complex operation. Allografts are the transfer of tissue between different persons of the same genera. Xenografts are tissue transfer between different genera. Allografts and xenografts have also been used for tissue deficiency problems. These type of transplantations provide their own environment to the wound which have significant disadvantages. Since allografts are obtained from living organisms, there is a great risk of transportation of several diseases such as AIDS, hepatitis B and C. Therefore, recently there has been a tendency towards biomaterial applications for wound healing treatment. In recent years, the wound dressings have been made of synthetic and natural polymers which are widely used according to the type of wound. These type of materials can easily be applied to the wound area (Ramos-e-Silva and Ribeiro de Castro 2002; Zhong et al. 2010).

2.4.2. Traditional Wound Dressings

Traditional wound dressings are made from natural, synthetic or semi-synthetic materials which are in dry form. The main goal of these dressings is to protect the wound from external factors and to absorb the liquid on the wound. Conventional dressings are generally made of cellulose, cotton fibers and polyamide. They have several advantages such as high absorption capacity and thermal insulation. However, the major drawback of these wound dressings is that they cannot provide a moist environment on the wound. It is not protective against bacterial contamination. In addition, fibrous structures are more likely to break up. For these reasons, modern wound dressings have been started to be designed (Boateng et al. 2008; Dhivya et al. 2015).

2.4.3. Modern Wound Dressings

Modern dressings have been developed to cover the wound, keep the wound area moist and promote healing. Modern dressings can be grouped in three classes: passive, active and bioactive dressing (Paul and Sharma 2004). Passive dressings can only cover the wound and protect the wound from external factors. There is no significant effect of passive type dressings to the healing process. Unlike, passive dressings, interactive products which has a certain moisture permeability, are more effective in wound healing. Example of interactive dressings that are semi-permeable films, hydrogels, alginate dressing and foams. Bioactive products play an active role in wound healing by releasing bioactive substances into the wound area (Degreef 1998; Strecker et al. 2007).

2.4.4. Semi Permeable Film Dressings

Semi permeable films are generally fabricated by solvent casting method. One side of these dressings consists of acrylic adhesive and the other side is made up of polyurethane films. Synthetic adhesive films have elastic and flexible structure. Therefore, they do not restrict patient movement. Besides, these type of dressings also prevent the passage of bacteria into the wound (Moshakis et al. 1984). Semi-permeable films are watertight biomaterials, but they allow to passage of the water vapor with

oxygen and carbon dioxide. These type of wound dressings do not have a liquid absorption feature. Therefore, they could cause fluid accumulation in the wound area. These wound dressings are suitable for covering narrow areas with superficial and less fluid accumulation since healthy skin is needed for the adhesion of the wound dressing to the skin (Seaman 2002).

2.4.5. Semi Permeable Foams

Generally, gas foaming technique and freeze drying method are used for the production of foams used in skin regeneration. These foams have a flexible, porous structure which allows the of water vapor transition (Ramos-e-Silva and Ribeiro de Castro 2002a). These dressings are mostly fabricated from polyurethane and silicon. Polyurethanes are synthesized from both hydrophilic and hydrophobic monomers. Thus, these foams can be produced with different ranges of porosity. Hence, these materials allow the passage of water vapor due to their porous structure. The outward facing side of the wound cover prevents the passage of liquid with its hydrophobic property. Foam dressings are capable of absorbing different liquids depending on the depth of the wound and can be easily applied and removed from the wound site. When they were placed on the wound, they easily adapt to the wound due to their swelling capacity and accelerates granulation formation. Foams are used in mid-wound exudates and leg ulcers. Unfortunately, they are not suitable for low exudate wounds and dry wounds (Boateng et al. 2008)**.**

2.4.6. Hydrocolloid Dressings

Hydrocolloid dressings are wound care products that are formed by gelatinizing agents such as cellulose, gelatin and pectin together with elastomer and adhesive products (Boateng et al. 2008). Hydrocolloid dressings are easy to use materials. The inner part of these covers is composed of liquid impervious to the outer part of the hydrocolloid. When the wound dressing is in contact with the wound, the hydrocolloid part absorbs the liquid in the wound and becomes a gel and wound is covered with a moist layer. Thus, no secondary cover is needed. The advantages of these covers are that they provide a moist

environment and gas permeability to the wound area. Hydrocolloid dressings can be used in mild to moderate exudative wounds, pressure sores and traumatic wounds. The main disadvantage of these dressings is not suitable for high exudate and infectious wounds (Stashak et al. 2004).

2.4.7. Hydrogels Dressings

Hydrogels are generally produced by freeze drying method and particulate-leaching method. These are three-dimensional structures of hydrophilic polymers. Hydrogels are easy to use and do not damage the wound when removed from the wound. These dressings provide a moist environment at the wound area. The barrier property of these materials to the bacteria is poor. Therefore, secondary covering is needed to provide antimicrobial barrier (Hanna and Giacopelli 1997). They can be used in dry and burn wounds. Hydrogel dressings can be used for any stages of wound healing, except for infectious and severe wounds (Dhivya et al. 2015).

2.4.8. Nanofiber Dressings

Nanofibers which have three-dimensional (3D) structure can also be used as wound dressings. They are fabricated by electrospinning method. The electrospinning system consists of power supply, syringe, syringe pump and metal collector and shown in Figure 2.2. The polymer solution is loaded into the syringe and placed in the syringe pump. The syringe pump is set to the desired flow and subject to an electric field which causes the elongation of the droplets. The polymer solution is loaded electrically in the form of a jet and moves towards the collector. Taylor's cone is formed at tip of the droplet, before the electrical compressive force overcome the surface tension. When the electric field is further increased, the polymer solution cannot resist electrostatic forces. It is moved to the collector in the form of a jet cone. Solvent evaporates, nanofibers accumulate randomly in the collector (Kurečič and Smole 2016; Bhardwaj and Kundu 2010).
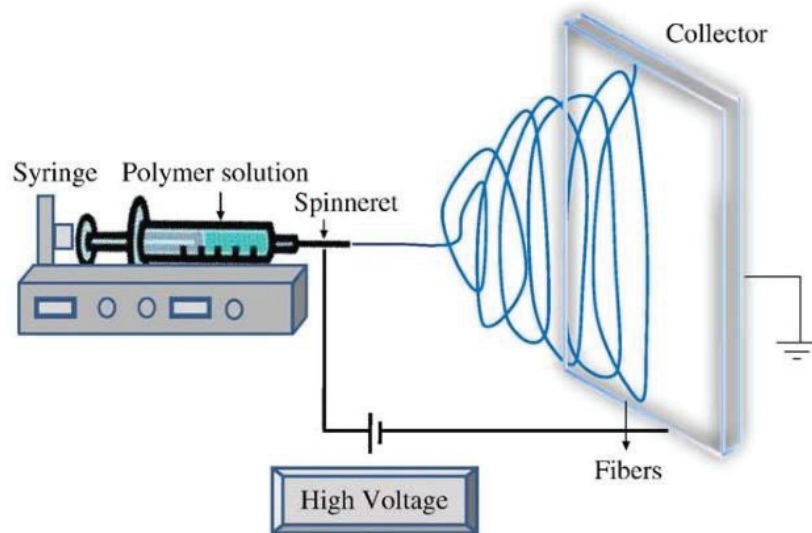
Figure 2. 2. Electrospinning System (Source:Bhardwaj and Kundu 2010)

Wound dressings which are produced by electrospinning method have many advantages over wound dressings produced by traditional methods. Nanofibers fabricated with electrospinning show random arranged nanostructure and mimic the extracellular matrix (ECM) which is a complex structure between the cells in cartilage, bone and skin tissue. ECM supports cells and provide tissue integrity. The main component is collagen with a fibrous structure. ECM acts as a support and tissue scaffold between cells in wound healing and provides the necessary conditions from cell attachment to differentiation. The collagen in the ECM secrete growth and angiogenic factors for tissue repair. In addition, nanofibers act as a barrier against bacteria and are also permeable to oxygen due to their microporous structure. It has a flexible structure and easy to apply on the wound. (Chen et al 2008; Gholipour et al 2010; Mogoşanu and Grumezescu 2014)

2.4.9. Commercial Skin Substitutes for Skin Regeneration

In skin transplantation procedures, skin grafts that consist of epidermis and dermis layers of the skin are used as wound dressing materials. Therefore, commercial skin graft designs have focused on mimicking this multilayered structure of skin. These grafts are used in burns and chronic wounds in diabetic foot ulcers. Commercial skin grafts including products like Biobrane ™, Integra ™, Suprathel™, Dermagraft-TC etc.

Biobrane ™ are comprised of two-layer, outer part are composed of silicone, and inner part is covered with a type-1 collagen that is similar to the dermis. Integra ™ consists of two layers. Outer layer is composed of silicon and inner part is composed of chondroitin-6-sulphate and bovine collagen. This cover serves as a dermis in the wound. Suprathel™ is a synthetic dressing with DL-Lactid, trimethylencarbonate and e-caprolacton. Dermagraft-TC outer part is made of synthetic material. This wound dressing is composed of swine dermal collagen and contains biologically active growth factors. However, they have some limitations such as low water absorption capacity, low flexibility and high price fags. (Dhivya et al 2015; Altan and Oğurtan 2016; Kimna et al 2018)

2.5. Biopolymer Based Wound Dressings for Skin Regeneration

In recent years, synthetic and natural polymers have been used in skin regeneration due to their biocompatibility and regenerative properties. Some of the synthetic polymers used in wound healing are poly(glycolic acid), poly(caprolactone), poly(ethylene glycol), poly-1-lactide and poly(lactide-co-glycolide). These polymers accelerate epithelization in wound healing. The wound dressings based on synthetic polymers are generally produced by electrospinning method (Khang et al. 2010; Supaphol et al. 2011; Goh et al 2013). Although the synthetic polymers can be easily electrospun, they have some disadvantages compared to natural polymers. Cell attachment and proliferation ability of synthetic polymers is lower than natural polymers (Mohiti et al. 2016). Predominantly, biopolymers show biocompatible and biodegradable characteristics. In literature, natural polymers used in wound healing applications are mostly alginate, pectin, cellulose, collagen, gelatin, keratin, silk fibrin and chitosan. These polymers are preferred as wound dressings due to their similarity with extracellular matrix (ECM) in skin tissue. This structural similarity induces and stimulates cells around the wound area (Mogoşanu and Grumezescu 2014). In addition, natural polymers are non-toxic and biodegradable. Thus, they can be preferred as wound dressings for long treatment periods without any side effects.

Natural polymers show significant bioactivity in wound healing by taking an active role in the formation of new tissue in the damaged area, increasing cell migration and inducing cell proliferation and granulation formation. Additionally, when the natural

polymers are loaded with bioactive agents such as antioxidants, growth factors or herbal extracts, they show superior properties in tissue regeneration (Altiok et al. 2010; Dhurai et al. 2013; Mohandas et al. 2015; Güneş and Tıhmınlıoğlu 2017).

2.6. Natural Polymers for Wound Healing Applications

Alginate, cellulose, collagen, gelatin, silk fibrin and chitosan are commonly used for wound healing applications.

2.6.1. Alginate

Alginate is a biodegradable polymer and obtained from brown seaweeds. It has high liquid absorption capability. Therefore, wound dressings from alginate form a hydrophilic gel when in contact with the wound. It should be replaced after taking enough liquid on the wound. If wound dressing is not changed after filling with liquid, it can damage the healthy tissue around the wound. Moist environment is required for the performance of alginate dressings. Therefore, it should not be used in dry wounds while used in medium and heavy drainage wounds (Boateng et al. 2008). In literature, there are numerous alginate based wound dressing studies. Various alginate dressings have been produced showing antimicrobial effect and accelerating wound healing. Mohandas et al. (2015) prepared nano-zinc oxide loaded composite bandages having 60-70% porosity by freeze drying method. These wound dressings showed antimicrobial activity against *Escherichia coli*, *Staphylococcus aureus*, *Candida albicans*, and methicillin resistant *S. aureus* (MRSA) bacteria. Wound dressings have been observed to be effective in wound healing for infected wounds (Mohandas et al. 2015). In another study, alginate based double layer hydrocolloid film was fabricated. The hydrocolloid film consisted of drug (ibuprofen) loaded upper layer and a speed controlling sublayer to slow drug release. Controlled release was obtained with bilayer films. At the same time, bilayer films showed better mechanical properties compared to single layer films. Drug-loaded films also accelerated the formation of granulation in tissue (Thu et al. 2012).

2.6.2. Cellulose

Cellulose is a polysaccharide based, biocompatible, biodegradable and hydrophilic biopolymer. It provides support for granulation and epithelization. Also, Biosynthetic bacterial cellulose from *Acetobacter xylinum* is also used in regenerative medicine. This polymer supports the healing process by reducing pain. Non-toxic microbial cellulose dressings with antimicrobial action can be applied to burn wounds (Muangman et al. 2011; Park et al. 2014). Since bacterial cellulose fibers accelerate new tissue formation due to their similarity to ECM (Bhattarai et al. 2005). Islam et al. (2013) have fabricated bacterial cellulose- montmorillonite composite films for wound healing applications. Cellulose- MMT composite films showed antimicrobial properties against *E. coli* and *S. aureus* (Islam et al. 2013). In another study, the release and antimicrobial activities of cellulose hydrogels loaded with chloramphenicol (active agent) were investigated. Almost all chloramphenicol was released from the hydrogel in 24 hours. Hydrogels with active showed antimicrobial activity agent loaded against *S. pneumonia, S. aureus* and *E. coli* bacteria (Laçin 2014).

2.6.3. Collagen

Collagen is a protein found in human body and it is biocompatible, biodegradable and non-toxic. The collagen produced by fibroblasts have been effectively used in makes great contributions to wound healing and new tissue development (Mogoşanu and Grumezescu 2014). It provides support in all phases of wound healing. There are many studies about collagen based wound dressings for skin tissue regeneration. In the literature, mostly nanofibers and vascular graft forms of collagen were developed for wound healing (Fullana and Wnek 2012). It was observed that collagen wound dressings supported the accumulation of collagen fibrils in the wound area (Aravinthan et al. 2018). The epidermal growth factor-containing sponges were investigated *in vitro* and in vivo and shown to be effective in wound healing (Kondo and Kuroyanagi 2012). In another study, collagen and a-tocopherol which is an antioxidant used in skin diseases were prepared for topical applications and this collagen-derived biomaterial was found suitable for biomedical applications.

2.6.4. Gelatin

Gelatin is a natural polymer produced from collagen derivatives of animal origin. It is a preferred polymer in drug delivery systems and wound healing. However, it is generally used with another polymer as gel form due to its low mechanical properties and thermal stability (Mogoşanu and Grumezescu 2014). Boateng et al. fabricated and characterized silver sulfadiazine-loaded alginate/gelatin composite wafers for infectious chronic wounds. Drug release from composites was observed for 7 hours to prevent bacterial infection (Boateng et al. 2008). In another study, effect of blending of different mass ratios of chitosan, honey and gelatin on the properties of the film was studied for burn wound dressing applications. Antimicrobial activity and rabbit's back burn model were examined. The film at optimum composition showed antimicrobial activity against *S. aureus* and *E. coli*. Films were examined for 12 days in wound model and positive results were obtained in wound closure (Wang et al. 2012).

2.6.5. Silk Fibroin

Silk fibroin is a natural polymer used in vascular grafts, drug delivery systems and wound dressings due to its biocompatibility, biodegradability, good mechanical properties and ease of use. Silk fibroin can be processed in different forms such as film, micro-nano particle, fiber or hydrogel thanks to its easy processability (Qi et al. 2017). Lee and his co-workers prepared hydrocolloid films containing silk fibroin nanoparticle for burn wounds. Structural, mechanical properties and cell compatibility tests were performed and the dressings was investigated in rabbit model. Hydrocolloid films containing silk fibroin showed good mechanical properties and accelerated wound healing (Lee et al. 2016). In another study, silver nanoparticle coated silk fibroin fibers were fabricated as wound dressings. It was shown that fibers exhibited antimicrobial activity against *S. aureus* and *P. aeruginosa* bacteria (Uttayarat et al. 2012). In another study, silk fibroin/alginate composite membranes were tested for wound healing applications. Structural and mechanical properties, water vapor transmission rate and toxicity of membranes were investigated. As the amount of silk fibroin increased, higher

mechanical strength was observed. Composite membranes were shown to be non-toxic with good swelling capacity and water transmission rate (Moraes and Beppu 2013).

2.6.6. Chitosan

Chitosan is one of the most abundant polymers in nature. Chitin is found abundantly in shells of shellfish, and also in the cell walls of yeast and fungus. The use of chitin is limited due to its low solubility. Therefore, chitosan is obtained from chitin as its deacetylated derivative (Figure 2.3). Chitosan is dissolved in dilute acidic solutions and used in different application areas (Dai et al. 2011). It is biodegradable, biocompatible, non-toxic, hydrophilic and antimicrobial activity. Because of these properties, chitosan is generally preferred in biomedical applications. Chitosan as well, has some limitations such as low stability and mechanical properties. Chitosan can form polyelectrolyte complexes with anionic alginate, gelatin, carboxymethyl cellulose to increase the stability and enhance mechanical properties. In the literature, chitosan/ alginate nanospheres and silver sulfadiazine complexes were fabricated to obtain stable biomaterials with better mechanical properties (Meng et al. 2010; Fan et al. 2016).
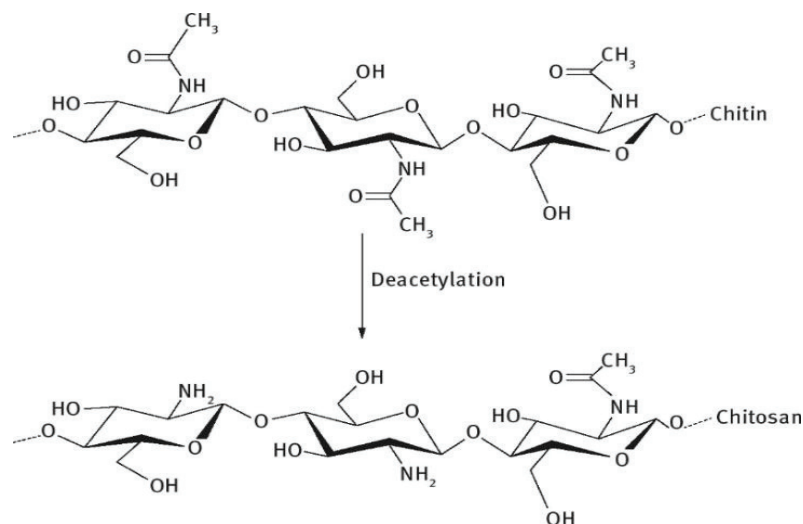
Figure 2. 3. Deacetylation of chitin to chitosan (Source:Berezina 2016)

Crosslinkers are also used with chitosan matrix to enhance its stability. Generally, glutaraldehyde, tripolyphosphate (TPP) and genipin have been used as crosslinkers.

Glutaraldehyde which is highly reactive, may interact with cell surface and cause toxic effects result in cell death (Lai et al 2012). TPP is an ionic cross-linker known as a physical cross-linker. Chemical crosslinkers are more potent binders than physical crosslinkers. The chemical crosslinking is irreversible but physical crosslinking is reversed by change in temperature or pH (Mane et al. 2015). Thus, in recent years, genipin as being a natural compound with no toxic effect, has been preferred as a crosslinker for biomedical applications. In literature, it was found that genipin cross-linked nanofibers exhibited better swelling and enzymatic degradation behavior compared to non-cross-linked nanofibers. It was also observed that L929 fibroblast cells incubated on genipin cross-linked nanofibers showed favorable attachment and growth (Li et al. 2015). Another way to increase mechanical properties and stability of polymer matrix is to use nanoparticles in polymer matrix to obtain composite structures. These nanoparticles can be carbon based particles, silica based hydrophilic nanoclays or synthetic hybrid nanoparticles such as polyhedral oligomeric silsesquioxanes (POSS) (Li et al. 2012; Malesu et al. 2019). Polymer composite materials with enhanced mechanical, thermal and physicochemical properties can be obtained by dispersing these nanoscale materials in polymer matrix homogenously.

Additionally, chitosan has a cationic structure. Hence, a biomaterial obtained from chitosan can easily interact with the negatively charged moieties present in the cell membrane (Kumari et al. 2010). The anionic parts of the cell membrane and the cationic parts of the chitosan interact to prevent the formation of any bacteria. N-acetyl-β-D-glucosamine units of chitosan released by degradation induces wound healing (Pillai et al. 2009). Chitosan helps blood clotting and chitosan bandages have been approved by the US for use in wound healing (Dai et al. 2011). It also supports the granulation in wound area.

2.7. Chitosan Based Wound Dressing Material

There are many studies related to the chitosan based wound dressing materials in different forms such as film, fiber or sponge (Table 2.1.) Also, there are numerous biomaterial studies with chitosan-induced antimicrobial activity, including bioactive, antibiotics, vitamins or growth factors to support wound healing.

Table 2. 1. Chitosan based wound dressing

Form	Purpose	References
Fiber	Wound dressing	(Zhou et al. 2013)
Film	Wound healing	(Díez and Díez 2015)
Sponges	Full-thickness wound healing and extract release	(Dai et al. 2009)
Membrane	Wound dressing material	(Silva et al. 2013)
Scaffold	Treatment of chronic skin ulcer, wound dressing material	(Mori et al. 2016)

2.7.1. Chitosan Film Wound Dressings

The wound dressings in the form of film allow the passage of water vapor and protecting the wound from bacteria. These dressings are suitable for more superficial wounds and low exudate wounds. In a study, ZnO nanoparticles modified and castor oil loaded chitosan films were prepared by the solvent casting method. Porosity, water absorption, and water vapor permeability of chitosan films were increased after modification with ZnO nanoparticles. Non-toxic films showed antimicrobial activity against gram negative and gram positive bacteria. The castor oil/chitosan-ZnO films tested on the rat model healed the wound faster than commercial products (Diez and Diez 2015). Ma et al prepared tetracycline hydrochloride and silver sulfadiazine loaded chitosan membranes using the solvent casting technique. Water vapor transmission rate, antimicrobial activity, and drug release behavior of the films were examined. Water vapor transmission rates of the films were found between 1240 to 2036 g / m^{2}day. This range is suitable for wound dressing materials. Percent release of antimicrobial drugs was determined as 52% and 75% cumulative release in the first 6 hours of silver sulfadiazine, tetracycline hydrochloride, respectively. Chitosan membranes showed antimicrobial activity against *E. coli* and *S. aureus* bacteria (Ma et al. 2017). In another study, Altıok et al. produced chitosan films containing thyme oil as a wound dressing material. The water transmission rate of control group chitosan and thyme oil loaded chitosan films was found between 200 g / m^{2}day and 300 g / m^{2}day. Films had antioxidant activity and they were showed antimicrobial activity against gram negative and positive bacteria (Altiok et al. 2010). In addition, chitosan films containing *hypericum perforatum* oil as wound dressing

material were prepared by the solvent casting method. The water vapor transmission rate of the films was found between 292.4 g / m^{2}day and 429.2 g / m^{2}day. Oil containing films showed antimicrobial activity against E.coli and S. aureus bacteria. Furthermore, the films showed no toxic effect against 3T3 fibroblast cells, promoted cell adhesion and proliferation (Güneş and Tıhmınlıoğlu 2017).

2.7.2. Chitosan Hydrogel Wound Dressings

Hydrogels are 3D structures of hydrophilic polymers. Hydrogel dressings have been used for any stages of wound healing, except for severe wounds. Secondary dressing is needed to provide antimicrobial barrier. In one study, zinc oxide nanoparticles were incorporated in chitosan hydrogels to impart an antimicrobial activity and hydrogels did not show toxic effects. It was tested in vivo on the rat model and shown to accelerate wound healing by increasing the collagen deposition of hydrogels. It was concluded that hydrogels could be preferred diabetic foot ulcers, chronic and burned wounds (Kumar et al. 2012). β-Chitin hydrogel / nano zinc oxide composite bandages were developed with freeze drying method. This biomaterial had antimicrobial activity against *S. aureus* and *E. coli* are also it has blood clotting ability, it was concluded that the bandage had a toxic effect and the collagen deposition was supported (Sudheesh Kumar et al. 2013). In another study, Obora et al. produced fibroblast growth factor-containing chitosan hydrogels. They were applied to healing-impaired diabetic (db/db) mice. Growth factor-containing chitosan hydrogels were showed 60% healing in the wound on the second day. (Obara et al. 2003). In another study, hydrogels containing chitosan, gelatin and honey, were prepared for burn wounds. These non-toxic hydrogels were showed antimicrobial activity against S. aureus and E.coli bacteria. The hydrogels were tested in the rat model in vivo and supported to wound healing (Wang et al. 2012). Xyloglucan (isolated materials from chia seed gum) containing chitosan hydrogels were produced as wound dressing by freeze-drying method. The addition of xyloglucan improved the mechanical properties of chitosan hydrogels and they were showed antimicrobial activity against S. aureus bacteria (Martínez-Ibarra et al. 2018). Ciprofloxacin loaded chitosan hydrogels were produced for use as wound dressing material. Ciprofloxacin release from hydrogels was examined. The drug was reached 70-80% cumulative release in 48 hours. In addition,

drug-loaded hydrogels which exhibited no toxic effects but showed antimicrobial activity against E. coli (Radhakumary et al. 2011).

2.7.3. Chitosan Sponge Wound Dressings

Sponges, which are the modern dressings, protect the wound from the bacteria, provide an appropriate healing environment and support healing. Sponges are used in exudative wounds because they have high swelling percentages (Boateng et al. 2008). In the literature, chitosan sponges crosslinked with carboxymethyl conjugate glucomannan were produced as wound dressings. These sponges had a suitable swelling ratio and water vapor permeability that could accelerate tissue regeneration. In addition, sponges were evaluated in vivo on the mouse and shown to accelerated wound healing (Xie et al. 2018). As a model drug fluorescein sodium loaded chitosan/polyethylene glycol sponges were produced with a 3D approach. Drug release from 3D sponges reached 70% in 5 hours. Human fibroblast cells on sponges have exhibited high cell viability (90%) at 48 hours. Therefore, these sponges can be considered as potential wound dressings for use in chronic wounds (Hafezi et al. 2019). In another study, chitin/ nano silver sponges were developed as wound dressings. The sponges showed antimicrobial activity against *S. aureus* and *E. coli* bacteria and blood clotting activity but they did not show toxic effects against L929 mouse cells (Madhumathi et al. 2010). Anisha et al. produced chitosan-hyaluronic acid sponges containing nano silver for diabetic foot ulcers against bacterial infection. They showed antimicrobial activity against gram negative and gram positive bacteria. Furthermore, cytotoxicity was tested using human dermal fibroblast cells. The sponges showed increased toxic effect with increasing concentration of nano silver. Cell attachment of sponges was examined, and found that cell attachment decreased with increasing nano silver concentration (Anisha et al. 2013).

2.7.4. Chitosan Fiber Wound Dressings

Nanofibers produced by electrospinning methods mimic the structure of the ECM, which act as a support between cells in wound healing. It also provides as a barrier

property against bacteria and can be easily applied to the wound. In the study of Mohsena et al., chitin/chitosan-glucan complex based fibers were produced by wet-dry-spinning technique. Fibers showed antimicrobial activity against *Escherichia coli, Klebsiella pneumoniae, Basillus subtilis* and *Staphylococcus aureus* bacteria. In addition, cytotoxicity of the materials and in vivo tests against rats were performed. It was concluded that the wound dressings were not toxic and the fibers accelerated wound healing in in vivo tests on rats (Abdel-Mohsen et al. 2016). In another study, nanofibers originating from lysozyme-containing chitosan were produced. Lysozyme showed approximately 80% release within 4 hours and fast release lysozyme accelerated wound healing. In addition, Fibers and gauze were tested and compared on rat. It was observed that it showed faster wound healing than control. (Charernsriwilaiwat et al. 2012). Chitosan/polyvinyl alcohol/starch nanocomposite fibers were produced and characterized by electrospinning method. Nanofibers have 91% porosity and the water vapor permeability of nanofibers was found to be 2340-3318 g/m ^{2}day and was in the appropriate range for wound healing. Nanofibers did not show toxic effects against L929 cells and showed antimicrobial activity against gram negative and gram positive bacteria, which would help protect the wound from the bacteria during the wound healing process. Scratch assay was tested with L929 cells by using extract media. After 24 h, cell migration occurred in the wound gap area (Adeli et al. 2019).

2.7.5. Chitosan Bilayer Wound Dressings

Bilayer wound dressings contribute to wound healing because they mimic the epidermis and dermis layers of the skin. In one study, cotton fabric surfaces were coated with a mixture of chitosan, polyethylene glycol and polyvinyl pyrrolidone with antimicrobial activity containing and tetracycline hydrochloride antibiotic. Water vapor transmission rate (WVTR), drug release, and antimicrobial activity of the dressing were investigated. The WVTR was found within the appropriate range for the wound dressing and the drug was released in 48 hours. Antibiotic loaded dressings showed antimicrobial activity against *E. coli* and *S. aureus* bacteria. The dressings were also examined in rat model and promote healing of wound in 12 days. It was observed that chitosan accelerated wound healing (Anjum et al. 2016). In another study, genipin cross-linked chitosan bilayer dressings were produced. The lower layer is made up of chitosan film and the

upper layer is made of non-woven fabric consisting of soybean. The water vapor permeability of the dressings was approximately 2137 g/m^{2}day and showed good mechanical properties. These dressings tested on a rat model accelerated epithelization and were easily removed from the wound surface (Liu et al. 2008). In a study, polycaprolactone fibers for ligament regeneration were coated on chitosan-hyaluronic acid composite hydrogel to produce bilayer biomaterial. The tensile strength of the double layer structure was found between 0.93 ± 0.1MPa and 1.55 ± 0.67 MPa. Bilayer biomaterials did not show any toxic effect. (Deepthi et al. 2015).

2.8. The Role of Polyhedral Oligomeric Silsesquioxane (POSS) in Tissue Engineering

In recent years, the use of nanofillers and nanoparticles has increased in order to produce biomaterials with better mechanical and physical properties. Silica is one of the most studied nanofiller materials in biomedical applications. *Polyhedral Oligomeric Silsesquioxane (*POSS) is also known as silica nanoparticle, because silica is located in the core of the cage (Figure 2.4).The molecular formula of is $RSiO_{1.5}$, (R is organic functional groups such as hydrogen, alkyne or hydroxyl). POSS nanostructures can be in different molecular structures such as random, staircase, partial cage.
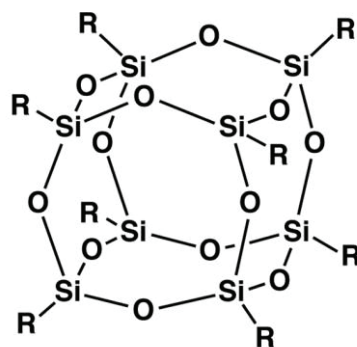
Figure 2. 4. Polyhedral Oligomeric Silsesquioxane (POSS) Structure

The organic R groups on the outer side of the POSS nanocage structure provide its structure compatibility with many polymers. The POSS nanoparticle dispersions in polymer matrix increase mechanical strength and toughness of the sample. Park et al. produced chitosan / silica hybrid sponges. They characterized these sponges in vivo and *in vitro* and also compared chitosan-silica hybrid sponges with 3 different commercial

dressing materials (gauze, polyurethane (PU), and silver - containing hydrophilic (HF - Ag). As a result of the in vivo experiments, the chitosan/silica hybrid sponges increased cell proliferation, and collagen synthesis at the early stage, thus improved wound healing. Commercial dressings played a passive role in wound healing and infection prevention in early stages (Park et al. 2017). In 2018, Park and his coworkers have developed chitosan/silica hybrid sponges and demonstrated the importance of silica in wound healing. These sponges were examined by opening full thickness wound in the pig model. It has been observed that sponges increase cell retention and proliferation at the wound site. These sponges were suggested as a potential artificial skin for humans. (Park et al. 2018).

2.9.   Bioactive Extract Loaded Chitosan Wound Dressings

Antibiotic or antimicrobial drugs, as well as some herbal extracts are known to accelerate wound healing. The use of herbal extracts in tissue engineering, as well as supporting the wound healing, has a positive effect on the wound healing process with antioxidant, anti-inflammatory and antimicrobial effect. Nguyen et al. prepared curcumin loaded chitosan / gelatin sponges by freeze drying method. Antimicrobial activity, extract release and extracts loaded with extracts examined in vivo showed antimicrobial activity against Pseudomonas aeruginosa, releasing about 90% extract in 96 hours. In an in vivo study, wound was opened on the back of the rabbit and wound healing was examined for 21 days on control sponge (without extract) and extract-loaded sponges. Extract loaded sponges accelerated wound healing at the end of 21 days (Nguyen, et al 2013). In another study, curcumin loaded chitosan/polylactic acid nanofibers were prepared and characterized by Dhurai et al. Extract release was carried out rapidly for 6 hours. Nanofibers showed no toxic effect when examined *in vitro*. In vivo tests on the rat model showed that nanofibers loaded with curcumin significantly accelerated wound healing (Dhurai et al. 2013). Charernsriwilaiwat et al. have produced garcinia mangostana extract loaded chitosan-ethylenediamine tetra acetic acid / polyvinyl alcohol composite nanofibers by electrospinning method. It was found that extract loaded composite fibers showed a rapid release at 8 hours, as well as antimicrobial activity against *S. aureus* and *E. coli*. The extract loaded composite fibers were examined by cytotoxicity analysis, Nanofibers did not show toxic effects (Charernsriwilaiwat et al. 2013). In another study,

Yousefi et al. produced chitosan nanofibers loaded with henna extract which showed antimicrobial activity and accelerated wound healing. The henna-containing nanofibers showed antimicrobial activity against *E. coli* and *S. aureus* bacteria. Normal human foreskin fibroblast cells were used in *in vitro* studies. Nanofibers loaded with henna extract support cell proliferation and proliferation (Yousefi et al. 2017).

2.10. *Cissus quadrangularis* as an Extract in Wound Dressing

Cissus quadrangularis is a medicinal plant grown in India, which belongs to the Vitaceae family. CQ is a traditional herb that is also used in Ayurveda as alternative drug therapy. CQ is known to be effective for many diseases. For example, it has been traditionally used in India for irregular menstruation, stomach disorders, bone fractures, skin infections, wound and burn treatments (Malik et al. 2012). There are many bioactive components in the content of CQ which are quercetin, vitamin C, calcium oxalate, carotene, sitosterol, ketosteroid, and ascorbic acid. CQ shows anti-inflammatory, anti-microbial, anti-bacterial and anti-fungal activity. CQ extract showed antimicrobial and antifungal activity against *escherichia coli*, *staphylococcus aureus*, *pseudomonas aeruginosa*, *proteus mirabilis*, *penicillium sp.*, *mucor sp.*, *aspergillus niger* and *candida albicans* (Jabamalai 2014; Selvamaleeswaran et al. 2016). CQ has been only used for bone tissue regeneration in tissue engineering (Tamburaci et al. 2018). It is also known that the CQ used in Ayurveda has a blood clotting effect and contributes to wound healing. In the literature, only CQ crude extract has been studied in vivo for wound healing. Mohanty et al. extracted the CQ plant successively with petroleum ether, and chloroform. The excision and incision wound model was applied to the rat model. Quercetin, vitamin C, ascorbic acid and phenols which are ingredient of CQ, support the wound healing. Quercetin stimulates myofibroblasts and provides contraction around the wound thus supporting healing. Ascorbic acid is needed for collagen synthesis, while Vitamin C helps in the formation of connective tissue, phenols can cause a synergistic effect in wound healing (Mohanty et al. 2010). In 2014, the methanolic and aqueous extracts of the CQ plant were tested on the rat model. These extracts stimulate cell proliferation of the extracts applied to the wound area, increasing the content of collagen. In addition, phenols present in CQ content also supports the wound healing process (Matadeen et al. 2014). CQ was only potentially studied in wound healing as a crude

extract. However, if used directly in the form of extracts, it may cause toxic effects or side effects in excessive use. Therefore, the extract can be loaded into the polymer systems and sustained and controlled extract release can be observed. Controlled delivery systems enable the active agent to release at regional or systemically predetermined rates and at specific time intervals. Controlled delivery systems that reduce toxicity and increase bioavailability, are administered locally at constant concentration with sustained release.

CHAPTER 3

MATERIALS AND METHOD

3.1. Materials

High molecular weight chitosan (Sigma-Aldrich), medium molecular weight (Sigma-Aldrich) and low molecular weight chitosan (Sigma-Aldrich) were used for nanosphere, nanofiber and sponge production, respectively. Acetic acid was purchased from Merck and used as a solvent for preparation of chitosan solution. Polyhedral Oligomeric Silsesquioxane (POSS) (Hybrid Plastics^{TM}) was used as a nanofiller for preparation of bottom layer of wound dressing material. The upper layer was made of chitosan nanofiber or nanospheres consisting of *Cissus quadrangularis* (CQ) (3% ketosteroid content; Ambe Phytoextracts Pvt.) that was selected as an antimicrobial and bioactive extract for wound healing. Phosphate buffer saline (PBS) tablets (Invitrogen, Thermofisher Scientific) were used *in vitro* extract release study and swelling studies. Dulbecco's Modified Eagle Medium (DMEM, Serox), fetal bovine serum (FBS, Serox), penicillin and streptomycin antibiotic solution (Serox), were used for cell culture. The WST-1 assay (Biovision) was used for *in vitro* cytotoxicity test.

3.2. Preparation of Extract Loaded Nanospheres/Fibers (Upper Layer)

In order to prepare bilayer dressings, firstly the upper layer was prepared using CQ extract loaded chitosan nanospheres and nanofibers. Subsequently, chitosan / POSS sponges were prepared as the bottom layer.

3.2.1. Nanosphere Production with electrospraying method

1(w/v) % chitosan solution was prepared by mixing high molecular weight chitosan and the 90 (v/v) % acetic acid solution and mixed for 24 h by magnetic stirrer. 1, 2 and 3 (w/w CHI) % genipin as a crosslinker was added in the chitosan solution. Then, *Cissus quadrangularis* extract powder (CQ) was dispersed in 2 ml distilled water and

added to chitosan genipin solution. According to preliminary solubility studies, polymer:extract (P:E) ratios were determined as 2.5:1, 5:1 and 7.5:1. CQ loaded chitosan nanospheres were prepared by electrospraying technique. Optimization of electrospraying operating conditions was done by altering voltage, distance and flow rate using 3 level 2 factorial design. The high and low level of parameters for experimental design was given in Table 1. Optimum electrospraying conditions were determined using Design Expert 11 (Trial version) program based on the particle size, uniformity and morphology of the nanospheres. All statistical analysis was done by using analysis of variance (ANOVA).

Table 3. 1. Levels of operating parameters of electrospraying for experimental design

Factor	Low Level	High Level
Voltage (kV)	10	20
Flow rate (ml/h)	1	3
Distance (cm)	10	15

3.2.2. Nanofiber Production with Electrospinning Method

2% (w/v) medium molecular weight chitosan solution was prepared by dissolving chitosan in 70% (v/v) acetic acid solution for 24 h using magnetic stirrer. Then, 0.5, 1, 2, 3 % (w/w CHI) genipin as a natural crosslinker agent and polyethylene oxide (PEO)(CHI:PEO;80:20) as plasticizer to liquefy and to obtain fiber morphology were added into chitosan solution. Then *cissus quadrangularis* extract (Polymer: Extract ratio 2.5:1, 5:1, 7.5:1) powder was dispersed in 2 ml of distilled water and added dropwise in genipin crosslinked chitosan solution and mixed for 1h. The final solution was electrospun by using electrospinning apparatus to produce extract loaded nanofibers. The extract loaded nanofibers were produced at the process conditions of 10 cm of distance, 1.5 ml/h of flow rate and 20 kV of voltage.

3.2.3. Fabrication of CHI-POSS Sponge (Bottom Layer)

Firstly, 2% (w/v) low molecular weight chitosan was dissolved in 2% (v/v) acetic acid solution and stirred overnight. Then, POSS nanoparticles (CHI:POSS; 95:5) was dispersed in 5 ml distilled water. POSS dispersion was added to homogeneous chitosan solution and mixed for 1 hour. Then chitosan/POSS solution was ultrasonicated for 30 min by using Misonix Ultrasonicator to disperse POSS nanoparticles in chitosan matrix effectively. Finally, chitosan/POSS dispersion was poured into petri dish and then it was prefrozen at -20 °C for 24 h. Later, the samples were lyophilized in freeze dryer (Labconco, FreeZone 4.5 liter Freeze Dry Systems, 77500-77510 Series Models) for 48 h at -46 °C and 0.018 mbar vacuum.

3.2.4. Fabrication of Bilayer Wound Dressing

Bilayer wound dressing was prepared by coating CQ loaded nanospheres (upper layer) on top of the chitosan/POSS sponge layer (bottom layer) by using electrospraying method. Effects of CQ/chitosan ratio and genipin crosslinker concentration on the properties of wound dressing materials were studied.

3.3. Characterization of Bilayer Sponges

After wound dressings were produced, they were characterized. Characterization tests of bilayer dressings are given below.

3.3.1. Morphology

SEM analysis (Quanta FEG 250, 7×10^{-2} mbar and 15mA) was performed to observe the morphology of the upper layer, nanospheres, nanofibers, as well as the bottom layer, sponge composites. In addition, structural integrity of bilayer composite and

thickness of each layer were observed with SEM. Before SEM analyses, samples were coated with gold in the presence of Argon gas using Emitech K550X Spot Coater. Image J software was used to calculate nanosphere particle size and nanofiber diameters by using SEM images. The average dimensions were reported.

3.3.2. Fourier Transform Infrared Spectroscopy (FT-IR) Analysis

Chemical characteristic peaks of CQ extract and POSS nanoparticles were investigated with ATR instrument (Shimadzu FTIR-8400 s) at a wavelength range from 4000 to 400 cm^{-1} at a resolution of 4 cm^{-1}. In addition, chemical interaction between CQ-chitosan and chitosan/POSS were determined.

3.3.3. Swelling Study

The water uptake capacity of each layer and bilayer composites were determined by swelling test. Before test, dry samples (W_d) were weighed. Then the samples were incubated in 1X PBS solution for 4 hours, 24 hours and 48 hours at 37 ° C to mimic human body condition. Finally, wet samples were taken from 1XPBS solution and weighed (W_w). Swelling rate (SR) was calculated according to Equation 3.1.

$$SR = ((W_w - W_d)/W_d)*100 \tag{3.1}$$

3.3.4. Porosity Measurement by Liquid Displacement

Open porosity was determined with liquid displacement method where ethanol was used as a liquid phase. Samples was put into graduated cylinder containing 20 ml of ethanol (V_1) and incubated in the vacuum oven for 1-2 minutes to remove air trapped in porous structure. The ethanol was entered when air was exited the structure. The total volume of both ethanol and samples was measured as V_2 value. Then, samples were removed from graduated cylinder containing of ethanol and recorded as V_3. Open porosity was calculated according to Equation 3.2.

$$\varepsilon = (V_1 - V_3)/(V_2 - V_3) \quad\quad\quad (3.2)$$

3.3.5. Water Vapor Transmission Rate

Water vapor permeability of chitosan-POSS sponges was measured with the operating system which consists of two chambers. The bottom chamber was filled with deionized water in a small container to maintain 100% relative humidity. The upper chamber comprises a moisture probe. This probe is connected to the Datalogger SK-L 200 TH system. The humidity probe at the top records the relative humidity and temperature. Sponges are cut in a diameter of 4 cm and placed between two compartments. Before starting the test, the relative humidity in the upper chamber is reduced to 5% with the anhydrous $CaSO_4$ column. Then, water vapor is allowed from the bottom to the sponge. Data is recorded to the computer at 1 minute intervals via Datalogger. Water vapor permeability (WVP) is calculated with the following Equation 3.3.

$$(WVP) = (Slope \times L \times V) / (A \times R \times T) \quad\quad\quad (3.3)$$

The slope of the equation is calculated from the time graph with $[(P_{IL} - P_{1ui}) / (P_{IL} - P_{1ut})]$. P_{1L} and P_{1u} are partial pressure in the upper and lower chambers, respectively. A is the transfer area of the exposed film surface (m^2), t is the test time, R is a gas constant, V is the volume of the chamber. WVP of chitosan-POSS sponges was calculated in mol/min cm kPa units. Water vapor transmission rates (WVTR) of the sponges were also calculated as g / m^2 day.

3.3.6. Mechanical properties

Mechanical properties of chitosan/POSS sponges (bottom layer) were determined with tension test according to ASTM D882 standard using TA XT plus Texture Analyzer (Stable Micro Systems, UK). Before tension test, chitosan/POSS sponges were cut into rectangular shape (1cmx6cm) and conditioned in humidity chamber at 25°C and 55% relative humidity conditions for 24 h. Digital calipers (Mitutoyo) was used to measure thickness of chitosan/POSS sponges. Tensile test was carried out using 5 kgf load cell

that have tensile grips at a crosshead speed of 10 mm min^{-1}. Tensile strength, Young's moduli and maximum stress of samples were measured.

3.3.7. Encapsulation Efficiency and *In vitro* Drug Release Profile

The amount of extract encapsulated in bilayer wound dressing was determined by dissolving certain amount of nanospheres / nanofibers in 1XPBS solution and detection of extract at specific wavelength by spectroscopy method. Chitosan nanospheres and nanofibers were dissolved in ultrasonic bath for 30 minutes in order to destroy the polymer structure. The amount of *Cissus quadrangularis* released from the nanospheres and nanofibers was determined by UV-spectrophotometer (Varioskan) at 230 nm. The encapsulation efficiency (% EE) was calculated by the equation given below (Equation 3.4).

$$ EE\ (\%) = \frac{Amount\ of\ extract\ loaded}{The\ theoretical\ amount\ of\ extract\ loading}\ 100 \qquad (3.4) $$

In vitro release assay was performed with bilayer composites which were placed on 24 well plate and incubated in 1 ml 1XPBS. Samples was incubated at 55 rpm and at 37 ° C in orbital shaker (Thermoshake, Gerhardt). The release rate of the samples collected at certain time intervals was determined with the absorbance data obtained using UV-spectrophotometer at 230 nm. The volume of the incubation medium was kept constant thus the collected medium was replaced with fresh 1XPBS at every detection times.

3.3.8. *In vitro* Release Kinetics

There are some semi-empirical and full empirical models for the prediction of the drug release mechanism. In this study, First order, Higuchi, and Korsmeyer-Peppas release models were used to determine the kinetics and the dominant mechanism of CQ release from the bilayer wound dressing.

First Order Kinetic Model: In the first order release model, the extract release is related to the extract concentration. The assumption of this model is the constant surface area during the dissolution of extract. Release definition was given in Equation 3.5.

$$M_t = M_0 e^{-K_1 t} \tag{3.5}$$

where, M is the released extract amount at a certain time t, K_1 is the first order rate constant. The semi-log plot of cumulative percentage of remained extract versus time was plotted to evaluate the kinetic parameters of the first-order release model.

Higuchi Model: Higuchi model is the most applied model for polymer release system. Assumptions of the Higuchi model are:

- Pseudo-steady approach

- Edges are negligible

- The thickness of the carrier is bigger than extract particles

- Dissolution and the swelling behavior of the polymer system are neglected.

Higuchi model is simply expressed with Equation 3.6.

$$\frac{M_t}{M_0} = K_H t^{1/2} \tag{3.6}$$

where, K_H is the Higuchi dissolution constant. The slope of the cumulative percentage of extract release versus square-root of time plot gives the K_H value.

Korsmeyer-Peppas model (The Power Law): Korsmeyer-Peppas is a semi-empirical model. This model is applied to the first 60% of the cumulative release in the model.

$$\frac{M_t}{M_\infty} = K t^n \tag{3.7}$$

where, n is the release constant. This constant defines the Korsmeyer-Peppas mechanism. K is the release constant, M_t is the release extract amount at time t and also M is the release amount at equilibrium time. The slope of the graph of $\log(M_t/M_\infty)$ versus $\log(\text{time})$ was drawn to obtain n value of Korsmeyer-Peppas release model. According to the geometry of the drug carrier systems, the release mechanism of the carrier system is

determined. Table 3.1 gives the n values and mechanism types for different morphologies of drug carrier systems.

Table 3. 1. Release coefficient ranges to determine the mechanism

Release Exponent (n)			Release mechanism
Thin film	Sphere	Cylinder	
n ≤ 0.5	n ≤ 0.45	n ≤ 0.43	Fickian diffusion
0.5<n<1	0.45<n<0.89	0.43<n<0.85	Anomalous diffusion or non-Fickian diffusion
n ≥1	n ≥0.89	n ≥0.85	Case-II transport

3.3.9. Antimicrobial activity of the wound dressing material

CQ release media, was collected from *in vitro* release study at predetermined time periods of 1 hour, 6 hours and 24 hours, was used for antimicrobial activity test by disk diffusion method. CQ release media was tested on gram positive Staphylococcus epidermidis (RSKK 1009 strain) and gram negative Echerichia coli (ATCC® 25922) microorganisms. Activated cultures of microorganisms in Nutrient Broth for 24 hours at 37 ° C were used. The bacteria concentration was set at 0.5 McFarland. Then, bacteria solution was placed on the agar. Blank disks (Oxoid™) were placed on the petri dish that contain bacteria. Then 10 μl of extract release media collected at specific times (1 hour, 6 hours, 24 hours) was dropped on blank discs. Amoxicillin (antibiotic) disks was used as a positive control. Petri dishes were incubated at 37°C for 24 h. After 1 day, clear inhibition zones around the discs were measured and recorded as the average of four replicates.

3.3.10. *In Vitro* Cytotoxicity Determination

Cytotoxicity of single layer and bilayer composite sponges was determined according to ISO 10993-5 using WST-1 assay. 3T3 (NIH/3T3 (ATCC® CRL-1658)

fibroblast viability was measured using indirection extraction method. Extract loaded nanofibers (upper single layer) and extract loaded coated Ch/POSS sponges were extracted in DMEM at 24 h at 37°C. NIH/3T3 (ATCC® CRL-1658) on 96 well plate with a density of 10^5 cell/ml and incubated with 100 µl extraction media for 72 h. %Cell viability was determined during 72 h spectrophotometrically at 440 nm and calculated according to Equation 3.5. (ABS: Average absorbance value, NC: Negative control) by normalizing the absorbance data with a negative control that includes fresh medium.

$$\text{Cell viability \%} = (\text{ABS of sample}/\text{ABS of NC}) \times 100 \qquad (3.8)$$

3.3.11. Statistical Analysis

The experimental data are presented as mean ± standard deviation (SD). The differences between groups were analyzed using a two-way Analysis of Variance (ANOVA) with Tukey's multiple comparison test.

CHAPTER 4

RESULTS AND DISCUSSION

4.1. Morphology and Structure of Composite Sponges (Bottom Layer)

The pore structure, dimensions, and morphology of the sponges were examined by SEM analysis. The pore sizes of the sponges were measured using Image J software. The average pore size of the chitosan control group and chitosan / POSS sponges were found as 163 ± 7 μm and 137 ± 8 μm, respectively. The pore sizes of chitosan/POSS sponges were reduced when the POSS was added to the chitosan sponges. In addition, chitosan / POSS composite sponges have more homogeneous pores than chitosan sponges. Pore sizes and structure of chitosan and chitosan / POSS composite sponges are shown in Figure 4.1. The inclusion of POSS in sponges increased wall thicknesses. In the study, Tamburacı produced POSS reinforced chitosan sponges for bone tissue regeneration. Pore size was decreased and scaffold walls were thickened when the POSS was added to the chitosan scaffold (Tamburaci 2016).
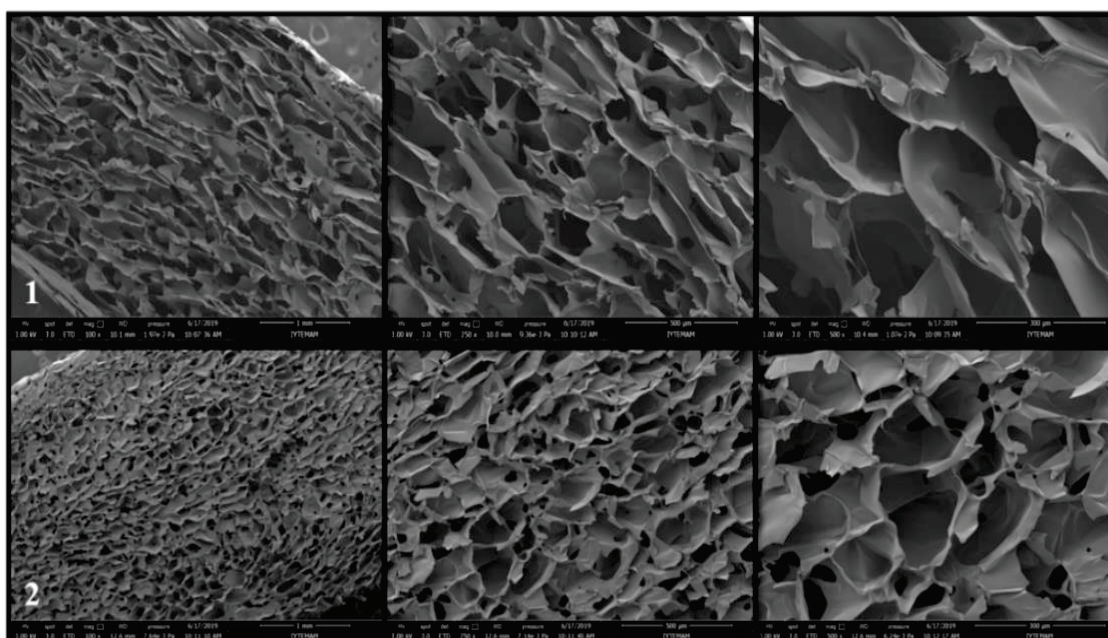

Figure 4. 1. SEM images of chitosan(1) and chitosan/POSS(2) composite sponges with 100x, 250x and 500x magnification

4.2. Optimization of Electrospraying and Electrospinning Parameters for the Production of Nanosphere and Nanofiber (Upper layer)

Electrospinning method is used in the production of nanofibers and microfibers with appropriate efficiency. There are many advantages of this method such as high encapsulation efficiency, high active loading capacity, and uniform fiber formation. In electrospinning method, voltage, distance, flow rate, and solution concentration are important parameters affecting fiber and sphere formation. The formation of sphere or fiber structures were optimized by changing these parameters. Solution concentration and working parameters were, nanospheres structure can be obtained the metal surface that defined the electrospray technique. In this study, extract loaded nanospheres and nanofibers were produced as the upper layer and operating parameters are optimized for having a uniform morphology and high encapsulation efficiency.

4.2.1. Nanosphere Morphology

In this study, 1(w/v) % chitosan solution was prepared via dissolution of high molecular weight chitosan into the 90 (v/v) acetic acid and mixed for an 24 h to prepare nanospheres. 0.2 g of CQ (P:E ratio 5:1) was dissolved in 2 ml of water and then added to the solution and stirred for 1 hour. The constant extract ratio was used in nanosphere and nanofiber fabrication. Electrospray parameters were determined with 3-level 2 factorial experimental design by using the flow rate, distance and voltage as design parameters. Table 4.1 shows the flow rate, distance and voltage ranges that are used in the experimental design.

Table 4. 1. Experimental design parameters for electrospray method

Factor	Low Level	High Level
Voltage (kV)	10	20
Flow rate (ml/h)	1	3
Distance (cm)	10	15

Experimental design groups are given in Table 4.2. Optimum electrospray conditions were determined according to the results of the examination of encapsulation efficiency and morphological structures.

The voltage, distance and flow rate are optimized in order to obtain nanospheres in smooth morphology and high encapsulation. The morphology of the nanospheres was examined with SEM analysis and the diameters of the spheres were measured by Image J program. Figure 4.2 illustrates morphology of all design groups. For nanosphere fabrication, smooth nanosphere morphology is important as well as experimental design results. Nanosphere dimensions of all experimental design groups are found in the range of 50-950 nm. When SEM images were examined, it was observed that spherical morphology deteriorated, and fiber formation occurred. It was revealed that the encapsulation efficiency decreased as the distance increased in the design groups. When the responses of the design groups (encapsulation efficiencies and morphologies) were investigated, the parameters for the uniform nanosphere morphology and high encapsulation efficiency are found as 2 ml/h flow rate, 20 kV voltage and 10 cm distance (Group 10). After the electrospray parameters were optimized, CQ loaded chitosan spheres were coated on the sponge with varying volume (4 ml, 2 ml and 1 ml) of CQ extract loaded chitosan solutions. Figure 4.3 shows the images of CQ extract loaded chitosan nanospheres with varying thickness or volume on sponges.

When the coating thickness of bilayer dressings was examined, it was seen that nanospheres were adhered on each other and disturbed their morphology with 4 ml and 2 ml coating of extract loaded chitosan solutions. However, 1 ml coating gave smooth surface structure (Figure 4.3). Therefore, 1ml coating volume was used for fabrication of nanospheres on sponge. The cross-sectional images of the CQ loaded chitosan (1ml) nanosphere coated wound dressings are given in Figure 4.4. It is known that skin grafts should be thinner than 400 μm to promote vascularization for nutrient delivery to epidermal layer. In this study, the thickness of the upper layer was measured as 0.97 μm with image J software. This range is found to be suitable range for epidermal layers (MacNeil 2007). In addition, the thickness of the dermis layer is reported in the range of 1-3 mm (Kruglikov 2016; Joodaki and Panzer 2018) . The thickness of the sponge prepared in this study which mimics the dermis layer was found to be 2.7 mm.

Table 4. 2. Experimental design groups

Groups	Flow Rate (ml/h)	Voltage (kV)	Distance (cm)	EE%	Particle Size (nm)
1	3	20	12.5	63.77±1.81	87-758
2	1	10	12.5	49.61±12.34	68-390
3	2	15	12.5	70.99±10.76	56-599
4	2	10	15	11.93±1.01	62-510
5	2	15	12.5	20.42±5.45	79-509
6	1	15	10	51.49±8.67	65-435
7	3	15	10	90.14±4.21	100-832
8	2	15	12.5	53.83±3.36	50-553
9	2	20	15	33.58±3.72	74-708
10	2	20	10	70.80±4.94	87-738
11	3	10	12.5	18.11±4.22	62-881
12	1	20	12.5	59.46±7.53	123-904
13	1	15	15	33.41±9.25	69-950
14	3	15	15	35.76±7.06	53-525
15	2	15	12.5	82.05±3.91	52-522
16	2	10	10	64.31±12.12	83-940
17	2	15	12.5	64.78±1.69	55-908
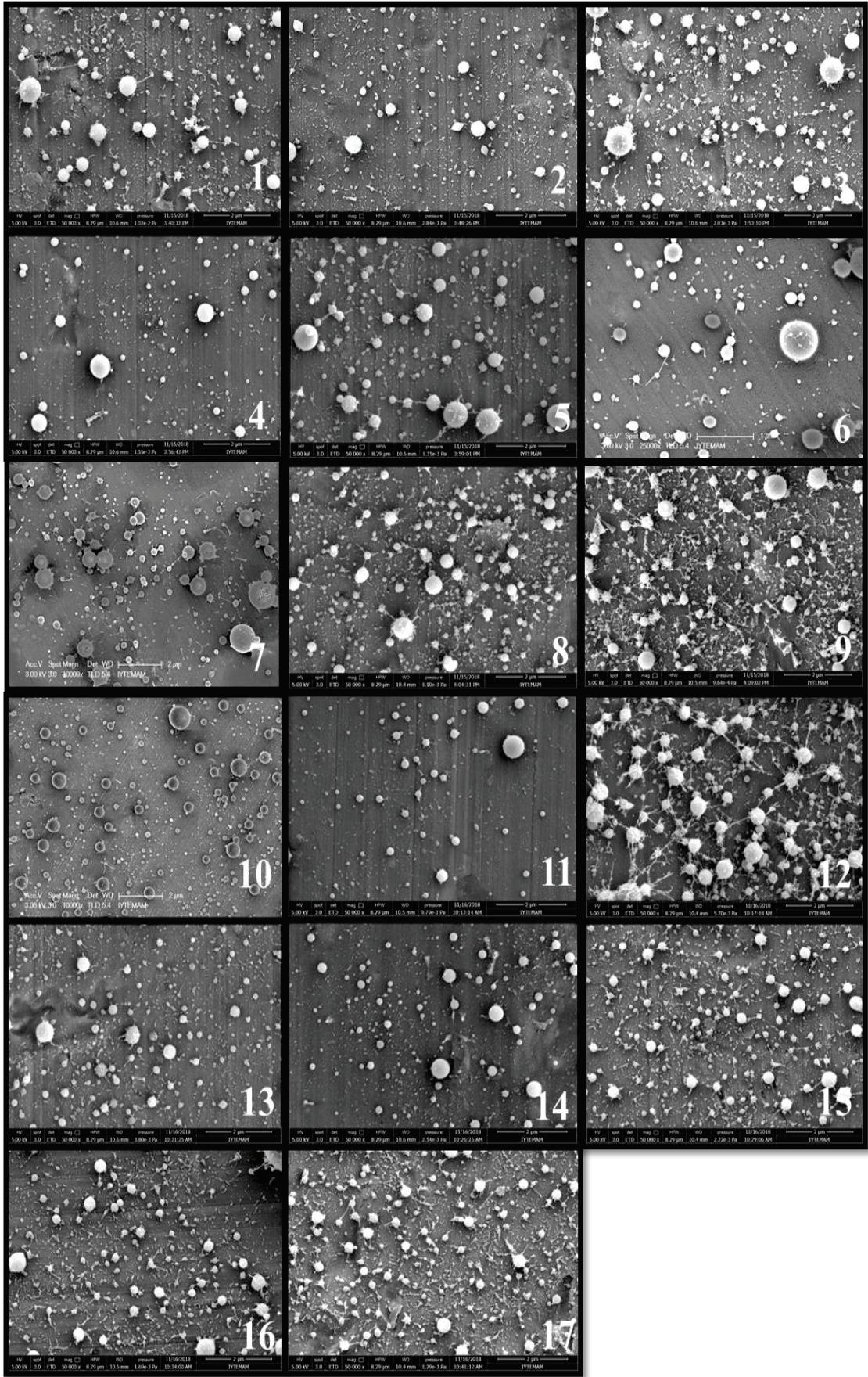
Figure 4. 2. SEM images of experimental design groups
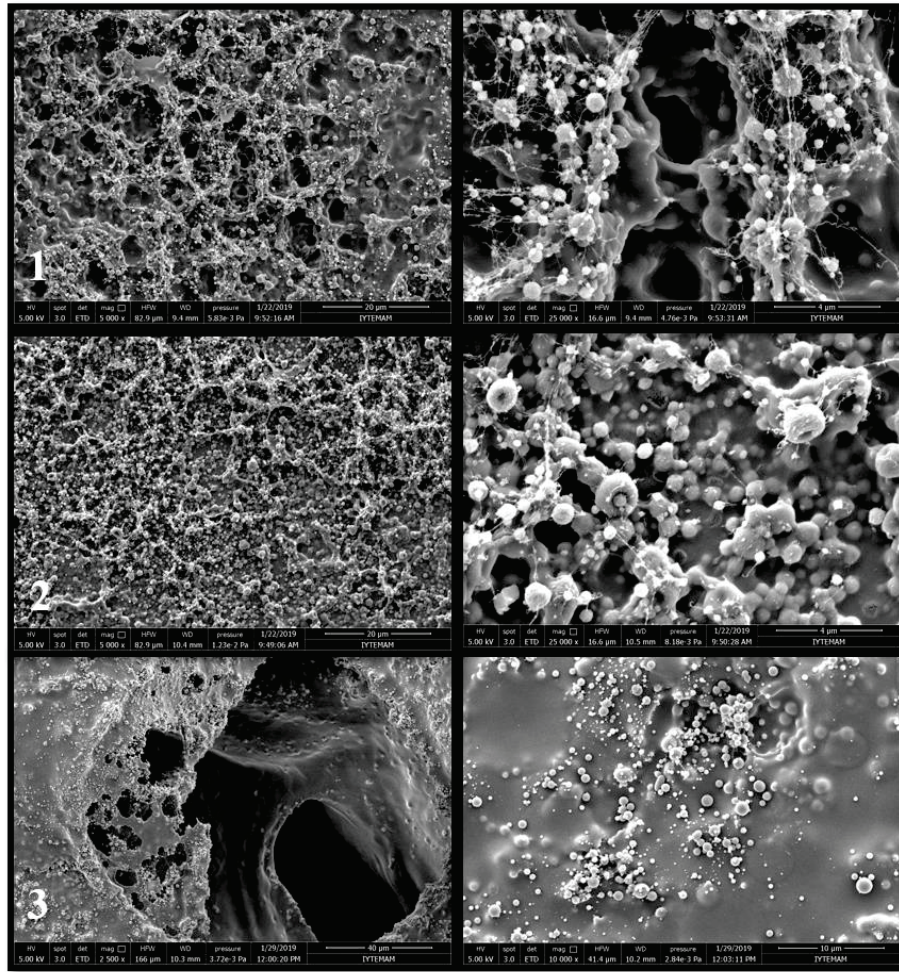
Figure 4. 3. SEM images of chitosan nanofiber coating with varying thickness on sponges 1) 4ml, 2) 2ml, and 3) 1ml
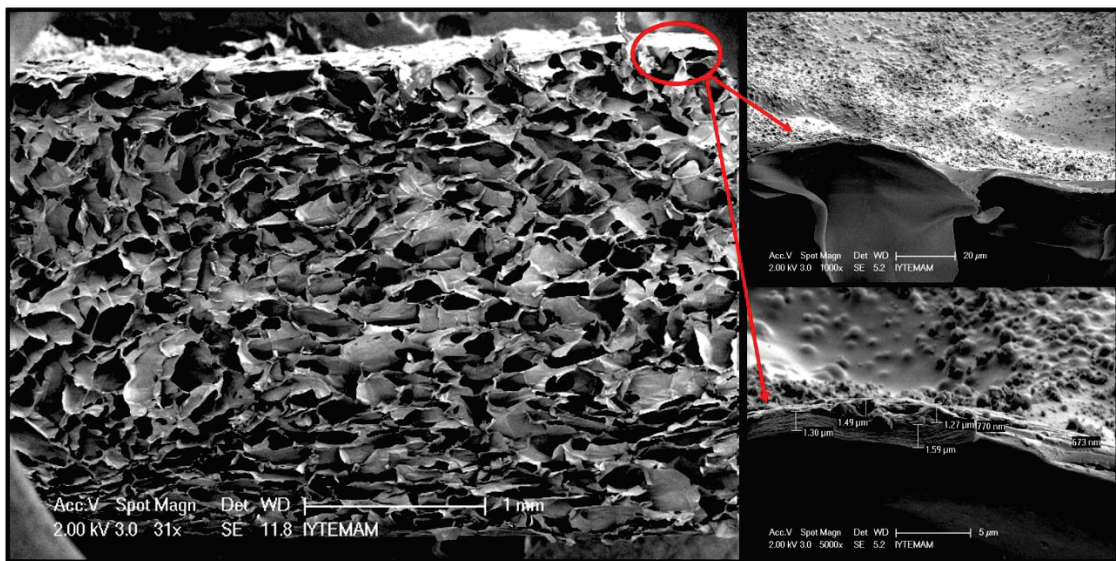
Figure 4. 4. SEM image of cross section of CQ loaded chitosan nanospheres coated a sponges

Genipin was used as a crosslinker to enhance the stability of the chitosan nanospheres. Figure 4.5 shows the SEM images of genipin crosslinked nanospheres prepared with different genipin ratios. In the case of 3 % (w/w CHI) genipin crosslinking, morphology of the nanospheres deteriorated and fiber-like structures were observed. When CQ loaded chitosan was crosslinked with 2 % (w/w CHI) genipin, the nanospheres were embedded in sponge layer and the structure of nanospheres were demolished due to this adhesion. There was no change in the morphology of the nanospheres with 1% (w/w CHI) genipin crosslinking. Nanospheres showed uniform morphology and structure. Therefore, genipin concentration was selected as 1% (w/w CHI).
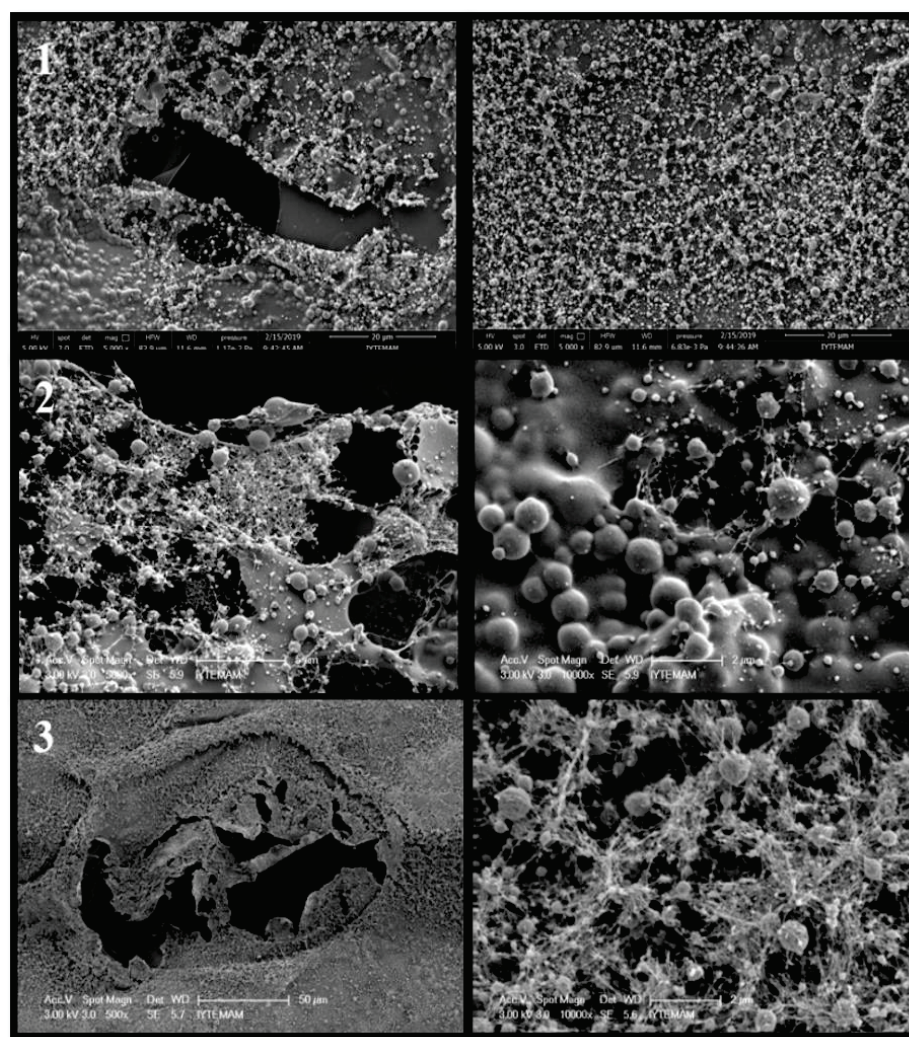
Figure 4. 5. SEM images of nanospheres coated on the sponge with different genipin ratio
1) 1%, 2) 2% 3) 3%

4.2.2. Nanofibers Morphology

The electrospinning method was used in the fabrication of the upper layer with fiber morphology. Voltage (15-20 kV), flow rate (1-1.5-2-3ml / h), acetic acid ratio (70-80-90%), and CHI:PEO ratios (CHI: PEO; 90: 10-80: 20-70: 30) were changed to produce the most uniform fiber morphology. Figure 4.6 shows effects of flow rate and CHI:PEO ratio on the morphology of fiber. It was seen that nanosphere-fiber mixture was obtained at all 3 different flow rates and PEO concentrations. Although full fiber structure was not obtained, more fiber structure formation was observed with an increase in the ratio of PEO concentration. However, uniform fiber morphology could not be observed due to excess acetic acid concentration.
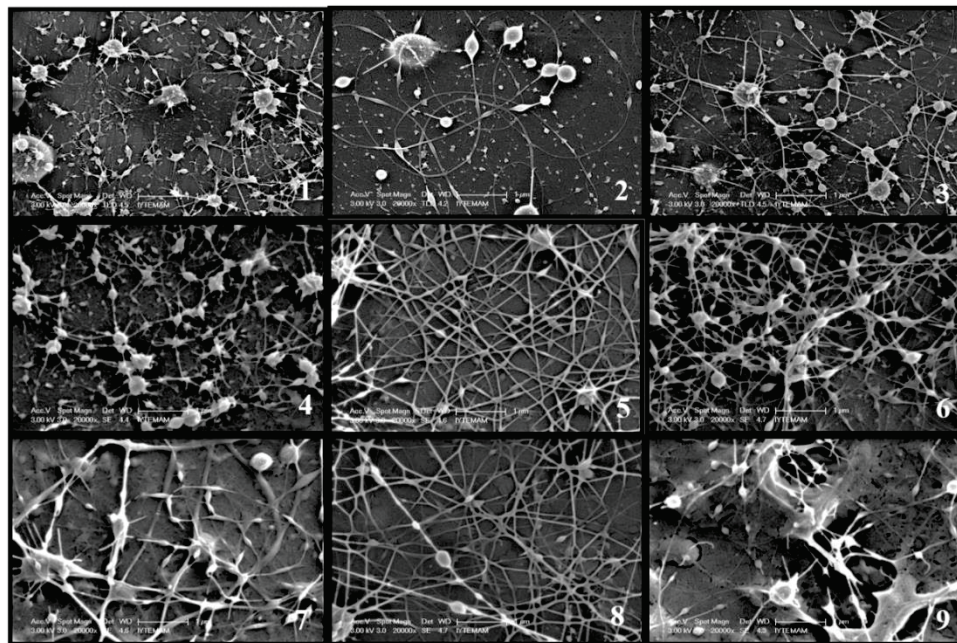
Figure 4.6. SEM images of different electrospraying production parameters: 1) 1 ml/h,.CHI:PEO 90:10, 2) 2 ml/h, CHI:PEO 90:10, 3) 3 ml/h, CHI:PEO 90:10, 4)1ml/h, CHI:PEO 80:20, 5) 2 ml/h, CHI:PEO 80:20, 6) 3 ml/h, CHI:PEO 80:20, 7)1ml/h, CHI:PEO 70:30, 8) 2 ml/h, CHI:PEO 70:30, 9) 3 ml/h, CHI:PEO 70:30 ; voltage of 20 kV, distance of 10 cm, acetic acid concentration 90%.

In the next step, the acetic acid concentration was reduced to 80% and 70% and CHI: PEO was kept constant with a ratio of 80:20. In addition, electrospinning parameters

were kept constant at 20 kV, 1.5 ml/h and 10 cm distance. Figure 4.7 shows the effect of acid concentration on the morphology of electrospun fibers (70-80%).
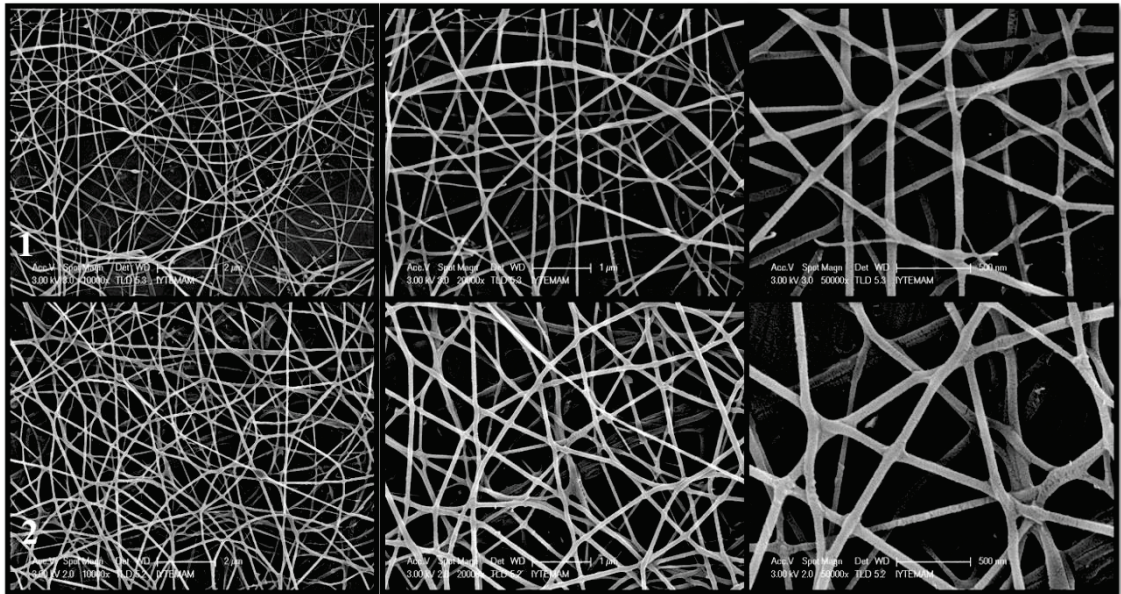
Figure 4. 7. SEM images of electrospun fibers with different acid concentrations: 1) 70%, 2) 80%; voltage of 20 kV, flow rate of 1.5 ml/h, distance of 10 cm, CHI:PEO 80:20

It is observed that the fibers produced with lower acid concentrations have a smooth morphology. The mean fiber diameters of the group containing 80% acetic acid were 70.8 ± 2.42 nm and the group containing 70% acetic acid was 65 ± 3.35 nm. Encapsulation efficiencies were determined as $60.6 \pm 4.74\%$, and $70.17 \pm 2.12\%$ for 80% and 70% acetic acid concentration, respectively. As a result of parametric study based on evaluation of the fiber diameter, morphology and encapsulation efficiency, 70% acetic acid concentration and CHI:PEO ratio of 80:20 were selected due to the higher encapsulation efficiency and smooth fiber structure. The most suitable electrospinning production parameters are found as voltage of 20 kV, flow rate of 1.5ml /h and distance of 10 cm.

Genipin as a cross-linker at different concentrations (0.5%, 1%, 2%, 3% (w/w CHI)) was used to enhance the stability of chitosan fibers as in the case of nanosphere production. The effect of genipin cross-linker on fiber morphology was investigated by SEM analysis. Figure 4.8 shows the morphology of chitosan nanofiber at different ratios of genipin loading. It was seen that morphologies of the fiber groups containing 1% and 2% (w/w CHI) are smooth, however nanofiber's structure became thinner as the ratio of

genipin concentration increases. Fiber diameters were found as 89.9±5 nm, 77.9±4 nm, 55.1±3 nm, 50.7±5nm for groups with a genipin ratio of 0.5%, 1%, 2% and 3% (w/w CHI), respectively.
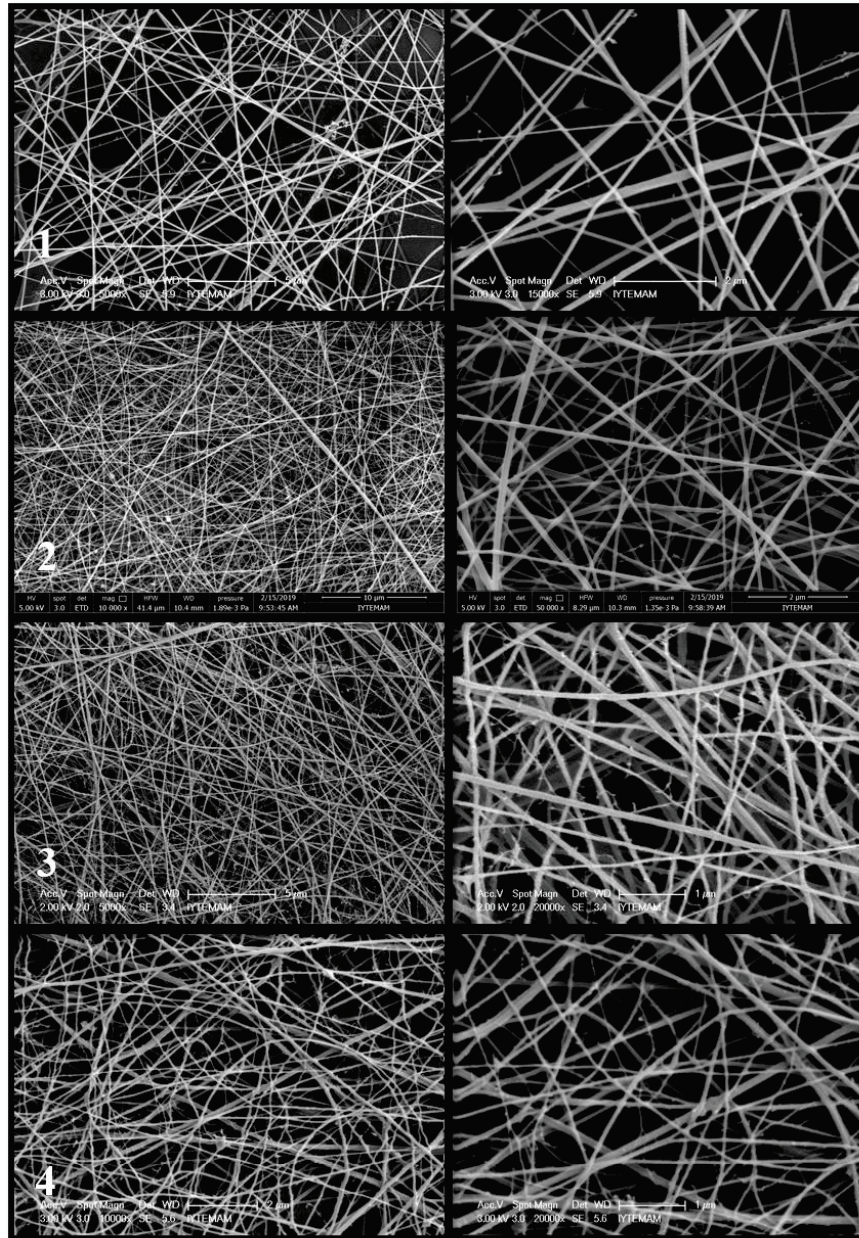
Figure 4. 8. SEM images of nanospheres coated on the sponge with different genipin ratio 1)0.5%, 2)1%, 3)2%, 4)3% (w/w CHI)

Nanofibers are coated on the sponge by using 1 ml volume of extract loaded solution. As seen in Figure 4.9, nanofibers are coated uniformly and covered on the sponge. The coating thickness of the fibers was measured as 1.5 μm. This range is a suitable range for the epidermis layer. On the other hand, thickness of sponges was

measured as 3.02 mm by Image J software. Since the thickness of dermis is in the range 1 mm-3 mm according the body region (Kruglikov 2016; Joodaki and Panzer 2018), the sponge prepared (3.02 mm) in this study can represent the dermis layer.
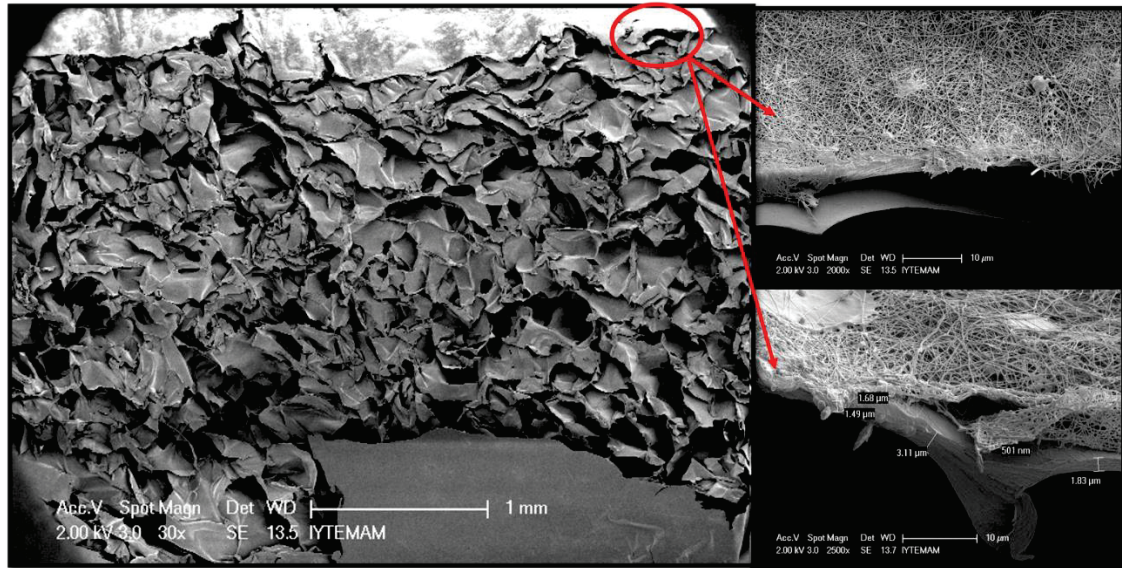
Figure 4. 9. SEM image of a cross-section of CQ loaded chitosan nanofibers coated sponges

Effect of extract concentration on the surface morphology of nanofibers was also studied in the study. Nanofibers were prepared at three different polymer:extract ratios, P:E's (P: E 2.5: 1, P:E 5:1, and P:E 7.5:1). Figure 4.10 shows SEM images of the nanofibers loaded with different extract ratios. The extract ratio did not much affect the structure of the fibers. Fiber diameters were found as 97.4±4 nm, 77.9±4 nm and 83.2±3 nm in groups with a P:E 2.5, 5:1 and 7.5, respectively. In a study, Geng et al. have produced chitosan fibers that are in the range of diameter sizes of 100-130 nm (Geng et al. 2005). In another study, chitosan-based nanofibers were produced by the electrospinning method and fiber diameters were found in the range of 20-100 nm (Hsieh 2006). Chen et al. produced biomimetic nanostructured chitosan-collagen fibers for tissue engineering. It was observed that, while the average nanofiber diameter of pure collagen fibers was 810 ± 580 nm, the average diameter of pure chitosan fibers was 415 ± 286 nm. As the chitosan ratio increased in collagen-chitosan nanofibers, nanofiber diameters decreased (Chen et al. 2010). In the study of Vrieze et al., optimum conditions for the production of chitosan nanofiber structures were investigated. Under appropriate conditions, chitosan nanofiber diameters were found to be 70 ± 45 nm (Vrieze et al. 2007). In another study, effect of molecular weight of chitosan on nanofiber morphology was

investigated. The average diameters of low, medium and high molecular weight chitosan nanofibers were found 74±28nm, 77±29nm and 108±42 nm, respectively (Schiffman and Schauer 2006). In native skin tissue, type I collagen fibril diameters vary between 50-500 nm (Liu et al. 2010). The diameters of the extract loaded chitosan nanofibers produced in this study were found to be in the appropriate range to mimic the structure of the ECM.
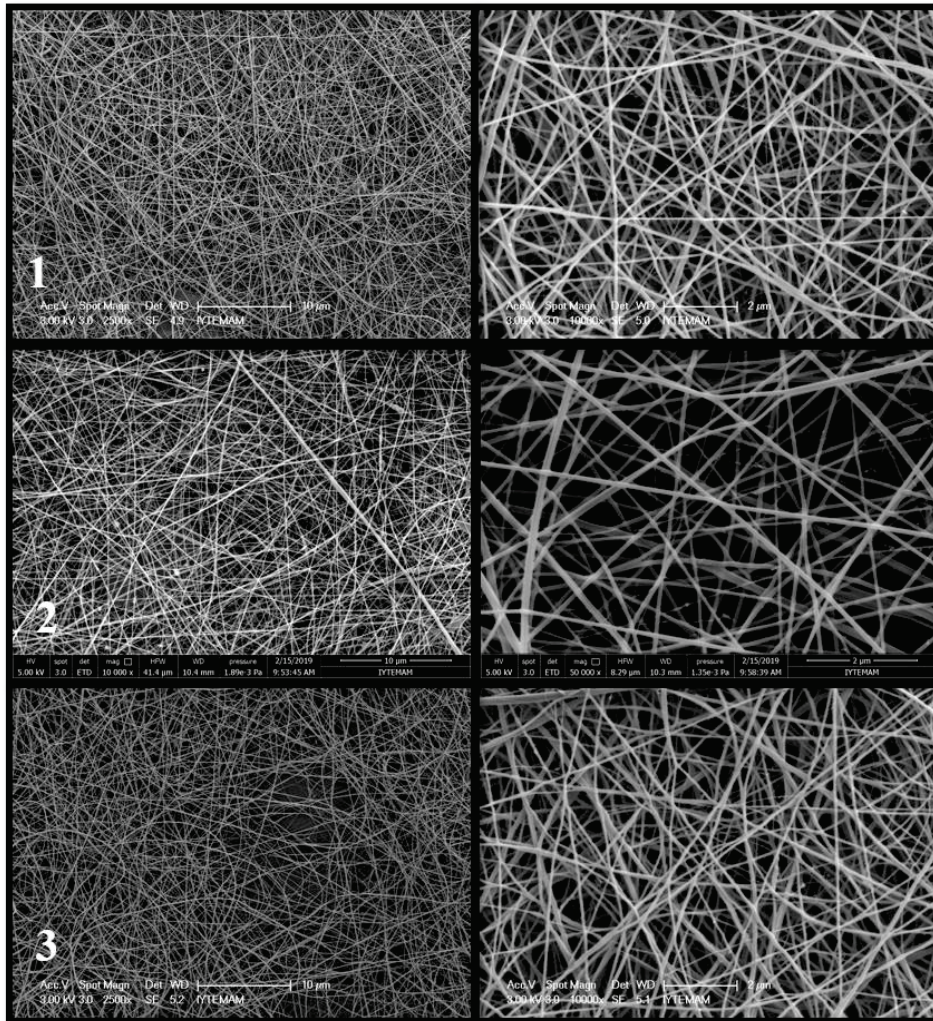

Figure 4. 10. SEM image of extract loaded chitosan nanofibers coated on the sponge at different P:E ratio; 1) 2.5:1, 2) 5:1, 3) 7.5:1

4.3. Characterization of Bilayer Wound Dressings

The results of the characterization tests of the bilayer wound dressings are given below, respectively.

4.3.1. *In vitro* Extract Release Profile

Before *in vitro* extract release studies, encapsulation efficiency of CQ was determined. Then the release profile and kinetics were examined.

4.3.1.1. Encapsulation Efficiency of CQ

In this study, nano-sized material is coated on the surface of the sponge with two different morphologies as nanofiber and nanospheres. The encapsulation efficiencies were calculated before the nanospheres and nanofibers as upper layer were coated on the bottom layer (sponge). The encapsulation efficiency of the extract in nanospheres and nanofibers were found by the standard calibration curve. Appendix B shows *Cissus quadrangularis* calibration curve. Table 4.3 shows the encapsulation efficiency of both nanofibers and nanospheres. Effect of P:E ratio on the encapsulation efficiency was studied for nanofiber production. It was found that as the P:E ratio increased, the encapsulation efficiency was increased. The encapsulation efficiencies of the CQ loaded nanofibers were found as 60.00±1.78%, 70.17±2.12% and 76.86±1.98% according to P:E ratio of 2.5:1, 5:1, 7.5:1, respectively. In the nanosphere morphology, CQ extract was loaded into nanospheres at constant ratio. The encapsulation efficiency of CQ loaded nanospheres was found as 76.48±3.63 for the P:E of 5:1. (Table 4.3.) The reason for testing only one extract ratio was burst release of the nanospheres. The encapsulation efficiency of nanospheres and nanofibers were found to be close to each other. In addition, the CQ extract release of the nanofibers was slower and more controlled than the CQ extract release of the nanospheres. Therefore, 3 different concentration of CQ extracts were tested in nanofiber morphology. (*in vitro* CQ extract release will be explained in detail in section 4.2.1.2). In literature, it was found that the nanofiber structures produced by the electrospinning method, showed high encapsulation efficiency and increased the stability of the bioactive compounds (Wen et al. 2017). In a study, raspberry leaf, hawthorn, ground ivy, yarrow, nettle, and olive leaf extracts were encapsulated in chitosan/alginate microspheres for food applications. The encapsulation efficiency of different extract loaded microspheres was found between 80-89% (Cvitanović et al. 2011). In another study, Moringa oleifera gelatin, which is a herbal extract, was encapsulated into a biopolymer using the electrospinning method. The encapsulation

efficiency of nanofibers loaded with different concentration of herbal extracts was found to be between 80-85% (Hani et al. 2017)

Table 4. 3. Encapsulation efficiencies of extract loaded nanospheres and nanofibers

Material	Polymer : Extract	Encapsulation Efficiency(%)
Genipin Crosslinked Chitosan Nanofibers	2.5:1	60.00±1.78
	5:1	70.17±2.12
	7.5:1	76.86±1.98
Genipin Crosslinked Chitosan Nanospheres	5:1	76.48±3.63

4.3.1.2. Extract Release Profile and Kinetics

In this study, CQ-loaded nanosphere and nanofiber coated sponges were evaluated for wound healing applications. *In vitro* release of CQ extract-loaded nanosphere and nanofiber coated sponges was examined at 37°C in 1x PBS (pH 7.4). Firstly, in vitro release of the CQ loaded nanosphere coated sponges was examined. Crosslinking effect and its concentration at three different ratios of genipin (1% , 2% and 3% (w/w CHI)) were studied at constant P: E; 5: 1. It was seen that the addition of genipin led to the slower release of the CQ extract. 78% of the extract was released in the first 4 hours without crosslinker.   Figure 4.11. shows the release of CQ extract from nanosphere coated sponges with and without genipin crosslinker.

1% (w/w CHI) genipin crosslinked chitosan nanosphere coated sponges reached 78% burst release in the first 6 hours while 2% and 3% (w/w CHI) genipin crosslinked bilayer wound dressings released 72% and 68% of extract from, respectively after 6 hours. The extract release reached 80% cumulative release on the 2nd day. As a result, the CQ release rate slowed down with increasing genipin concentration.

Figure 4. 11. The cumulative release of extract from nanosphere coated sponges with and without genipin

Secondly, extract release from nanofiber coated sponges was examined. 81% of extract was released in 6 hours without crosslinking. Thus, genipin crosslinker was used to slow down the rapid release. Four different concentrations of genipin were used to obtain the appropriate cross-linking ratio. These ratios are 0.5% (w/w CHI), 1% (w/w CHI), 2% (w/w CHI) and 3% (w/w CHI), respectively. The extract ratio (P: E; 5: 1) was kept constant. Figures 4.12. and 4.13. show the release of extract from nanofiber coated sponges with and without genipin at different ratios. *In vitro* release results showed that, 74% of the extract was released within 6 hours from 0.5% (w/w CHI) genipin crosslinked CQ-loaded chitosan nanofiber-coated sponges. It reached a cumulative release of 86% on the 2nd day. %50 of the extract release was obtained from 1% (w/w CHI) genipin crosslinked bilayer wound dressings after first 6 hours and the extract release reached a cumulative release of 79% on the 4th day. 2% (w/w CHI) genipin crosslinked bilayer wound dressings were reached 49% burst release in the 6 hours. Extract release reached

a 75% cumulative release on the 4th day. Finally, 3% (w/w CHI) genipin crosslinked bilayer wound dressing was examined, 52% of the extract was released in 6 hours. It was reached 83% were released in 4 days. As effect of crosslinking ratio was evaluated, it was found that crosslinking definitely slowed down the release rate, however no significant differences between 1% genipin crosslinked nanospheres and the higher crosslinking ones (2% and 3% crosslinked nanospheres) was obtained. Therefore, 1% (w/w CHI) genipin ratio was found to be sufficient for chitosan nanofiber fabrication.
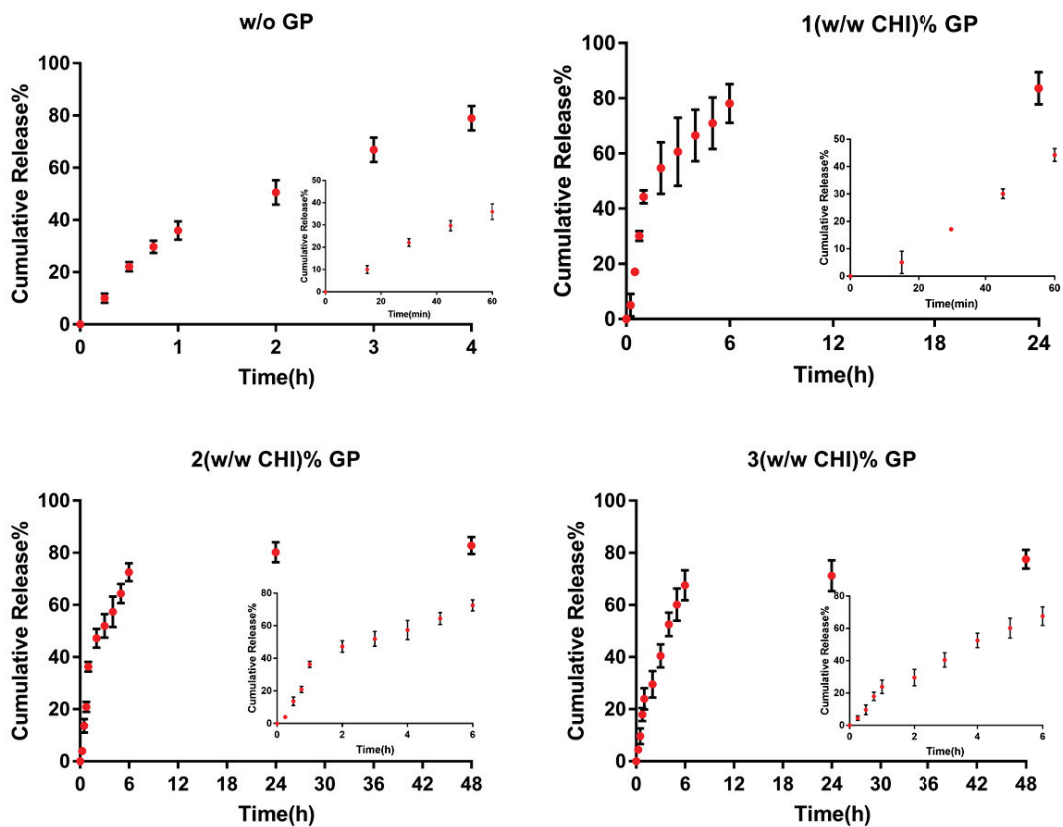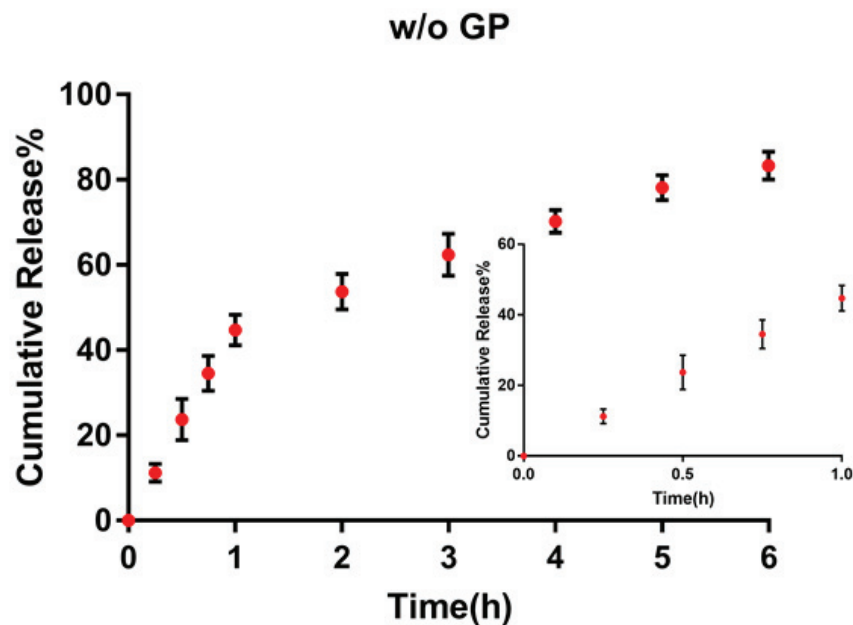

Figure 4. 12. The cumulative release of extract from nanofiber coated sponges with and without genipin

Extract loaded nanofiber coated sponges showed more controlled release compared to extract loaded nanosphere coated sponges. This is due to the fact that the disintegration of the nanospheres was faster than the nanofibers. Although the genipin cross-linker was added, extract release from nanospheres was more rapid compared to nanofibers. Therefore, nanofiber structure was chosen as the upper layer of wound dressing design in our study.
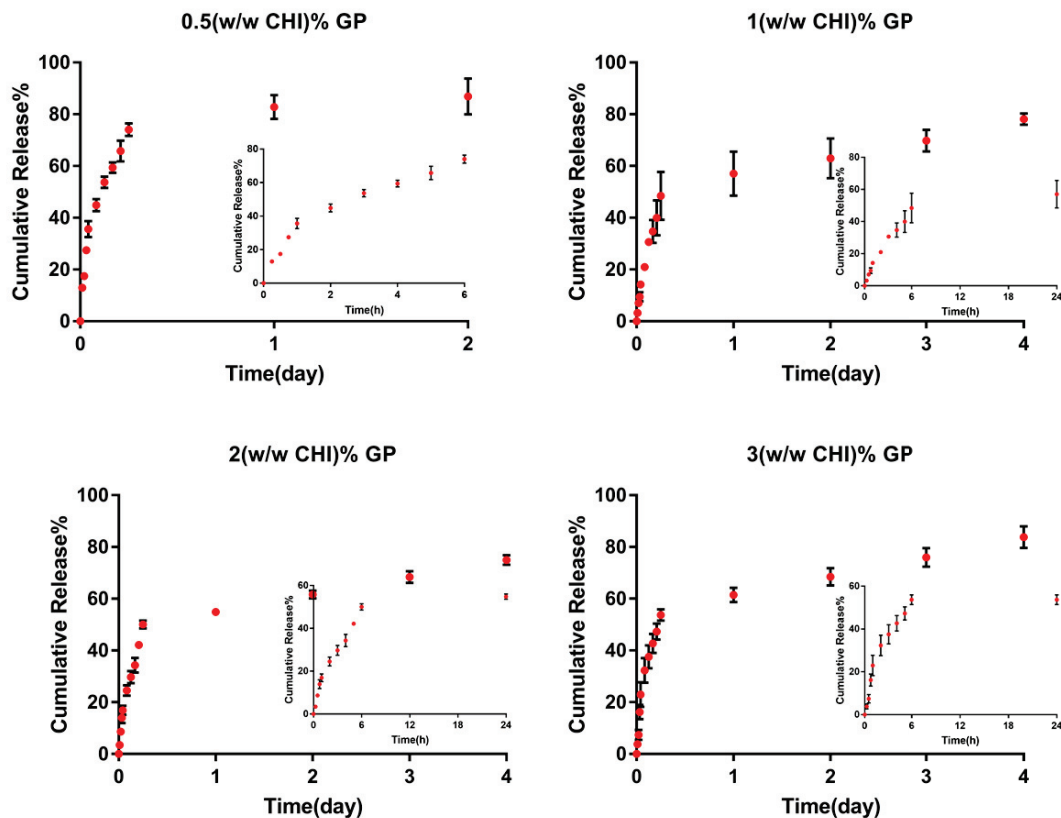
Figure 4. 13. The cumulative release of extract from nanofiber coated sponges with different amount genipin

Effect of polymer:extract ratio (P:E) on the release rate was also studied. Three different extract ratios (2.5:1, 5:1, and 7.5:1) were used at constant genipin concentration (1% (w/w CHI). The release profiles of extract from nanofiber coated sponge were examined at three different P:E ratios. Figures 4.14-4.16 show the release profile of extract from bilayer sponges loaded with three different extract ratios. According to the in vitro release profile, 54% of the extract was released from the bilayer wound dressing (P:E ratio 2.5:1). These wound dressings reached 80% cumulative release in 4th day of incubation. The release profile of the bilayer dressing with P:E 5:1 extract ratio showed 50% release in first 6 hours and reached 75% cumulative release at the end of the 4th day. Finally, the release of bilayer dressings with P:E 7.5:1 ratio was examined. 49% of the extract was released from bilayer wound dressings in 6 hours and reached 78% cumulative release on the 4th day of incubation. In the first 6 hours, the burst release occurred from all bilayer dressings. This is due to the fact that extract was rapidly

released from the surface of the nanofibers. However, as the P:E ratio is increased , % cumulative release decreased from 54% to 49%.

CHI:CQ 2.5:1 GP:1%
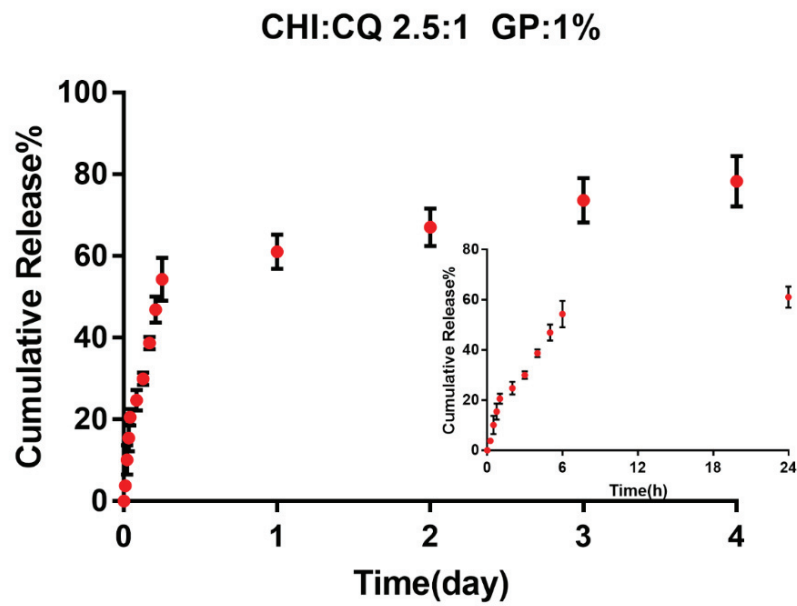
Figure 4. 14. The cumulative release of extract from nanofibers coated sponge for P:E ratio 2.5:1

CHI:CQ 5:1 GP:1%
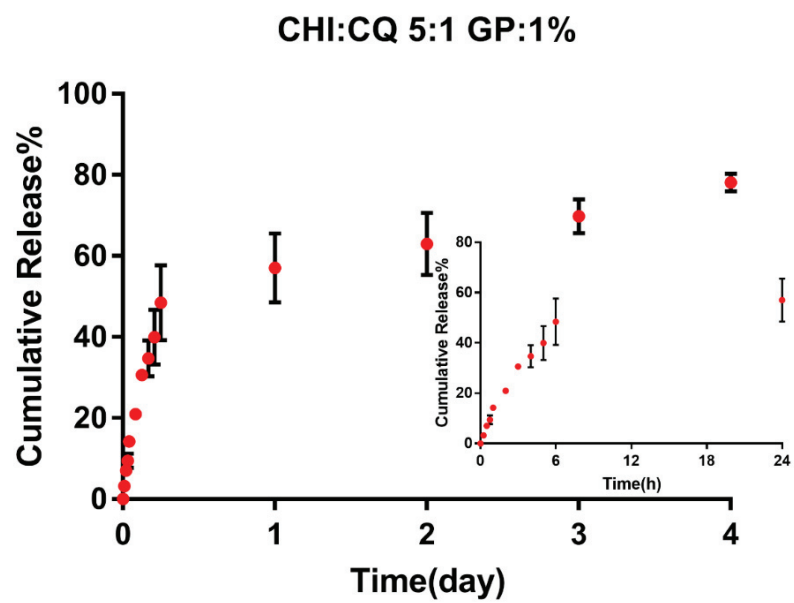
Figure 4. 15. The cumulative release of extract from nanofibers coated sponge for P:E ratio 5:1
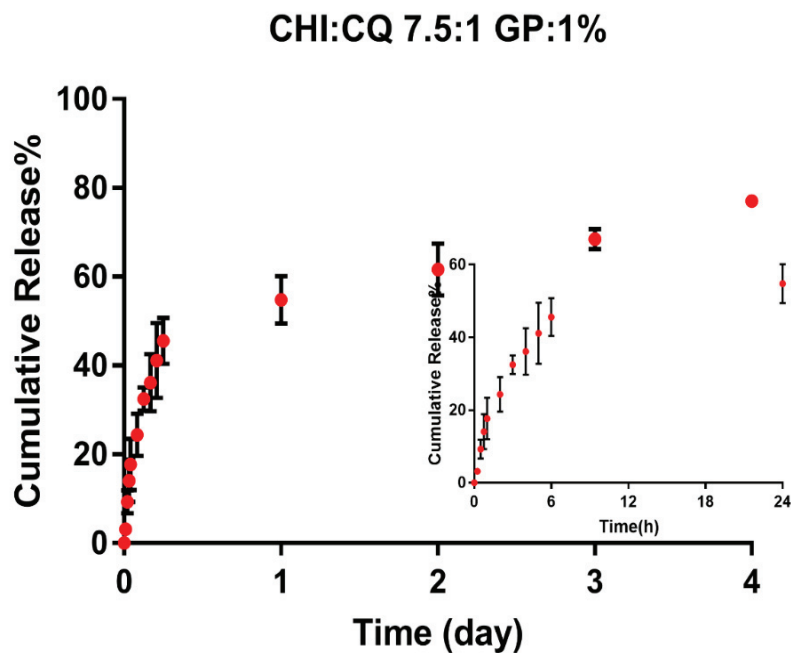
Figure 4. 16. The cumulative release of extract from nanofibers coated sponge for P:E ratio 7.5:1

A few studies exist in the literature regarding to extract loaded chitosan based wound healing materials. In the study of Charernsriwilaiwat et al., Garcinia mangostana extract was incorporated into chitosan-ethylenediaminetetraacetic acid/polyvinyl alcohol (CS-EDTA / PVA) mats by electrospinning for wound healing. The 80% of extract was released in 60 minutes. At the end of the 8th hour, it reached a 90% cumulative release (Charernsriwilaiwat et al. 2013). In another study of Nguyen et al., curcumin loaded chitosan/gelatin sponges were produced for wound healing applications. Extract loaded chitosan/gelatin sponges showed 30% burst release in the first 6 hours. Extract loaded sponges was reached 90% cumulative release at the end of the 5 days (Nguyen, et al. 2013).

In this study, CQ was used as a bioactive herbal extract and according to our knowledge, there is no study in literature concerning the encapsulation of CQ extract into polymer matrix as a sustained release system. Besides, there is limited literature knowledge about the use of CQ extract for wound healing applications.

Mathematical relations corresponding to extract release during the incubation period were utilized to predict the release rate at the specified time. First-order, Higuchi, Korsmeyer-Peppas models were applied to determine release kinetics and the dominant

mechanism of CQ release from the bilayer wound dressing. Mathematical models were separately applied for two different regions of release data. The first region consists of the first 6 hours of the release data which is named as burst release, and the release data between the first and fourth days are consisted of the second region, named as sustained release. Mathematical models were applied to experimental data and correlated as shown in Figures 17-19.

It was found that First order, Higuchi and Korsmeyer-Peppas models fit the extract release data according to their high R^2 values. Korsmeyer-Peppas model is not only suitable for the Fickian diffusion-controlled system but also applicable for non-Fickian diffusion and case-2 transport. Non-Fickian diffusion has more than one mechanism that directs the release rate. Case-II transport is related to polymer swelling and disentanglement. The increment for the extract loading ratio on the fiber layer leads to the suitability of different mechanism types for wound dressings with different extract ratio. In this case, when considering the fiber layer as a thin film layer, it was found that Non-Fickian diffusion mechanism is a dominant mechanism for all samples where n is between 0.83-0.94. In a study, PVA/chitosan/ lidocaine hydrochloride nanofibers containing erythromycin loaded gelatin nanoparticles were produced by electrospinning method for wound dressing application. Korsmeyer-Peppas and Higuchi kinetic models were used to investigate the drug release mechanism. Drug release from polymer system was mostly fit to Korsmeyer-Peppas model with R^2 value of 0.98 (Fathollahipour et al. 2015). In another study, the release kinetics of sulfodazine loaded alginate/chitosan fibers were investigated. It was determined that the release of model drug, sulfodazine, matched First order model and the release mechanism was governed by the Korsmeyer-Peppas model (Sibaja et al. 2015). Das and his coworkers have produced curcumin loaded alginate/chitosan pluronic composite nanoparticles and investigated the release mechanism of curcumin. First order, Higuchi and Korsmeyer-Peppas were applied to the experimental data. R^2 value showed that release kinetic data of curcumin was best fitted to the Korsmeyer Peppas model. Also, It was found that anomalous transport is a dominant mechanism of curcumin release. (Das et al. 2010).
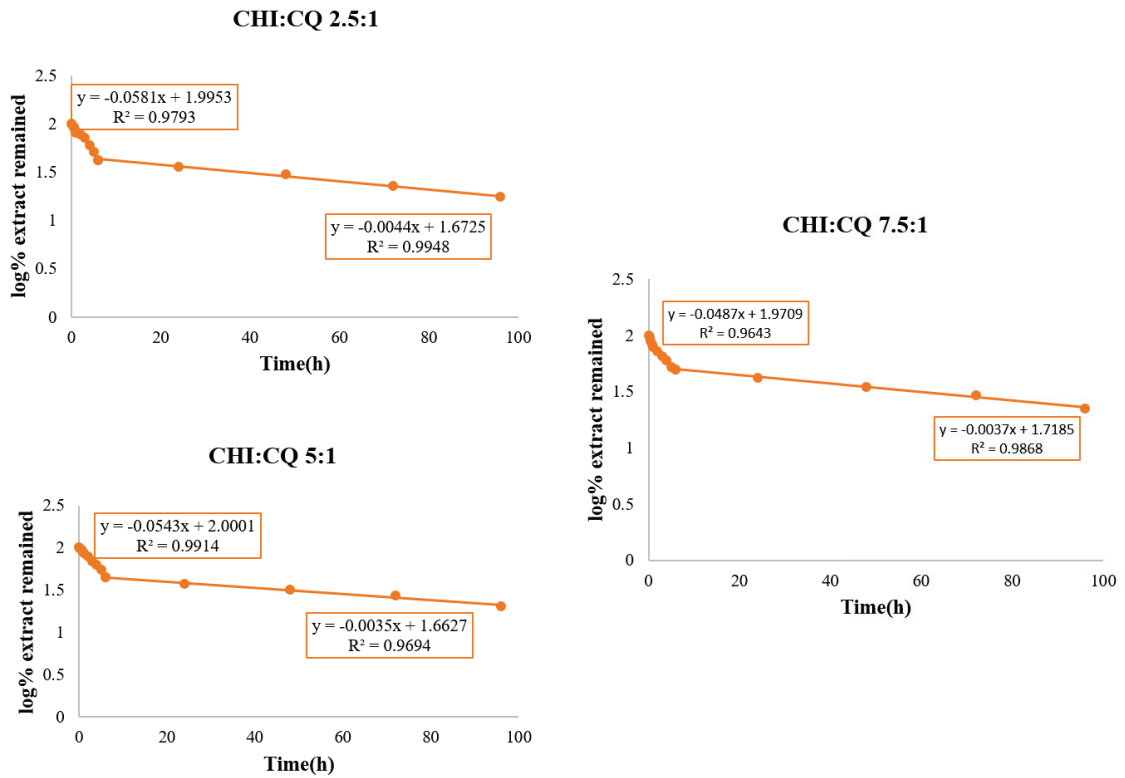
Figure 4. 17. First order release model for extract loaded bilayer dressings
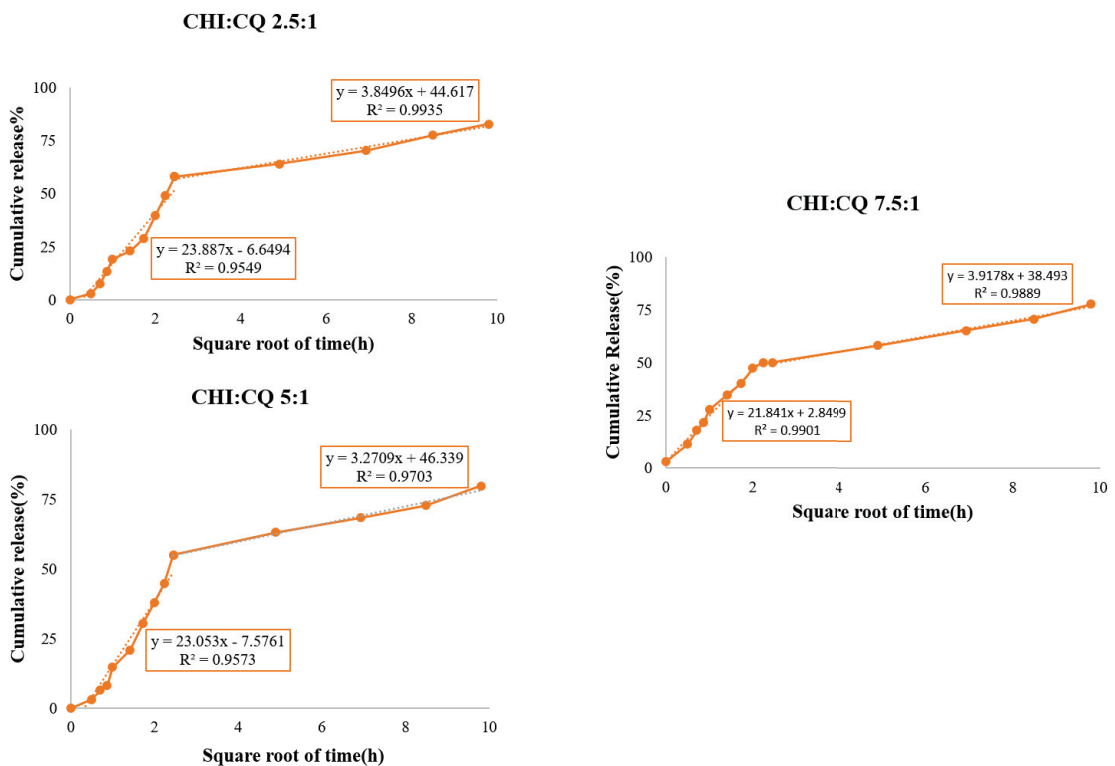
Figure 4. 18 Higuchi release model for extract loaded bilayer dressings

CHI:CQ 2.5:1

y = 0.8368x - 0.877
R² = 0.9563

CHI:CQ 7.5:1

y = 0.9418x - 0.4329
R² = 0.9215

CHI:CQ 5:1

y = 0.9038x - 0.6962
R² = 0.9792
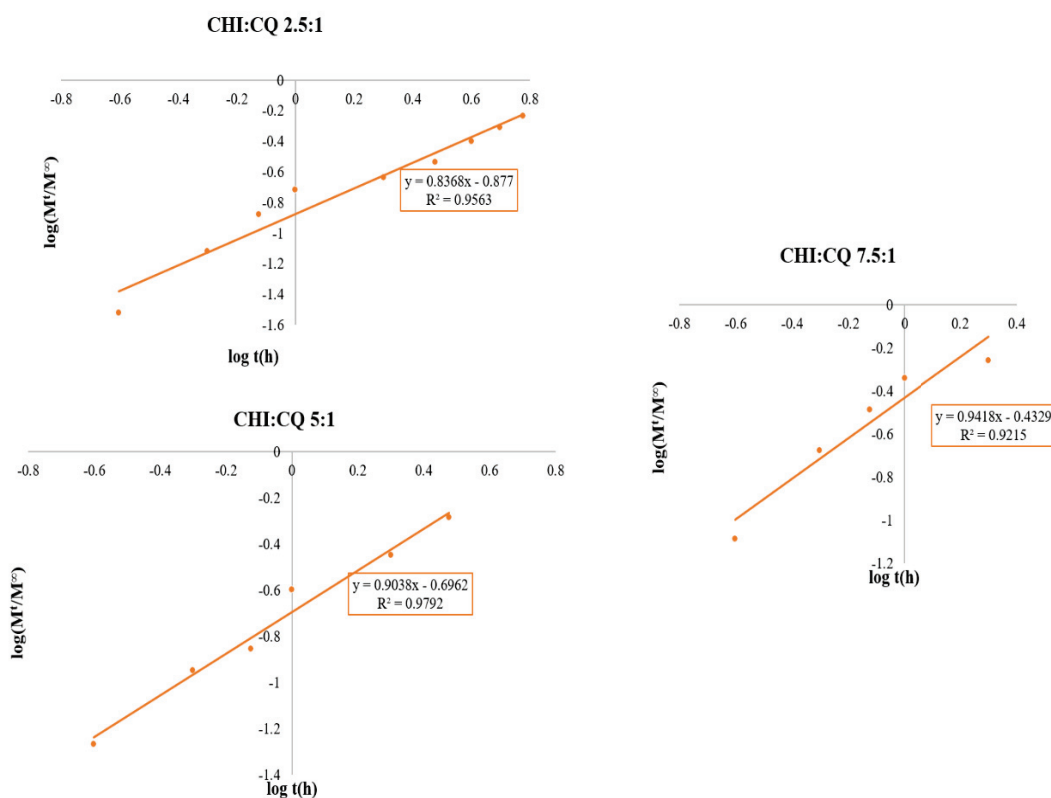
Figure 4. 19. Korsmeyer-Peppas release model for extract loaded bilayer dressings

4.3.2. Antimicrobial Activity

One of the most effective bacteria in wound infections is known as *S. epidermidis*. This bacterium can be caused by a peripheral skin and is frequently seen in wound infections. Another bacterium that is effective in wounds such as traumatic wounds and burns wounds is *E. coli*. These bacteria can cause infection in the wound area due to environmental causes (Gülay Görak 1997; Bowler et al. 2001). The use of antibiotics or bioactive extracts not only promotes wound healing but also protects the wound from bacterial infections. For this reason, in this study, CQ was used as a herbal extract to support wound healing and to prevent bacterial infections in wound. The antimicrobial activity of release media of bilayer dressings as well as ethanolic CQ extract was tested on gram-negative bacteria, *E. coli*, and gram-positive bacteria *S. epidermidis* with *in vitro* release media. In disc diffusion method, the release media of bilayer dressings (1h, 6h, and 24h) were dropped to the blank discs and after 24 hours of incubation, the inhibition zones around the disc were measured. The effect of the released CQ extracts on the inhibition of *E. coli* and *S. epidermidis* are shown in Figures 4.20 - 4.23.
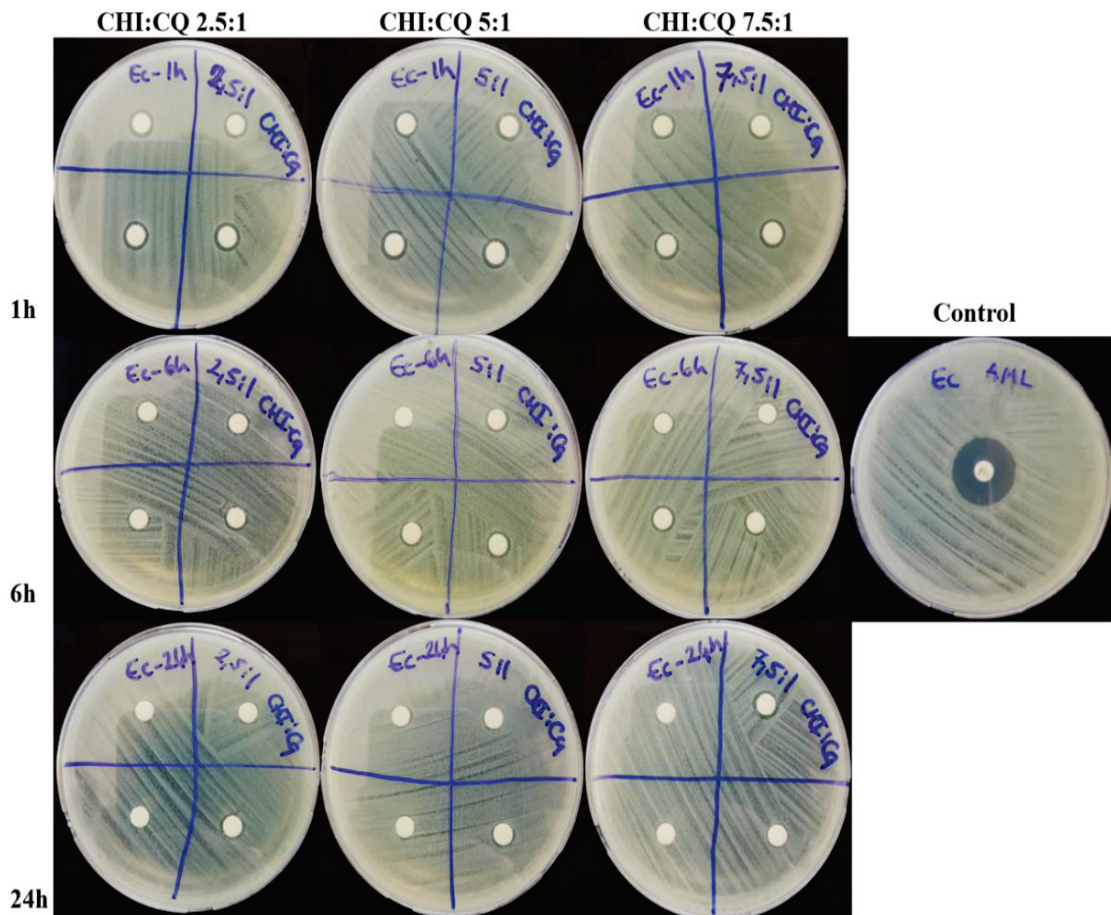
Figure 4. 20. Effect of Release media against *E. coli* at incubation times of 1hour, 6 hours and 24 hours
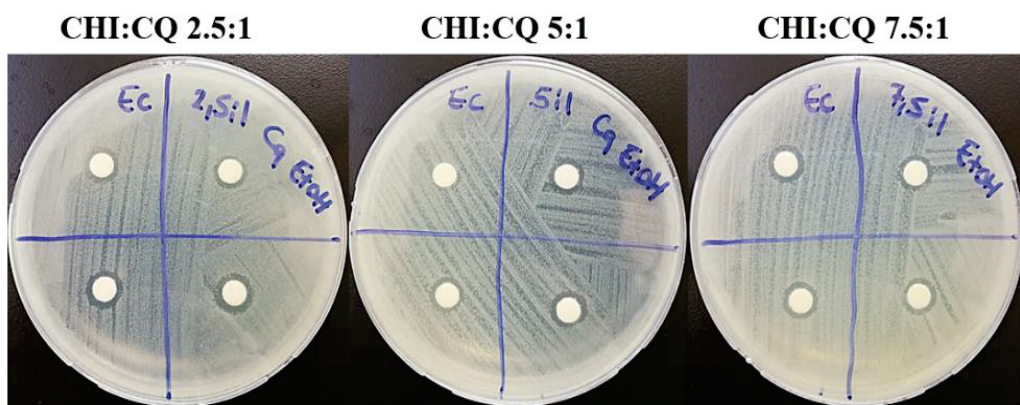
Figure 4. 21. Effect of CQ extract against gram negative bacteria for three different P:E ratios.
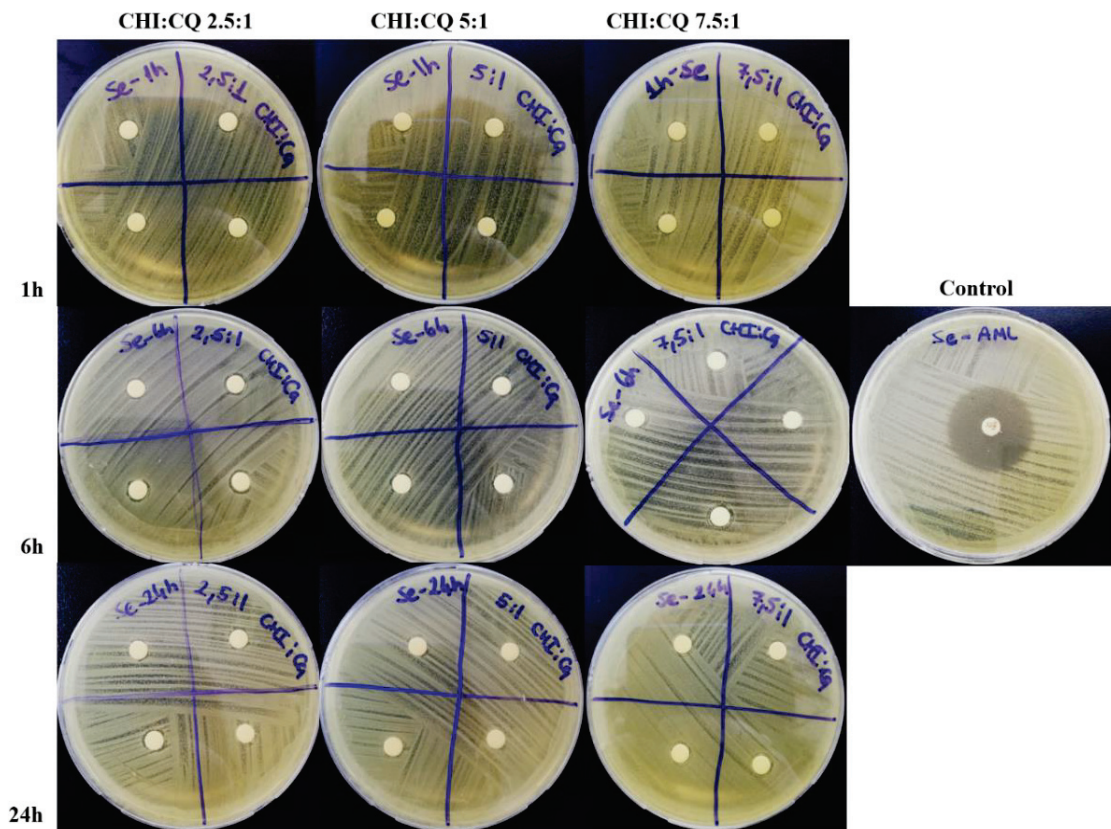
Figure 4. 22. Effect of Release media against *S. epidermidis* at incubation times of 1 hour, 6 hours and 24 hours
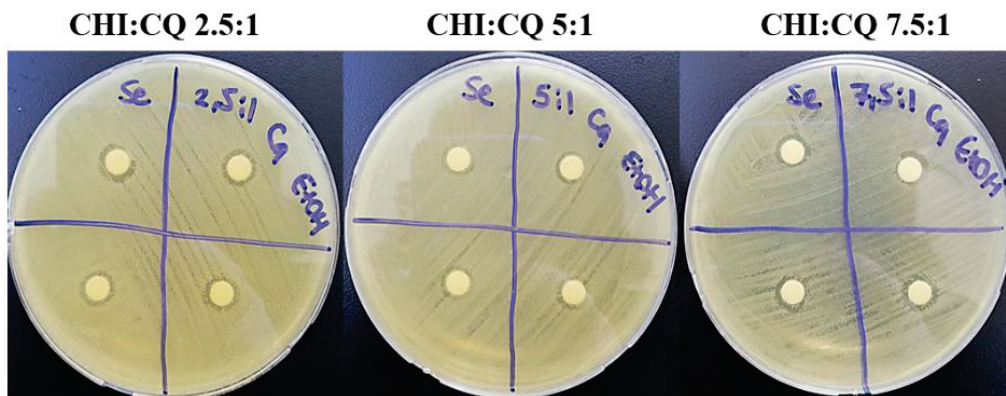
Figure 4. 23. Effect of CQ extract against gram positive bacteria for three different P:E ratios

Release media of bilayer dressing showed antimicrobial effect on both two pathogens when released in certain proportions. Also, the diameters of inhibition zones are shown in Tables 4.4 and 4.5. Release media of bilayer wound dressings and three different ratios of ethanolic CQ extract showed effective antimicrobial activity in the first hours for both two pathogens due to the burst release of the extract.

Also, when the ratio of ethanolic CQ extract increased, zone diameter increased. In addition, it was found that zone diameters obtained against *E. coli* and *S. epidermidis* increased with increasing CQ extract loading in bilayer wound dressings. It was also observed that the release media from bilayer dressings formed a larger zone diameter against *E.coli* compared to *S. epidermidis.*

Table 4. 4. Effect of *in vitro* release media (1h, 6h, 24h) against *E. coli*

Groups	Inhibition zone (mm)			
	1 hour	6 hours	24 hours	CQ extract
Positive control (Amoxicillin)	8			
CHI:CQ 2.5:1	1.62±0.08	1.40±0.10	1.30±0.12	2.18±0.09
CHI:CQ 5:1	1.00	0.96±0.03	0.86±0.06	2.00±0.01
CHI:CQ 7.5:1	1.00	0.83±0.08	1.00	1.89±0.08

Table 4. 5. Effect of *in vitro* release media (1h, 6h, 24h) against *S. epidermidis*

Groups	Inhibition zone (mm)			
	1 hour	6 hours	24 hours	CQ extract
Positive control (Amoxicillin)	11.00±0.30			
CHI:CQ 2.5:1	1.00±0.10	0.76±0.12	0.62±0.06	2.00±0.01
CHI:CQ 5:1	0.82±0.09	0.7±0.13	0.60±0.10	1.62±0.09
CHI:CQ 7.5:1	0.88±0.07	0.65±0.92	0.60±0.10	1.56±0.12

In the literature, it was observed that CQ extract showed antimicrobial activity against both gram negative and gram-positive bacteria (Chidambara Murthy et al. 2003; Jabamalai 2014; Kumar et al. 2017). The appropriate culture medium and temperature is provided for the growth of microorganisms in the antimicrobial test.

4.3.3. Fourier Transform Infrared Spectroscopy (FT-IR) Analysis

The characteristic peaks of chitosan, CQ and POSS as well as the chemical interaction between chitosan / POSS and chitosan-CQ were determined using FT-IR analysis. As seen in Figure 4.24, the main characteristic peaks of chitosan are C=O stretching (amide I) at 1651 cm^{-1} wavelength, N-H bending (amide II) at 1551cm^{-1} wavelength and C-N stretching and N-H bending of amide linkages at 1380cm^{-1}. (Baxter et al. 1992). When the characteristic peaks of POSS are examined, the Si-O-Si stress band are seen at wavelengths of 580 cm^{-1}, 1006 cm^{-1}, and 1095 cm^{-1}. The vibrations of the reactive groups of POSS nanocage (tetramethyl ammonium) were appeared at 1497 cm^{-1} and 1651 cm^{-1} (Tamburaci and Tihminlioglu 2018). Chitosan/POSS sponges showed characteristic peaks of both chitosan and POSS structures (Figure 4.24). Chitosan/POSS composite sponges showed slight shift in Si-O-Si peaks at 555-650 cm^{-1} ˌand 1070 cm^{-1} with stretching and bending vibrations, respectively. The main characteristic of chitosan and POSS were depicted in Table 4.
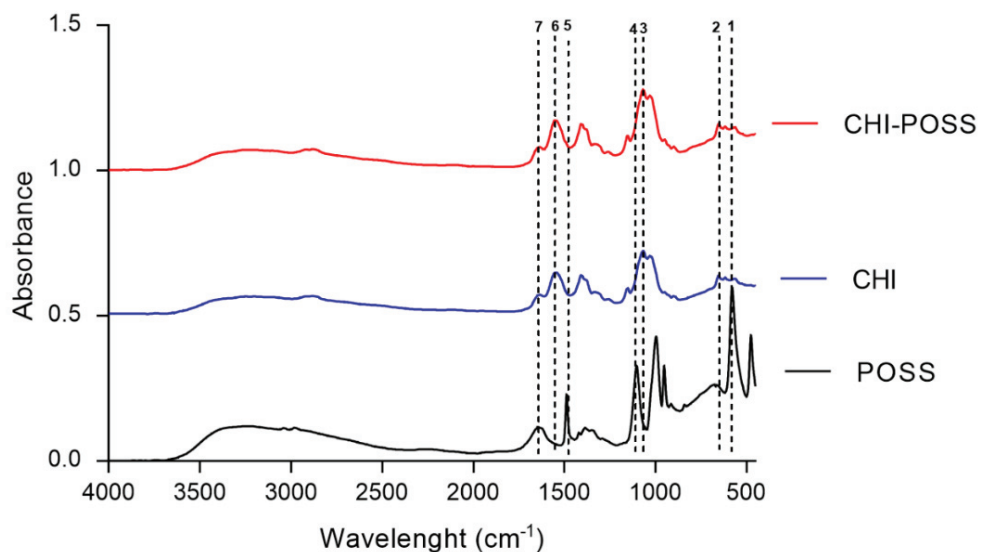
Figure 4. 24. FT-IR spectra of Chitosan, POSS and chitosan/POSS

The FT-IR spectrum of *Cissus quadrangularis* powder consists of characteristic bands appeared at 2922cm^{-1} and 2850 cm^{-1}(C-H stretching), 3220 cm^{-1} and 3290 cm^{-1} (OH stretching), between at 1600 cm^{-1} (C=O aromatic stretching) and ˏ at 1396 cm^{-1} (C-

O stretching of phenol and ester) and at 1036 cm^{-1} (the alkoxy C-O band) (Indran and Raj 2015; Soumya et al. 2012).

Table 4. 6. Characteristic bands of CHI and POSS

No	Wavenumber (cm^{-1})	Band	Formulation
1	580	Si-O-Si stretching	POSS
2	650	Si-O-Si stretching	POSS
3	1070	Si-O-Si bending	POSS
4	1095	Si-O-Si stretching	POSS
5	1497	Tetramethylammonium	POSS
6	1551	N-H bending (amide II)	CHI
7	1651	C=O stretching (amide I)	CHI
7	1651	Tetramethylammonium	POSS

Figure 4.25. shows the FT-IR spectra of extract loaded bilayer sponges with different extract concentrations. as well as chitosan fiber coated bilayer sponges as a control group. The main peaks of chitosan were appeared at for all samples, however the characteristic peak of CQ (at 2922 cm^{-1} and 2852 cm^{-1}) was only observed for high extract loaded nanospheres coating (P: E ratio of 2.5).
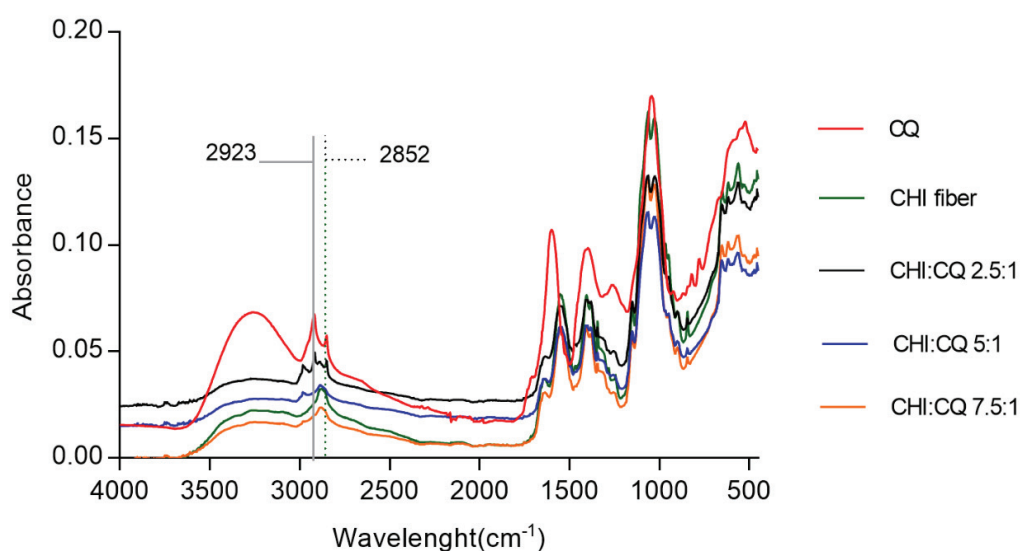
Figure 4. 25. FT-IR spectra of CHI fiber coated bilayer sponges with different P:E ratios

4.3.4. Swelling Study

Swelling tests were performed to determine the liquid absorption capacity of single and bilayer wound dressings. Swelling tests were calculated according to weight changes of samples at 4h, 24h, and 48h in 1xPBS. The swelling percentages of single and bilayer wound dressings are shown in Figure 4.26. Swelling results showed that water absorption capacity chitosan increased at 24h and decreased at 48 h due to the low stability of chitosan. According to statistical analysis, there is a significant difference in swelling % of chitosan control group (CHI) for 4 h and 24 h also, 24 and 48 h. However, POSS nanoparticle incorporation in chitosan matrix enhanced the swelling % for all incubation times.
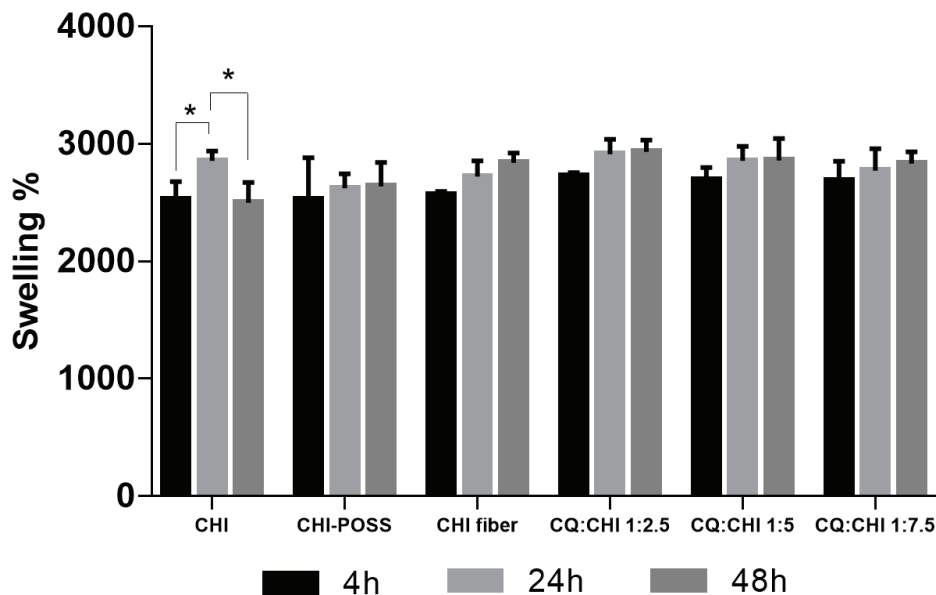
Figure 4. 26. The swelling percentages of single and bilayer wound dressings for 4, 24 and 48 h

When swelling behavior of bilayer dressings were examined, they exhibited the same swelling trend at 4 h, 24 h, and 48 h. Results indicated that chitosan nanofiber and CQ loaded chitosan nanofiber layers showed similar swelling % and increasing trend during 48 hours of incubation. Since the nanofiber layer is very thin layer compared to sponge layer, no increase in swelling % of bilayer wound dressings is expected.

4.3.5. Open Porosity Measurement by Liquid Displacement

The open porosity of the monolayer and bilayer wound dressings were determined by liquid displacement. Table 4.7 shows open porosity percentages of single layer and bilayer wound dressings. The porosity % of the single layer and bilayer sponges were found very similar. The open porosity % of the chitosan sponge was found to be 81.23 ± 1.4. POSS nanoparticle incorporation caused a slight decrease in open porosity of chitosan composite due to enlarging the pore wall surface and thickening of the walls of the sponges. The open porosity % of bilayer dressings were found between 77.56 ± 3.4. and 79.36 ± 4.0. The coating of chitosan/POSS composite sponges with and without CQ extract loaded nanofibers did not affect the open porosity.

Table 4. 7. Open porosity percentages of single layer and bilayer sponges

Groups	Open Porosity (%)
CHI	81.23±1.38
CHI/POSS	77.51±3.43
CHI fiber wo CQ	78.33±2.00
CHI:CQ 2.5:1	78.93±2.67
CHI:CQ 5:1	79.36±3.96
CHI:CQ 7.5:1	77.56±1.94

4.3.6. Water Vapor Transmission Rate

Water vapor permeability is an important feature in wound healing which affects the humidity at the wound site. Wound dressing should absorb excess fluid on the wound area. The wound should be kept at the proper humidity. The water vapor permeability of normal human skin is 204 g/m^2day. The ideal wound dressing should have water vapor permeability value in the range of 279-5138 g/m^2day depending on the wound type (Patel et al. 2018). In this study, water vapor permeability of chitosan, chitosan/POSS sponge, and bilayer sponges were investigated. Table 4.8 gives experimental permeability values of single layer chitosan, chitosan/POSS sponge and the bilayer sponge loaded with three

different CQ extract ratios The water vapor permeability of the single layer and bilayer sponges was found in the range of the ideal wound dressings.

Table 4. 8. WVP and WVTR values of single layer and bilayer layer sponges

Groups	WVP x 10^5 (mol min^{-1} cm^{-1} kPa^{-1})	WVTR (g m^{-2} day^{-1})
CHI	2.95±0.15	4251.97±150
CHI/POSS	3.15±0.54	4609.06±13
CHI:CQ 2.5:1	2.60±0.5	4013.16±36
CHI:CQ 5:1	2.60±0.4	4021.29±300
CHI:CQ 7.5:1	2.95±0.05	4243.1±330

The water vapor permeability of chitosan/POSS sponges was increased when the POSS nanoparticles were added to the chitosan matrix. However, nanofiber coated sponges showed reduced water vapor permeability. As the permeability pathway in the nanofiber coated sponges is slightly higher than that of the single chitosan/POSS sponge layer permeability decreases in the expected direction (Thu et al. 2012). At the same time, the nanofiber coating closed the surface pores of sponge. Thus, the permeability of sponge layer is reduced with nanofiber coating. Nanofibers prepared at different extract concentrations did not have a significant effect on the permeability of the bilayer sponges. When literature studies based on the permeability values of chitosan dressings were examined, it was found that the water vapor permeability of chitosan-based double layer dressings is 2137 g/m^2 day In another study, chitosan/gelatin hydrogels were prepared for wound healing. The water vapor permeability of hydrogels was found to be 2228 ± 31.8 g/ m^{2}day (Patel et al. 2018). It is very important for wound healing to have appropriate water vapor permeability. The bilayer layer dressings, which produced in the study, are in the ideal dressing range.

4.3.7. Mechanical Properties

Mechanical properties of single layer and bilayer dressings were examined with tension test in terms of tensile strength and Young's modulus. The tensile strength can be

stated as the maximum stress of the sponges in the unit area. Young's modulus and tensile strength results of single layer and bilayer dressings are given in Figures 4.27. and 4.28. The Young's moduli of single layer and bilayer dressings are in the range of 48.02 to 80.29 kPa. It was observed that Young's moduli of the sponges increased with the contribution of POSS nanoparticles to chitosan matrix. Generally, inorganic additives improve the mechanical properties polymers. Tamburaci&Tihminlioglu fabricated chitosan/diatom composite membranes and investigated the effect of diatom incorporation in terms of mechanical properties. Results showed that Young's moduli of composite membranes increased as the diatom content of chitosan membrane increased. Young's modulus of chitosan and composite membranes were found between 13.5-25.9 MPa (Tamburaci and Tihminlioglu 2017). Similarly, POSS incorporation into chitosan sponge matrix enhanced the mechanical properties of chitosan matrix. In addition, Young moduli of nanofiber coated sponge groups slightly decreased due to the formation of bilayer structure which has non-uniform morphology. However, nanofiber coating did not significantly affect the mechanical properties. When the Young modulus values of a natural skin are examined, it was seen that Young modulus values are changed between 5 kPa and 140 kPa depending on the skin region of body (Kalra et al. 2016).
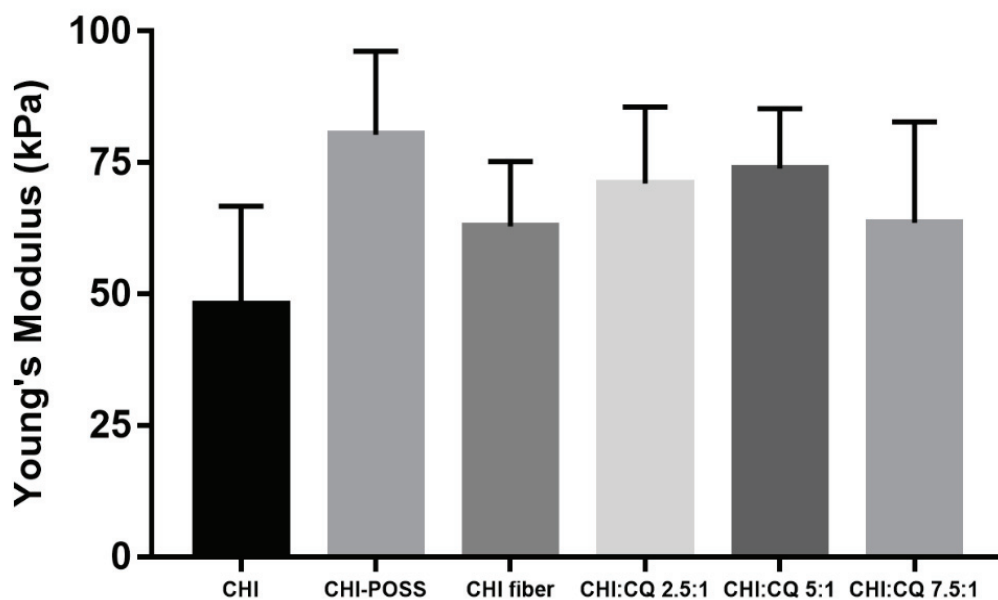
Figure 4. 27. Young's Module of single and bilayer wound dressings

When tensile strengths were examined, it was observed the contribution of POSS nanoparticles increased tensile strength chitosan sponge. In the literature, chitosan /POSS composite films were prepared by solvent casting method. It was observed that the POSS addition dramatically increased the tensile strength of chitosan membranes (Tamburaci and Tihminlioglu 2018). In this study, chitosan/POSS composites were fabricated with different method and porous sponge structures were obtained. Unlike literature, tensile strength values were found at lower. In the literature, the tensile strength of chitosan and chitosan / POSS films is 34.37 MPa and 60.28 MPa, respectively. In this study, the tensile strength of Chitosan and Chitosan / POSS sponges is found much lower values as 1.88 kPa and 3.17 kPa, respectivelt due to the porous sponge structure.
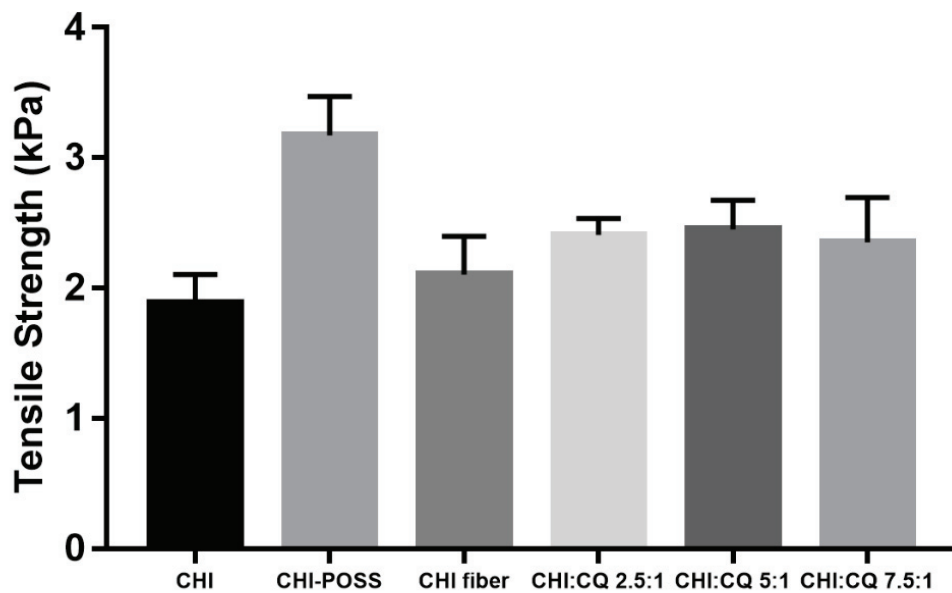
Figure 4. 28. Tensile Strength of single and bilayer wound dressings

4.3.8. *In Vitro* Cytotoxicity Determination

Cell viability of single layer and bilayer wound dressings was determined with WST-1 assay. It is known that fibroblast cells are mostly involved in wound healing process, especially in the proliferation phase (Güneş and Tıhmınlıoğlu 2017). In this study, NIH/3T3 fibroblast cells were used to investigate the *in vitro* cytotoxicity. Figure 4.29. shows the viability (%) of NIH/3T3 fibroblast cells incubated with the single layer

and bilayer wound dressings extraction media for 24 h, 48 h and 72 h. Single layer and bilayer wound dressings did not show any cytotoxic effects on fibroblast cells. In addition, it was observed that all groups have high cell viability. In addition, the highest cell viability (%) was observed for the bilayer sponge consisting of the polymer :extract ratio 2.5:1 and statistical significant difference in P:E 2.5:1 ratio group was obtained between 12 to 48 h and 48 to 72 h incubation times.
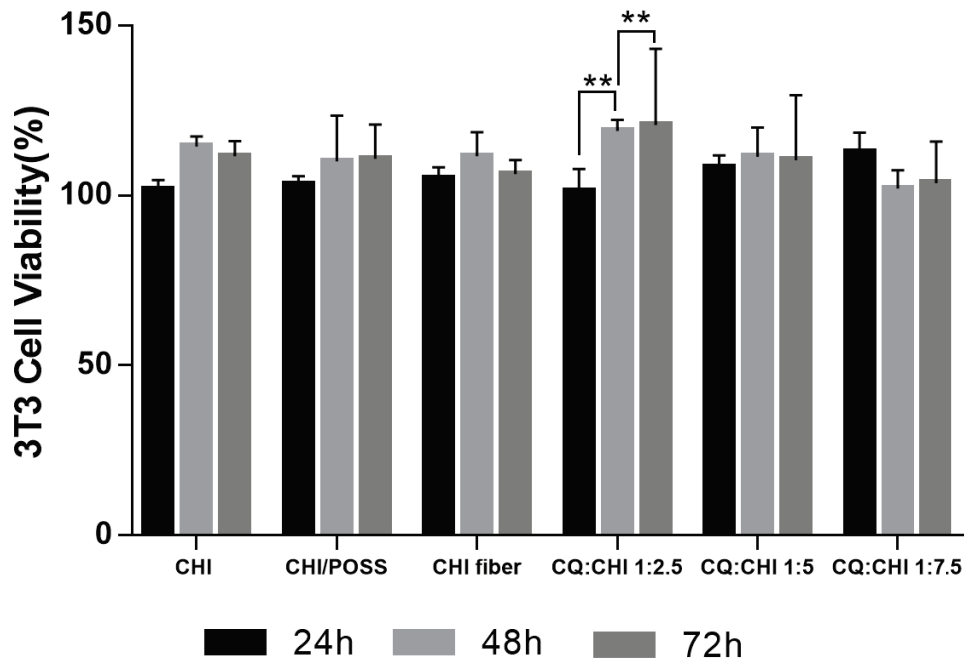
Figure 4. 29. *In vitro* Cytotoxicity of single and bilayer wound dressings

CHAPTER 5

CONCLUSIONS

Natural extracts contribute significantly to wound healing because of their advantages, but undesirable reactions can occur when directly applied to the wound. Thus, the extracts encapsulate into a polymer and controlled release is applied to the wound area to prevent these side effects.

The main objective of this study is to provide controlled extract release from *Cissus quadrangularis* loaded chitosan nanofiber coated chitosan/POSS nanocomposite sponges.

In this study, two different morphologies were used as the upper layer. Firstly, electrospray and electrospinning working parameters were optimized in order to produce smooth morphology and high encapsulation efficiency of CQ in nanospheres and nanofibers. The parameters were optimized and then the nanospheres were coated on the sponge. The mean distribution of the nanosphere sizes was found in the range of 87-738 nm and the average diameter for nanofiber was 77.9±4 nm. The encapsulation efficiencies of the nanospheres and nanofibers with CQ were determined as 76.48±3.63 and 70.17±2.12%, respectively. Then the release profiles of nanospheres and nanofibers coated sponges were investigated. The release studies were analyzed, genipin crosslinker was used to control the burst release. Firstly, the release profile of two different morphology coated sponges was examined, it was observed that nanospheres coated sponges released the extract faster. It was found that the release of extracts from the nanospheres coated sponges was 78% within 6 hours, however 49% of the extract was released in the first 6 hours and at the end of the 4th day, it reached 78% cumulative release for the nanofiber coated sponges. The stability of the nanofibers was found to be better than nanospheres ones due to the slower decomposition, thus resulting in a faster release in nanosphere coated sponges than the nanofiber coated sponges. For this reason, the nanofiber structure was chosen as the upper layer for further sponge production. It was found that the release medium obtained from bilayer sponges showed antimicrobial activity against *E. coli* and *S. epidermidis*.

The addition of POSS nanoparticles into sponges decreased porosity from 81.23 $\pm$ 1% to 77.51 $\pm$ 3%, because of the addition of POSS nanoparticles thickness the walls of the sponge. It was observed that, due to the low stability of the chitosan, swelling percentages increased at 24 hours and decreased at 48 hours. The addition of POSS ensured the swelling to be in a more controlled manner. The incorporation of POSS nanoparticles into the sponge structure resulted in improved mechanical properties. Young's modulus was increased from 48.02 kPa to 80.29 kPa with the contribution of POSS. Also, tensile strength was increased from 1.88 kPa to 3.17 kPa with the addition of POSS. In addition, POSS incorporation increased the permeability of the chitosan sponges. However, the permeability of nanofiber coated chitosan / POSS composite sponges was lower than the permeability of chitosan single layer sponge and has suitable value for wound dressing applications. Cytotoxicity results show that single and bilayer wound dressings did not show any toxic effects on fibroblast cells. In fact, the P:E ratio of 2.5:1 bilayer wound dressings showed the best increase in cell viability (%).

In conclusion, when these results were evaluated, CQ loaded bilayer wound dressings showed promising effects on wound healing. In future studies, bilayer dressings can be tested *in vitro* and *in vivo* studies to better understand the effect of natural extracts in wound healing mechanisms.

REFERENCES

A. Mohanty, P.K. Sahu, C.Das. 1Arnabaditya Mohanty, and Associate. 2010. "Wound Healing Activity of Methanolic Extract of Cissus." *International Journal of Drug Formulation & Research* 1 (2): 176–84.

A, Kalra, Lowe A, and Al-Jumaily AM. 2016. "Mechanical Behaviour of Skin: A Review." *Journal of Material Science & Engineering* 5 (4): 1–7.

Abdel-Mohsen, A.M., J. Jancar, D. Massoud, Z. Fohlerova, H. Elhadidy, Z. Spotz, and A. Hebeish. 2016. "Novel Chitin/Chitosan-Glucan Wound Dressing: Isolation, Characterization, Antibacterial Activity and Wound Healing Properties." *International Journal of Pharmaceutics* 510 (1): 86–99.

Adeli, Hassan, Mohammad Taghi Khorasani, and Mahmoud Parvazinia. 2019. "Wound Dressing Based on Electrospun PVA/Chitosan/Starch Nanofibrous Mats: Fabrication, Antibacterial and Cytocompatibility Evaluation and in Vitro Healing Assay." *International Journal of Biological Macromolecules* 122 (February): 238–54.

Altiok, Duygu, Evren Altiok, and Funda Tihminlioglu. 2010. "Physical, Antibacterial and Antioxidant Properties of Chitosan Films Incorporated with Thyme Oil for Potential Wound Healing Applications." *Journal of Materials Science: Materials in Medicine* 21 (7): 2227–36.

Anisha, B.S., Raja Biswas, K.P. Chennazhi, and R. Jayakumar. 2013. "Chitosan–hyaluronic Acid/Nano Silver Composite Sponges for Drug Resistant Bacteria Infected Diabetic Wounds." *International Journal of Biological Macromolecules* 62 (November): 310–20.

Anjum, Sadiya, Abha Arora, M.S. Alam, and Bhuvanesh Gupta. 2016. "Development of Antimicrobial and Scar Preventive Chitosan Hydrogel Wound Dressings." *International Journal of Pharmaceutics* 508 (1–2): 92–101.

Aravinthan, Adithan, Jeong-Kyu Park, Mohammad Amjad Hossain, Judith Sharmila, Han-Jong Kim, Chang-Won Kang, Nam Soo Kim, and Jong-Hoon Kim. 2018. "Collagen-Based Sponge Hastens Wound Healing via Decrease of Inflammatory Cytokines." *3 Biotech* 8 (12): 487.

Baum, Christian L, and Christopher J Arpey. 2005. "Normal Cutaneous Wound Healing: Clinical Correlation with Cellular and Molecular Events." *Dermatologic Surgery : Official Publication for American Society for Dermatologic Surgery [et Al.]* 31 (6): 674–86; discussion 686.

Baxter, Alasdair, Michael Dillon, K.D. Anthony Taylor, and George A.F. Roberts. 1992. "Improved Method for i.r. Determination of the Degree of N-Acetylation of Chitosan." *International Journal of Biological Macromolecules* 14 (3): 166–69.

Belščak-Cvitanović, Ana, Radoslava Stojanović, Verica Manojlović, Draženka Komes, Iva Juranović Cindrić, Viktor Nedović, and Branko Bugarski. 2011. "Encapsulation of Polyphenolic Antioxidants from Medicinal Plant Extracts in

Alginate–chitosan System Enhanced with Ascorbic Acid by Electrostatic Extrusion." *Food Research International* 44 (4): 1094–1101.

Berezina, Nathalie. 2016. "Production and Application of Chitin." *Physical Sciences Reviews* 1 (9).

Bhardwaj, Nandana, and Subhas C. Kundu. 2010. "Electrospinning: A Fascinating Fiber Fabrication Technique." *Biotechnology Advances* 28 (3): 325–47.

Bhattarai, Narayan, Dennis Edmondson, Omid Veiseh, Frederick A. Matsen, and Miqin Zhang. 2005. "Electrospun Chitosan-Based Nanofibers and Their Cellular Compatibility." *Biomaterials* 26 (31): 6176–84.

Boateng, Joshua S., Kerr H. Matthews, Howard N.E. Stevens, and Gillian M. Eccleston. 2008. "Wound Healing Dressings and Drug Delivery Systems: A Review." *Journal of Pharmaceutical Sciences* 97 (8): 2892–2923.

Bowler, P. G., B. I. Duerden, and D. G. Armstrong. 2001. "Wound Microbiology and Associated Approaches to Wound Management." *Clinical Microbiology Reviews* 14 (2): 244–69.

Charernsriwilaiwat, Natthan, Praneet Opanasopit, Theerasak Rojanarata, and Tanasait Ngawhirunpat. 2012. "Lysozyme-Loaded, Electrospun Chitosan-Based Nanofiber Mats for Wound Healing." *International Journal of Pharmaceutics* 427 (2): 379–84.

Charernsriwilaiwat, Natthan, Theerasak Rojanarata, Tanasait Ngawhirunpat, Monrudee Sukma, and Praneet Opanasopit. 2013. "Electrospun Chitosan-Based Nanofiber Mats Loaded with Garcinia Mangostana Extracts." *International Journal of Pharmaceutics* 452 (1–2): 333–43.

Chen, Jyh-Ping, Gwo-Yun Chang, and Jan-Kan Chen. 2008. "Electrospun Collagen/Chitosan Nanofibrous Membrane as Wound Dressing." *Colloids and Surfaces A: Physicochemical and Engineering Aspects* 313–314 (February): 183–88.

Chen, Z.G., P.W. Wang, B. Wei, X.M. Mo, and F.Z. Cui. 2010. "Electrospun Collagen–chitosan Nanofiber: A Biomimetic Extracellular Matrix for Endothelial Cell and Smooth Muscle Cell." *Acta Biomaterialia* 6 (2): 372–82.

Chidambara Murthy, K.N., A. Vanitha, M. Mahadeva Swamy, and G.A. Ravishankar. 2003. "Antioxidant and Antimicrobial Activity of *Cissus Quadrangularis* L." *Journal of Medicinal Food* 6 (2): 99–105.

Dai, Mei, XiuLing Zheng, Xu Xu, XiangYe Kong, XingYi Li, Gang Guo, Feng Luo, Xia Zhao, Yu Quan Wei, and Zhiyong Qian. 2009. "Chitosan-Alginate Sponge: Preparation and Application in Curcumin Delivery for Dermal Wound Healing in Rat." *Journal of Biomedicine and Biotechnology* 2009: 1–8.

Dai, Tianhong, Masamitsu Tanaka, Ying-Ying Huang, and Michael R Hamblin. 2011. "Chitosan Preparations for Wounds and Burns: Antimicrobial and Wound-Healing Effects." *Expert Review of Anti-Infective Therapy* 9 (7): 857–79.

Das, Ratul Kumar, Naresh Kasoju, and Utpal Bora. 2010. "Encapsulation of Curcumin in Alginate-Chitosan-Pluronic Composite Nanoparticles for Delivery to Cancer Cells." *Nanomedicine: Nanotechnology, Biology and Medicine* 6 (1): 153–60.

Daunton, C, S Kothari, L Smith, and D Steele. 2012. "A History of Materials and Practices for Wound Management." *Wound Practice & Research: The Australian Journal of Wound Management* 20 (4): 174–86.

Deepthi, S., K. Jeevitha, M. Nivedhitha Sundaram, K.P. Chennazhi, and R. Jayakumar. 2015. "Chitosan–hyaluronic Acid Hydrogel Coated Poly(Caprolactone) Multiscale Bilayer Scaffold for Ligament Regeneration." *Chemical Engineering Journal* 260 (January): 478–85.

Degreef, H J. 1998. "How to Heal a Wound Fast." *Dermatologic Clinics* 16 (2): 365–75.

Dhivya, Selvaraj, Viswanadha Vijaya Padma, and Elango Santhini. 2015. "Wound Dressings – a Review." *BioMedicine* 5 (4): 22.

Dhurai, Bhaarathi, Nachimuthu Saraswathy, Ramasamy Maheswaran, Ponnusamy Sethupathi, Palanisamy Vanitha, Sukumar Vigneshwaran, and Venugopal Rameshbabu. 2013. "Electrospinning of Curcumin Loaded Chitosan/Poly (Lactic Acid) Nanofilm and Evaluation of Its Medicinal Characteristics." *Frontiers of Materials Science* 7 (4): 350–61.

Díez-Pascual, Ana M., and Angel L. Díez-Vicente. 2015. "Wound Healing Bionanocomposites Based on Castor Oil Polymeric Films Reinforced with Chitosan-Modified ZnO Nanoparticles." *Biomacromolecules* 16 (9): 2631–44.

Fan, Lihong, Huan Yang, Jing Yang, Min Peng, and Jin Hu. 2016. "Preparation and Characterization of Chitosan/Gelatin/PVA Hydrogel for Wound Dressings." *Carbohydrate Polymers* 146 (August): 427–34.

Fathollahipour, Shahrzad, Ali Abouei Mehrizi, Azadeh Ghaee, and Mojtaba Koosha. 2015. "Electrospinning of PVA/Chitosan Nanocomposite Nanofibers Containing Gelatin Nanoparticles as a Dual Drug Delivery System." *Journal of Biomedical Materials Research Part A* 103 (12): 3852–62.

Firat Öztopalan, Dicle, Recep Işik, Ali Said Durmuş, Bağlar İlçe Gıda, and Tarım ve Hayvancılık Müdürlüğü. 2017. "Dicle Üniv Vet Fak Derg." Vol. 10.

Fullana, Matthew J., and Gary E. Wnek. 2012. "Electrospun Collagen and Its Applications in Regenerative Medicine." *Drug Delivery and Translational Research* 2 (5): 313–22.

Geng, Xinying, Oh Hyeong Kwon, and Jinho Jang. 2005. "Electrospinning of Chitosan Dissolved in Concentrated Acetic Acid Solution." *Biomaterials* 26 (27): 5427–32.

Gholipour Kanani, A., and S. Hajir Bahrami. 2010. "Review on Electrospun Nanofibres Scaffold and Biomedical Applications." *Trends in Biomaterials and Artificial Organs* 24 (2): 93–115.

Goh, Yi-Fan, Imran Shakir, and Rafaqat Hussain. 2013. "Electrospun Fibers for Tissue Engineering, Drug Delivery, and Wound Dressing." *Journal of Materials Science* 48 (8): 3027–54.

Gülay Görak. 1997. "Yogun Bakım Ünitelerinde Hastane Enfeksiyonlarının İnlenmesi[#278814]-260180.Pdf."

Güneş, Seda, and Funda Tıhmınlıoğlu. 2017. "Hypericum Perforatum Incorporated Chitosan Films as Potential Bioactive Wound Dressing Material." *International Journal of Biological Macromolecules* 102 (September): 933–43.

Hafezi, Forough, Nikolaos Scoutaris, Dennis Douroumis, and Joshua Boateng. 2019. "3D Printed Chitosan Dressing Crosslinked with Genipin for Potential Healing of Chronic Wounds." *International Journal of Pharmaceutics* 560 (April): 406–15.

Hani, Norziah M, Amir E Torkamani, Mohammad H Azarian, Kamil WA Mahmood, and Siti Hawa Ngalim. 2017. "Characterisation of Electrospun Gelatine Nanofibres Encapsulated with *Moringa Oleifera* Bioactive Extract." *Journal of the Science of Food and Agriculture* 97 (10): 3348–58.

Hanna, James R., and Joseph A. Giacopelli. 1997. "A Review of Wound Healing and Wound Dressing Products." *The Journal of Foot and Ankle Surgery* 36 (1): 2–14.

Indran, S., and R. Edwin Raj. 2015. "Characterization of New Natural Cellulosic Fiber from Cissus Quadrangularis Stem." *Carbohydrate Polymers* 117: 392–99.

Joodaki, Hamed, and Matthew B Panzer. 2018. "Skin Mechanical Properties and Modeling: A Review." *Proceedings of the Institution of Mechanical Engineers, Part H: Journal of Engineering in Medicine* 232 (4): 323–43.

Kanitakis, Jean. 2002. "Anatomy, Histology and Immunohistochemistry of Normal Human Skin." *European Journal of Dermatology : EJD* 12 (4): 390-9; quiz 400-1.

Khang, Dongwoo, Joseph Carpenter, Young Wook Chun, Rajesh Pareta, and Thomas J. Webster. 2010. "Nanotechnology for Regenerative Medicine." *Biomedical Microdevices* 12 (4): 575–87.

Kimna, Ceren, Sedef Tamburaci, and Funda Tihminlioglu. 2018. "Novel Zein-Based Multilayer Wound Dressing Membranes with Controlled Release of Gentamicin." *Journal of Biomedical Materials Research Part B: Applied Biomaterials*, December.

Kolarsick, Paul A. J., Maria Ann Kolarsick, and Carolyn Goodwin. 2011. "Anatomy and Physiology of the Skin." *Journal of the Dermatology Nurses' Association* 3 (4): 203–13.

Kondo, Shinya, and Yoshimitsu Kuroyanagi. 2012. "Development of a Wound Dressing Composed of Hyaluronic Acid and Collagen Sponge with Epidermal Growth Factor." *Journal of Biomaterials Science, Polymer Edition* 23 (5): 629–43.

Kruglikov, Ilja L. 2016. "Influence of the Dermis Thickness on the Results of the Skin Treatment with Monopolar and Bipolar Radiofrequency Currents." *BioMed Research International* 2016.

Kumar, Mangesh, Tamanna Talreja, Dinesh Jain, Asha Goswami, Tribhuwan Sharma, Correspondence Mangesh Kumar, and RK Dhuria. 2017. "Comparative Evaluation of in Vitro Antibacterial Activity of Several Extracts of Achyranthes Aspera, Azolla Pinnata, Cissus Quadrangularis and Tinospora Cordifolia." ~ *154* ~ *International Journal of Chemical Studies* 5 (1): 154–57.

Kumari, Avnesh, Sudesh Kumar Yadav, and Subhash C. Yadav. 2010. "Biodegradable Polymeric Nanoparticles Based Drug Delivery Systems." *Colloids and Surfaces B: Biointerfaces* 75 (1): 1–18.

Kurečič, Manja, and Majda Sfiligoj Smole. 2016. "Electrospinning: Nanofibre Production Method." *Tekstilec* 56 (1): 4–12.

Laçin, Nelisa Türkoğlu. 2014. "Development of Biodegradable Antibacterial Cellulose Based Hydrogel Membranes for Wound Healing." *International Journal of Biological Macromolecules* 67 (June): 22–27.

Lai, Jui-Yang, Lai, and Jui-Yang. 2012. "Biocompatibility of Genipin and Glutaraldehyde Cross-Linked Chitosan Materials in the Anterior Chamber of the Eye." *International Journal of Molecular Sciences* 13 (9): 10970–85.

Lee, Ok Joo, Jung-Ho Kim, Bo Mi Moon, Janet Ren Chao, Jaeho Yoon, Hyung Woo Ju, Jung Min Lee, et al. 2016. "Fabrication and Characterization of Hydrocolloid Dressing with Silk Fibroin Nanoparticles for Wound Healing." *Tissue Engineering and Regenerative Medicine* 13 (3): 218–26.

Li, Lei, and You-Lo Hsieh. 2006. "Chitosan Bicomponent Nanofibers and Nanoporous Fibers." *Carbohydrate Research* 341 (3): 374–81.

Li, Qin, Xianliu Wang, Xiangxin Lou, Huihua Yuan, Hongbin Tu, Biyun Li, and Yanzhong Zhang. 2015. "Genipin-Crosslinked Electrospun Chitosan Nanofibers: Determination of Crosslinking Conditions and Evaluation of Cytocompatibility." *Carbohydrate Polymers* 130 (October): 166–74.

Li, XingYi, KaiHui Nan, Shuai Shi, and Hao Chen. 2012. "Preparation and Characterization of Nano-Hydroxyapatite/Chitosan Cross-Linking Composite Membrane Intended for Tissue Engineering." *International Journal of Biological Macromolecules* 50 (1): 43–49.

Liu, Bai-Shuan, Chun-Hsu Yao, and Shr-Shin Fang. 2008. "Evaluation of a Non-Woven Fabric Coated with a Chitosan Bi-Layer Composite for Wound Dressing." *Macromolecular Bioscience* 8 (5): 432–40.

Liu, Shih-Jung, Yi-Chuan Kau, Chi-Yin Chou, Jan-Kan Chen, Ren-Chin Wu, and Wen-Ling Yeh. 2010. "Electrospun PLGA/Collagen Nanofibrous Membrane as Early-Stage Wound Dressing." *Journal of Membrane Science* 355 (1–2): 53–59.

Ma, Ye, Lian Xin, Huaping Tan, Ming Fan, Jianliang Li, Yang Jia, Zhonghua Ling, Yong Chen, and Xiaohong Hu. 2017. "Chitosan Membrane Dressings Toughened by Glycerol to Load Antibacterial Drugs for Wound Healing." *Materials Science and Engineering: C* 81 (December): 522–31.

MacNeil, Sheila. 2007. "Progress and Opportunities for Tissue-Engineered Skin." *Nature*. Nature Publishing Group.

Madhumathi, K., P. T. Sudheesh Kumar, S. Abhilash, V. Sreeja, H. Tamura, K. Manzoor, S. V. Nair, and R. Jayakumar. 2010. "Development of Novel Chitin/Nanosilver Composite Scaffolds for Wound Dressing Applications." *Journal of Materials Science: Materials in Medicine* 21 (2): 807–13.

Malesu, Vijay Kumar, Vijay Kumar Malesu, Debasish Sahoo, and P. L. Nayak. 2019 "Chıtosan–Sodıum Algınate Nanocomposıtes Blended Wıth Cloısıte 30b As A Novel Drug Delıvery System For Antıcancer Drug Curcumın." Accessed April 29, 2019.

Malik, C P, Poonam Garg, Yaksha Singh, and Staffi Grover. 2012. "Medicinal Uses, Chemical Constituents and Micro Propagation of Three Potential Medicinal Plants." *International Journal of Life Science and Pharma Research* 2 (3): 57–76.

Mane, Sachin, Surendra Ponrathnam, and Nayaku Chavan. 2015. "Effect of Chemical Cross-Linking on Properties of Polymer Microbeads: A Review" 3: 473–85.

Martin, P, and R Nunan. 2015. "Cellular and Molecular Mechanisms of Repair in Acute and Chronic Wound Healing." *The British Journal of Dermatology* 173 (2): 370–78.

Martínez-Ibarra, Diana M., Dalia I. Sánchez-Machado, Jaime López-Cervantes, Olga N. Campas-Baypoli, Ana Sanches-Silva, and Tomas J. Madera-Santana. 2018. "Hydrogel Wound Dressings Based on Chitosan and Xyloglucan: Development and Characterization." *Journal of Applied Polymer Science* 136 (12): 47342.

Matadeen Bharti, Kamlesh Borane, Amrita Singhasiya. 2014. "Evaluation of Wound Healing Activity of Cissus Quadrangularis" 3 (6): 822–34.

Meng, Xin, Feng Tian, Jian Yang, Chun-Nian He, Nan Xing, and Fan Li. 2010. "Chitosan and Alginate Polyelectrolyte Complex Membranes and Their Properties for Wound Dressing Application." *Journal of Materials Science: Materials in Medicine* 21 (5): 1751–59.

Mogoşanu, George Dan, and Alexandru Mihai Grumezescu. 2014. "Natural and Synthetic Polymers for Wounds and Burns Dressing." *International Journal of Pharmaceutics* 463 (2): 127–36.

Mohandas, Annapoorna, Sudheesh Kumar P T, Biswas Raja, Vinoth-Kumar Lakshmanan, and Rangasamy Jayakumar. 2015. "Exploration of Alginate Hydrogel/Nano Zinc Oxide Composite Bandages for Infected Wounds." *International Journal of Nanomedicine* 10 Suppl 1 (Suppl 1): 53–66.

Mohiti-Asli, M., and E.G. Loboa. 2016. "Nanofibrous Smart Bandages for Wound Care." *Wound Healing Biomaterials*, January, 483–99.

Moraes, Mariana Agostini de, and Marisa Masumi Beppu. 2013. "Biocomposite Membranes of Sodium Alginate and Silk Fibroin Fibers for Biomedical Applications." *Journal of Applied Polymer Science* 130 (5): 3451–57.

Mori, Michela, Silvia Rossi, Franca Ferrari, Maria Cristina Bonferoni, Giuseppina Sandri, Theodora Chlapanidas, Maria Luisa Torre, and Carla Caramella. 2016. "Sponge-Like Dressings Based on the Association of Chitosan and Sericin for the Treatment of Chronic Skin Ulcers. I. Design of Experiments–Assisted Development." *Journal of Pharmaceutical Sciences* 105 (3): 1180–87.

Moshakis, V, M J Fordyce, J D Griffiths, and J A McKinna. 1984. "Tegadern versus Gauze Dressing in Breast Surgery." *The British Journal of Clinical Practice* 38 (4): 149–52.

Muangman, Pornprom, Supaporn Opasanon, Supaparn Suwanchot, and Orapin Thangthed. 2011. "Efficiency of Microbial Cellulose Dressing in Partial-Thickness Burn Wounds." *The Journal of the American College of Certified Wound Specialists* 3 (1): 16–19.

Mutlu, Gözde. 2019 "Preparatıon And Characterızatıon Of Actıve Agent Loaded Nanofıbrıllar Structures For Tıssue Regeneratıon." Accessed May 8, 2019.

Nguyen, Van Cuong, Van Boi Nguyen, and Ming-Fa Hsieh. 2013. "Curcumin-Loaded Chitosan/Gelatin Composite Sponge for Wound Healing Application." *International Journal of Polymer Science* 2013 (July): 1–7.

Obara, Kiyohaya, Masayuki Ishihara, Toshiaki Ishizuka, Masanori Fujita, Yuichi Ozeki, Tadaaki Maehara, Yoshio Saito, et al. 2003. "Photocrosslinkable Chitosan Hydrogel Containing Fibroblast Growth Factor-2 Stimulates Wound Healing in Healing-Impaired Db/Db Mice." *Biomaterials* 24 (20): 3437–44.

P. T., Sudheesh Kumar, Vinoth-Kumar Lakshmanan, Mincy Raj, Raja Biswas, Tamura Hiroshi, Shantikumar V. Nair, and Rangasamy Jayakumar. 2013. "Evaluation of Wound Healing Potential of β-Chitin Hydrogel/Nano Zinc Oxide Composite Bandage." *Pharmaceutical Research* 30 (2): 523–37.

P, Selvamaleeswaran, Manimaran E, and Sureshkumar M. 2016. "Antimicrobial Activity of Medicinally Important Plant - Cissus Quadrangularis Linn against Some Pathogenic Bacteria." *Journal of Chemical and Pharmaceutical Research* 8 (11).

Park, Ji-Ung, Seol-Ha Jeong, Eun-Ho Song, Juha Song, Hyoun-Ee Kim, and Sukwha Kim. 2018. "Acceleration of the Healing Process of Full-Thickness Wounds Using Hydrophilic Chitosan–silica Hybrid Sponge in a Porcine Model." *Journal of Biomaterials Applications* 32 (8): 1011–23.

Park, Ji-Ung, Hyun-Do Jung, Eun-Ho Song, Tae-Hyun Choi, Hyoun-Ee Kim, Juha Song, and Sukwha Kim. 2017. "The Accelerating Effect of Chitosan-Silica Hybrid Dressing Materials on the Early Phase of Wound Healing." *Journal of Biomedical Materials Research Part B: Applied Biomaterials* 105 (7): 1828–39.

Park, Sang Uk, Byung Kwon Lee, Mi Sun Kim, Kwan Kyu Park, Woo Jung Sung, Hyun Yeon Kim, Dong Gil Han, et al. 2014. "The Possibility of Microbial Cellulose for Dressing and Scaffold Materials." *International Wound Journal* 11 (1): 35–43.

Patel, Satish, Shikha Srivastava, Manju Rawat Singh, and Deependra Singh. 2018. "Preparation and Optimization of Chitosan-Gelatin Films for Sustained Delivery of Lupeol for Wound Healing." *International Journal of Biological Macromolecules* 107 (February): 1888–97.

Paul, Willi, and Cp Sharma. 2004. "Chitosan and Alginate Wound Dressings: A Short Review." *Trends in Biomaterials and Artificial Organs* 18 (1): 18–23.

Pillai, C.K.S., Willi Paul, and Chandra P. Sharma. 2009. "Chitin and Chitosan Polymers: Chemistry, Solubility and Fiber Formation." *Progress in Polymer Science 34*(7): 641–78.

Qi, Yu, Hui Wang, Kai Wei, Ya Yang, Ru-Yue Zheng, Ick Kim, and Ke-Qin Zhang. 2017. "A Review of Structure Construction of Silk Fibroin Biomaterials from Single Structures to Multi-Level Structures." *International Journal of Molecular Sciences* 18 (3): 237.

Radhakumary, C., Molly Antonty, and K. Sreenivasan. 2011. "Drug Loaded Thermoresponsive and Cytocompatible Chitosan Based Hydrogel as a Potential Wound Dressing." *Carbohydrate Polymers* 83 (2): 705–13.

Ramasastry, Sai S. 2005. "Acute Wounds." *Clinics in Plastic Surgery* 32 (2): 195–208.

Ramos-e-Silva, Marcia, and Maria Cristina Ribeiro de Castro. 2002a. "New Dressings, Including Tissue-Engineered Living Skin." *Clinics in Dermatology* 20 (6): 715–23.

Seaman, Susie. 2002. "Dressing Selection in Chronic Wound Management." *Journal of the American Podiatric Medical Association* 92 (1): 24–33.

Sibaja, Bernal, Edward Culbertson, Patrick Marshall, Ramiz Boy, Roy M. Broughton, Alejandro Aguilar Solano, Marianelly Esquivel, Jennifer Parker, Leonardo De La Fuente, and Maria L. Auad. 2015. "Preparation of Alginate–chitosan Fibers with Potential Biomedical Applications." *Carbohydrate Polymers* 134 (December): 598–608.

Silva, S.S., E.G. Popa, M.E. Gomes, M. Cerqueira, A.P. Marques, S.G. Caridade, P. Teixeira, C. Sousa, J.F. Mano, and R.L. Reis. 2013. "An Investigation of the Potential Application of Chitosan/Aloe-Based Membranes for Regenerative Medicine." *Acta Biomaterialia* 9 (6): 6790–97.

Singer, Adam J., and Richard A.F. Clark. 1999. "Cutaneous Wound Healing." Edited by Franklin H. Epstein. *New England Journal of Medicine* 341 (10): 738–46.

Soumya, S., K. M. Sajesh, R. Jayakumar, S. V. Nair, and K. P. Chennazhi. 2012. "Development of a Phytochemical Scaffold for Bone Tissue Engineering Using Cissus Quadrangularis Extract." *Carbohydrate Polymers* 87 (2): 1787–95.

Stashak, Ted S., Ellis Farstvedt, and Ashlee Othic. 2004. "Update on Wound Dressings: Indications and Best Use." *Clinical Techniques in Equine Practice* 3 (2): 148–63.

Strecker-McGraw, Margaret K., Thomas Russel Jones, and David G. Baer. 2007. "Soft Tissue Wounds and Principles of Healing." *Emergency Medicine Clinics of North America* 25 (1): 1–22.

Sudheesh Kumar, P. T., Vinoth-Kumar Lakshmanan, T.V. Anilkumar, C. Ramya, P. Reshmi, A.G. Unnikrishnan, Shantikumar V. Nair, and R. Jayakumar. 2012. "Flexible and Microporous Chitosan Hydrogel/Nano ZnO Composite Bandages for Wound Dressing: In Vitro and In Vivo Evaluation." *ACS Applied Materials & Interfaces* 4 (5): 2618–29.

Supaphol, Pitt, Orawan Suwantong, Pakakrong Sangsanoh, Sowmya Srinivasan, Rangasamy Jayakumar, and Shantikumar V. Nair. 2011. "Electrospinning of Biocompatible Polymers and Their Potentials in Biomedical Applications." In , 213–39. Springer, Berlin, Heidelberg.

Tamburaci, Sedef. 2016. "Natural And Synthetic Silica Incorporated Chitosan Composite Scaffolds For Bone Tissue Engineering Applications A Thesis Submitted to in Bioengineering."

Tamburaci, Sedef, Ceren Kimna, and Funda Tihminlioglu. 2018. "Novel Phytochemical *Cissus Quadrangularis* Extract–loaded Chitosan/Na-Carboxymethyl Cellulose–based Scaffolds for Bone Regeneration." *Journal of Bioactive and Compatible Polymers* 33 (6): 629–46.

Tamburaci, Sedef, and Funda Tihminlioglu. 2017. "Diatomite Reinforced Chitosan Composite Membrane as Potential Scaffold for Guided Bone Regeneration." *Materials Science and Engineering: C* 80 (November): 222–31.

Thu, Hnin-Ei, Mohd Hanif Zulfakar, and Shiow-Fern Ng. 2012. "Alginate Based Bilayer Hydrocolloid Films as Potential Slow-Release Modern Wound Dressing." *International Journal of Pharmaceutics* 434 (1–2): 375–83.

Ul-Islam, Mazhar, Taous Khan, Waleed Ahmad Khattak, and Joong Kon Park. 2013. "Bacterial Cellulose-MMTs Nanoreinforced Composite Films: Novel Wound Dressing Material with Antibacterial Properties." *Cellulose* 20 (2): 589–96.

Uttayarat, Pimpon, Suwimol Jetawattana, Phiriyatorn Suwanmala, Jarurattana Eamsiri, Theeranan Tangthong, and Suchada Pongpat. 2012. "Antimicrobial Electrospun Silk Fibroin Mats with Silver Nanoparticles for Wound Dressing Application." *Fibers and Polymers* 13 (8): 999–1006.

Velnar, T, T Bailey, and V Smrkolj. 2009. "The Wound Healing Process: An Overview of the Cellular and Molecular Mechanisms." *Journal of International Medical Research 37*(5): 1528–42.

Vrieze, Sander De, A E Philippe, Westbroek Ae, Tamara Van Camp, A E Lieva, and Van Langenhove. n.d. "Electrospinning of Chitosan Nanofibrous Structures: Feasibility Study." Accessed June 13, 2019.

Wang, Tao, Xiao-Kang Zhu, Xu-Ting Xue, and Da-Yang Wu. 2012a. "Hydrogel Sheets of Chitosan, Honey and Gelatin as Burn Wound Dressings." *Carbohydrate Polymers* 88 (1): 75–83.

Wen, Peng, Min-Hua Zong, Robert J. Linhardt, Kun Feng, and Hong Wu. 2017. "Electrospinning: A Novel Nano-Encapsulation Approach for Bioactive Compounds." *Trends in Food Science & Technology* 70 (December): 56–68.

Wolcott, Randall D., Keith F. Cutting, Scot E. Dowd, and Steven L. Percival. 2010. "Types of Wounds and Infections." *Microbiology of Wounds*, no. July 2014: 219–32.

Xie, Yu, Zeng-xing Yi, Jian-xun Wang, Tong-gang Hou, and Qiong Jiang. 2018. "Carboxymethyl Konjac Glucomannan - Crosslinked Chitosan Sponges for Wound Dressing." *International Journal of Biological Macromolecules* 112 (June): 1225–33.

Yousefi, Iman, Mehdi Pakravan, Hoda Rahimi, Abbas Bahador, Zahra Farshadzadeh, and Ismael Haririan. 2017. "An Investigation of Electrospun Henna Leaves Extract-Loaded Chitosan Based Nanofibrous Mats for Skin Tissue Engineering." *Materials Science and Engineering: C* 75 (June): 433–44.

Zhong, S. P., Y. Z. Zhang, and C. T. Lim. 2010. "Tissue Scaffolds for Skin Wound Healing and Dermal Reconstruction." *Wiley Interdisciplinary Reviews: Nanomedicine and Nanobiotechnology* 2 (5): 510–25.

Zhou, Yingshan, Hongjun Yang, Xin Liu, Jun Mao, Shaojin Gu, and Weilin Xu. 2013. "Potential of Quaternization-Functionalized Chitosan Fiber for Wound Dressing." *International Journal of Biological Macromolecules* 52 (January): 327–32.
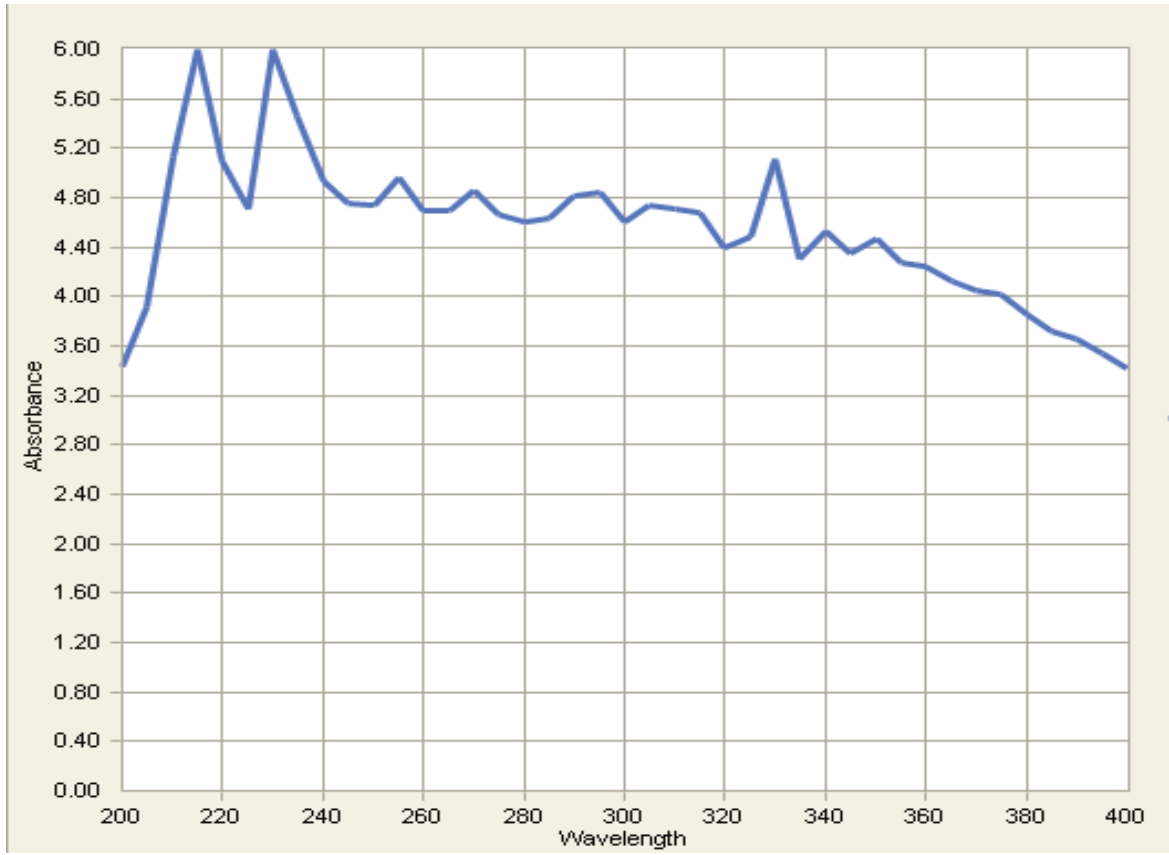
APPENDIX A

SCAN OF EXTRACT

Figure A. 1. UV Scan of *cissus quadrangularis*

APPENDIX B

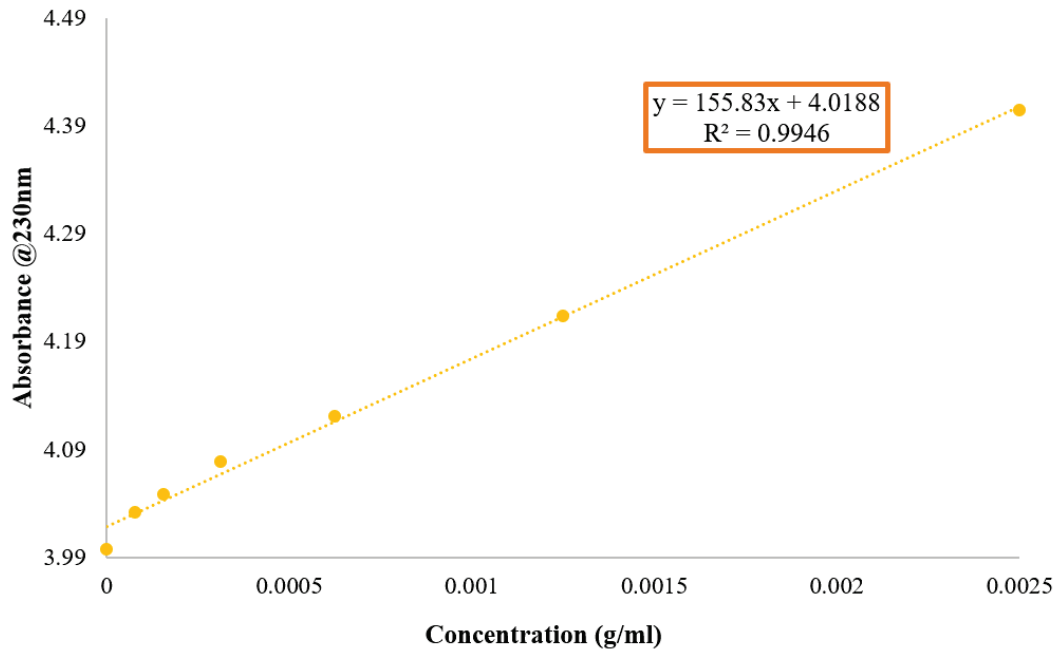# CALIBRATION CURVES OF EXTRACT

y = 155.83x + 4.0188
R² = 0.9946

Figure B. 1. Calibration curve of *cissus quadrangularis*